SYNTHESIS OF CARBON-BASED FLEXIBLE TEMPERATURE-CONTROLLED SEMICONDUCTIVE COMPOSITES

A Thesis Submitted to
the Graduate School of Engineering and Sciences of
İzmir Institute of Technology
in Partial Fulfillment of the Requirements for the Degree of

MASTER OF SCIENCE

in Chemical Engineering

by
Esra Sıla GÜNDÜZ

July 2024
İZMİR

We approve the thesis of **Esra Sıla GÜNDÜZ**

Examining Committee Members:

Prof. Dr. Mehmet POLAT
Department of Chemical Engineering, İzmir Institute of Technology

Prof. Dr. Ekrem ÖZDEMİR
Department of Chemical Engineering, İzmir Institute of Technology

Prof. Dr. Erol Kaya
Department of Mining Engineering, Dokuz Eylül University

10 July 2024

Prof. Dr. Mehmet POLAT
Supervisor, Department of Chemical Engineering, İzmir Institute of Technology

Prof. Dr. Hürriyet POLAT
Co-Supervisor, Department of Chemistry, İzmir Institute of Technology

Prof. Dr. Aysun SOFUOĞLU
Head of the Department of Chemical Engineering

Prof. Dr. Mehtap EANES
Dean of the Graduate School of Engineering and Sciences

ACKNOWLEDGEMENTS

First, I would like to express my thanks to my advisors Prof. Dr. Mehmet POLAT and Prof. Dr. Hürriyet POLAT for all their advice, guidance, motivation, patience information sharing, and endless support. Their perspectives helped me improve and challenge myself in both my academic and personal life. The guidance they provided made a great contribution to me during the research, implementation, and writing of the thesis.

I would like to thank Specialist Duygu OĞUZ KILIÇ, Zehra Sinem YILMAZ, and Mutlu DEVRAN YAMAN in the Material Research and Development Center of IZTECH for their valuable help in SEM analysis. I would also to thank Prof. Dr. Metin TANOĞLU for his support in the implementation of mechanical tests.

I would also like to thank my labmates, Tuğçe TUNÇ GULIYEV, Merve ÇEVİK EREN, and Hazal PAKER, for their support, patience, and motivation throughout my thesis process.

Last but not least; I would like to thank my boyfriend, Erdal ULAŞLI for his endless support, motivation, patience, and technical information during the thesis process. His endless support and trust in me from the beginning to the end of the thesis process helped me complete the process more easily. I would also like to thank him for his support in performing and interpreting mechanical tests.

Finally, I would like to express my sincere gratitude to my family, my mother Yıldız GÜNDÜZ, my father Bilgin GÜNDÜZ, and my sister Ezgi GÜNDÜZ, who are my biggest supporters. I could not have achieved this without my beloved family, who raised me, helped me find my way, supported me in every decision I made, and showed me their trust and endless love.

ABSTRACT

SYNTHESIS OF CARBON-BASED FLEXIBLE TEMPERATURE-CONTROLLED SEMICONDUCTIVE COMPOSITES

Semiconducting flexible polymer matrix composites with tunable temperature profiles find use in consumer goods, robotics, aerospace, and energy sectors. However, the manufacturing cost is high due to the need for expensive conductive phases, such as carbon nanotubes, graphene, or metal nanoparticles. This study aims to use inexpensive conductive materials, such as carbon blacks and natural graphite in polydimethylsiloxane matrix to manufacture such composites. The composite samples prepared by the solution-mixing approach were tested for dispersibility, electrical conductivity, thermal responsiveness, and mechanical and morphological characteristics. They displayed non-wettable and low-energy surfaces (26 J/m²) and, hence, were prone to agglomeration at high carbon contents (>30%). Surfactant addition was employed to counteract the negative consequences of agglomeration. Adjusting the carbon content could modulate conductivity between 0 and 10.79 S/m. A typical composite with 3.17 S/m conductivity showed a surface temperature of 49.7°C under a load of 30 V. Compared to bare PDMS, mechanical properties were favorable; a composite with optimal conductivity and temperature response showed increases of 97.8% in elastic modulus and 197% in tear strength, despite a 50% decrease in tensile strength. The study highlights significant economic potential in manufacturing semiconductive flexible composites with desired temperature profiles.

ÖZET

KARBON ESASLI ESNEK SICAKLIK KONTROLLÜ YARİİLETKEN KOMPOZİTLERİN SENTEZİ

Günümüzde, yarı iletken polimer matrisli kompozitler ve kullanım alanları araştırmacıların ilgisini çekmektedir. Ayarlanabilir sıcaklık profillerine sahip yarı iletken esnek polimer matrisli kompozitler, robotik, havacılık ve enerji sektörlerinde kullanım alanı bulmaktadır. Ancak karbon nanotüpler, grafen veya metal nanopartiküller gibi pahalı iletken fazlarlara duyulan ihtiyaç nedeniyle üretim maliyeti yüksektir. Bu çalışma, bu tür kompozitlerin üretimi için polidimetilsiloksan matrisinde karbon siyahı ve doğal grafit gibi ucuz iletken malzemelerin kullanılmasını amaçlamaktadır. Kompozitler "Çözelti karıştırma" yöntemiyle (%10 ila %35 metanolde) hazırlandı ve dağılabilirlik, elektriksel iletkenlik, termal tepki ve mekanik ve morfolojik özellikler açısından test edildi. Bu substratların yüzeylerinin ıslanmayan, düşük enerjili yüzeyler (Fowke teorisine göre 26 J/m^2) olduğu bulundu; bu nedenle parçacıklar daha yüksek konsantrasyonlarda (>%30) topaklanma eğilimliydiler. Aglomerasyonun olumsuz sonuçlarını ortadan kaldırmak için yüzey aktif madde ilavesi kullanıldı. Karbon içeriğinin ayarlanması iletkenliği 0 ile 10,79 S/m arasında modüle edilmesini sağlamıştır. 3,17 S/m iletkenliğe sahip tipik bir kompozit, 30 V yük altında 49,7°C yüzey sıcaklığı göstermiştir. PDMS ile karşılaştırıldığında kompozitlerin mekanik özellikler olumluydu; optimum iletkenliğe ve sıcaklık tepkisine sahip bir kompozit, çekme mukavemetinde %50'lik bir düşüşe rağmen elastik modülde %97,8 ve yırtılma mukavemetinde %197 artış gösterdi. Çalışma, istenen sıcaklık profillerine sahip yarı iletken esnek kompozitlerin üretiminde önemli ekonomik potansiyelin altını çiziyor.

TABLE OF CONTENTS

LIST OF FIGURES

Figure **Page**

Figure **Page**

Figure **Page**

LIST OF TABLES

CHAPTER 1

INTRODUCTION

Composite materials have been used since ancient times to combine the best properties of two or more varied materials into a single material. With the advancement of technology, composite production techniques are developed, and their usage areas are increased. Recently, the production of high-value-added polymer matrix composites has gained attention due to the ease of the process, economical production methods, lightness, and adjustable properties such as electrical, mechanical, and thermal (Kong et al. 2014; Sun et al. 2019). One of their emerging applications has been flexible semi-conductive polymer composites, which can be used as electromagnetic interference (EMI) protection, heating elements, transistors, supercapacitors, and electronic equipment (Zhang, Dehghani-Sanij, and Blackburn 2007). Semiconductor polymer composites can be developed by combining non-conductive polymers with conductive fillers such as metallic particles (MPs), metal wires (MWs), carbon black (CB), carbon nanotubes (CNTs), carbon fiber (CF), etc., or conductive polymers with non-conductive fillers (Mohd Radzuan, Sulong, and Sahari 2017; Thongruang, Spontak, and Balik 2002).

Materials with high conductivity, such as silver, gold, and copper, are good candidates for dispersed phases in manufacturing semi-conductive composites. However, such composites also possess high thermal conductivities, which can challenge temperature control and retention. Also, the high sensitivity of the fine metal powder in the composite to oxidation in water and air is another negative factor. On the contrary, carbon-based additives emerge as the best option due to their excellent thermal and electrical properties. In the literature, graphene and carbon nanotubes are frequently used in producing semiconductor flexible composites (Khan, Kausar, and Ullah 2016; Kim, Miura, and MacOsko 2010; Rahmat and Hubert 2011; Sun et al. 2019; Tian et al. 2015; Yan and Jeong 2014; Yao et al. 2013). However, the very high cost of these carbon-based materials makes them unsuitable for large-scale production purposes. Therefore, it becomes an important avenue for researching the possibility of using low-cost carbon-

based additives such as graphite or carbon black to produce composite materials with proper semi-conductive properties for use in flexible heating materials.

This thesis is about designing semi-conductive, flexible composite materials using low-cost carbon additives whose resistance could be adjusted to control the temperature sensitively within the desired range. Such a material will find use in applications such as heating devices, thermotherapy pads, or used in aerospace, though no specific application was aimed at this thesis. Composite design would require close control of material properties (dispersed or continuous phase), particle size and concentration, and surface energies. Therefore, the work in this study is an exercise in synthesis which requires a background in colloid and surface chemistry and particle technology.

CHAPTER 2

THE STATE OF THE ART OF SEMICONDUCTOR COMPOSITES

This thesis focuses on designing flexible semi-conductive composite materials whose temperature can be controlled sensitively within the desired range. The composites comprise a non-conductive continuous resin phase (polydimethylsiloxane, PDMS) and a conductive carbon-based dispersed powder phase. The carbon reinforcements tested for the purpose of the thesis consist of graphite and carbon black powder due to their low cost and availability in large quantities. Therefore, the following paragraphs will begin with a general introduction to composites and provide information about the matrix phase which includes polymers, and the dispersed phase under the title of polymer matrix composites. Then, it will continue with information about the current state of the art regarding semiconductor composites, production techniques, and their applications, which are the subject of the study.

2.1. Composites

Composite materials, consisting physical combination of two or more ingredients, are materials that show better properties than the components from which they are derived individually (Akaluzia et al. 2021; Campbell 2010). Composite materials have become indispensable in many industries due to their extraordinary qualities such as fracture toughness, resistance to wear and corrosion, and superior thermal properties (Sharma et al. 2020). The most important features of composite materials are their low density and light structure, as well as their high strength and stiffness (Campbell 2010).

Composite materials are formed by combining a matrix and one or more reinforcement elements. A representative image of composite materials is given in Figure 2.1.

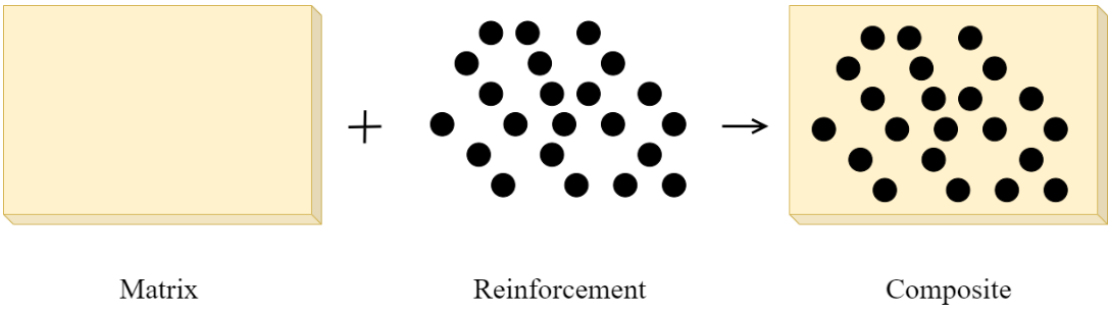

Figure 2.1. Composite Materials

The phase that provides stiffness and strength to the composite material is the reinforcement phase (Campbell 2010). Fibers, sheets, or particles are all considered forms of reinforcement elements (Akaluzia et al. 2021; Oladele et al. 2020; Ratna Prasad and Mohana Rao 2011). The use of particle-reinforced composites, which can have spherical or irregular/regular geometric shapes, is typically limited to 40–50% by volume due to their fragility and difficulty in processing, which makes them weaker than fiber reinforcements (Campbell 2010; Chawla 2019). Fibers can be dispersed continuously or discontinuously within the matrix in fiber-reinforced composites. Composites can be classified according to type of reinforcement and their details are given in Figure 2.2.

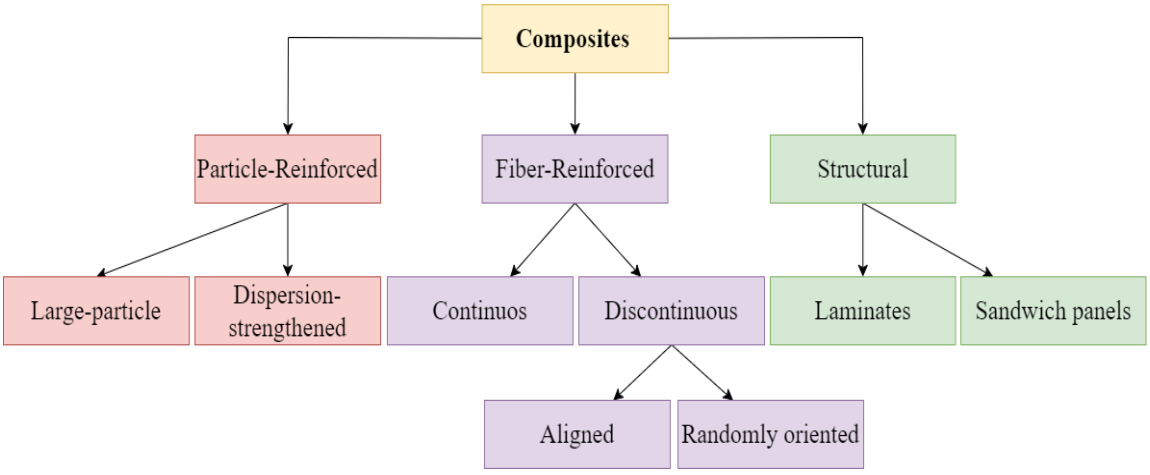

Figure 2.2. Composite classification according to the reinforcement type

Fiber types commonly used in the literature are carbon, glass, and aramid. Glass fibers are frequently used in different industries because they are economical, flexible,

light in weight, hard, and non-reactive (Altera et al. 2021). Carbon fibers are frequently used in the development of composites in different fields such as automotive, aerospace, sports equipment, and military because they are lighter and higher strength than steel, non-reactive, resistant to high temperatures, and good electrical properties (Shirvanimoghaddam et al. 2017).

The matrix, known as the continuous phase, holds and protects the dispersed phase. The matrix phase can have three different structures: polymer, metal, and ceramic, and composites are generally named according to the phase used in the matrix material (Akaluzia et al. 2021; Sharma et al. 2020; Sijo and Jayadevan 2016) as shown in Figure 2.3.

The most important advantages of metal matrix composites (MMCs) are high strength and stiffness, better wear and abrasion resistance, specific modulus, and high-temperature performances (Sharma, Mahant, and Upadhyay 2019; Sijo and Jayadevan 2016). MMCs have gained a notable position in a variety of industries, including aerospace, automotive, military, and electronic instruments (Sharma et al. 2020)The primary drawback of MMCs is the comparatively high cost of both the reinforcement materials and the fabrication process (Sijo and Jayadevan 2016).

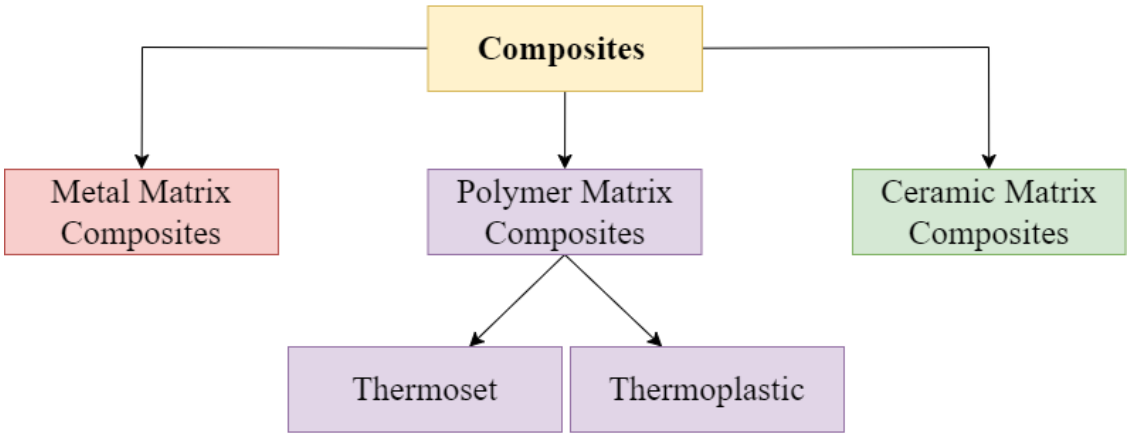

Figure 2.3. Composite classification according to the matrix type

Ceramic materials stand out with high stability at high temperatures, low density, and chemical inertness (Chawla 2012). However, their lack of toughness limits their use considerably. Consequently, the aim of ceramic matrix composites (CMCs) is primarily

to increase toughness (Campbell 2010). Because of their high-temperature resistance, CMCs are especially useful in applications requiring high temperatures, such as heat engines, gas turbines, furnace materials, jet aircraft, and energy conversion systems.

Polymer matrix composites (PMC) include different types of organic polymers that together with the dispersed phase form the continuous phase (Liew et al. 2021). Detailed information about PMCs is given in the following section.

2.2. Polymer Matrix Composites

Polymer matrix composites are attracting increasing attention due to their easy manufacturability, low cost, higher specific strength and stiffness, lightweight, good resistance to corrosion and abrasion, and adjustability of internal features (Kong et al. 2014). The use areas of polymer matrix composites, which have been used for years, especially in the aviation, space, and automotive sectors, are increasing in many fields such as maritime, energy, wearable technologies, and biomedical (Hamidi and Altan 2017).

The polymer matrix can be thermoplastic and thermoset. The matrix that forms the main backbone of the composite is determined according to the usage area of the composite (Hsissou et al. 2021). Particles and/or fibers are added to the polymer matrix to improve specific properties of the composite, such as thermal stability, conductivity, and hardness. Generally, micron-sized particles are used to increase thermal stability, while nanoparticles, fibers, and whiskers are used to improve physical and mechanical properties (Robinson, Greenhalgh, and Pinho 2012).

2.2.1. Matrix Phase: Polymers

Polymers are large molecules formed by polymerizing many repeating units called monomers. The earliest known polymers are natural products such as cotton, starch, protein, and wool (Sperling 2006). A revolution in polymer chemistry occurred in the

early 20th century with the production of Bakelite, the first synthetic polymer (Sperling 2006). Polymers have quickly gained a place in many different industries due to their affordable prices, lightness, inertness to chemicals, ease of processing, and lack of corrosion. Based on distinct criteria, the polymers are categorized into several types (Mishra 2018) and detailed in Figure 2.4.

One of the important features of the polymers is the glass transition temperature, T_g. Polymers have a rigid structure at temperatures below Tg and a flexible and soft structure at temperatures above T_g. The glass transition temperature value of polymers is important for classifying the material as thermoset or thermoplastic (Bîrca et al. 2019).

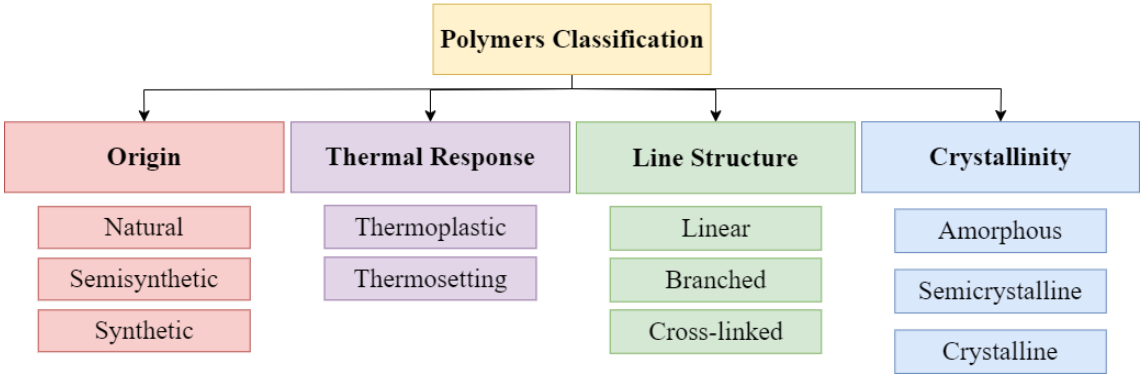

Figure 2.4. Classification of polymers according to different criteria

2.2.1.1. Thermosetting Polymers

Thermosetting polymers, also known as thermosets, are polymers that irreversibly change from liquid to solid during the heating process, known as the curing process (Pascault and Williams 2013). One of the important features of thermosetting polymers is that they are highly cross-linked, thus gaining high resistance to creep and solvent, and stable structure under high temperature and high strength (Bîrca et al. 2019; Kausar 2017). The structure of the thermosetting polymer is given in Figure 2.5.

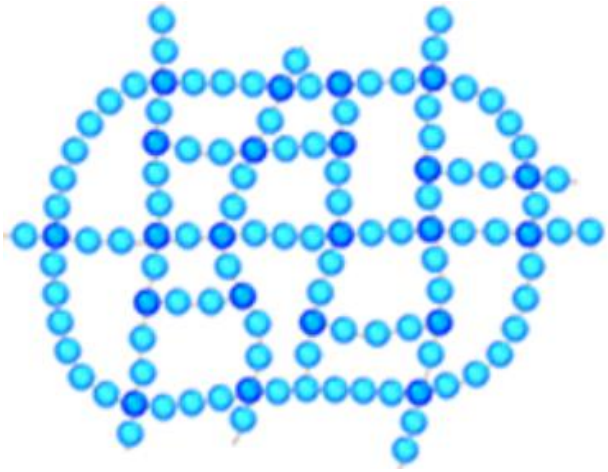

Figure 2.5. Thermosetting polymer structure (Source: Navin Baskar 2023)

Their irreversibility and resistance to heat make them useful in a variety of industries, including aerospace, coating, dentistry, electronics, and sporting products, etc. Epoxy, polyester, polyurethane, and phenolic polymers are the most well-known examples of thermosets. Epoxy resins are one of the most used thermosets in structural and specialty composite applications.

2.2.1.1.1. Epoxy

Epoxy resin is a thermoset resin with a molecular formula $C_{21}H_{25}ClO_5$, composed of more than one epoxy group (Takeichi and Furukawa 2012). Epoxy resins are low-viscosity materials that are combined with a curing agent and hardened by applying heat. Their low viscosity provides ease of processability.

The properties of epoxy resins vary depending on the curing agents and epoxy type, which provides the advantage of versatile use (Jin, Li, and Park 2015). Because of their good processing qualities and favorable properties, epoxy resins are used in a variety of applications, such as adhesives, paints and coatings, industrial tooling, biomedical systems, electronics for encapsulation, potting, and printed circuit boards, and aerospace as composite matrices (Dinu et al. 2022; Gergely et al. 2013; Jojibabu, Zhang, and Prusty 2020; Ogbonna, Popoola, and Popoola 2023; Wen et al. 2022).

2.2.1.2. Thermoplastics Polymers

Thermoplastics are a type of polymer that can reversibly transform from liquid to solid and vice versa. There are no cross-links between the chains of thermoplastic polymers. Therefore, it is reversibly recyclable, and the structure is given in Figure 2.6. However, these polymers only have a certain number of reversibility cycles, and exceeding this limit can change their structure, color, and mechanical properties (Bîrca et al. 2019; Oliveira et al. 2017; Radlmaier et al. 2017).

The important advantages of thermoplastics are that they release fewer chemicals, do not require curing, and are recyclable, re-shapeable, and sustainable (Almushaikeh et al. 2023). Thermoplastic polymers can be used in a variety of industries such as plastics, medicine, automobiles, electrical devices, packaging, and aerospace. Polyethylene, polypropylene, polystyrene, nylon, and polyvinyl chloride are a few examples of thermoplastic polymers.

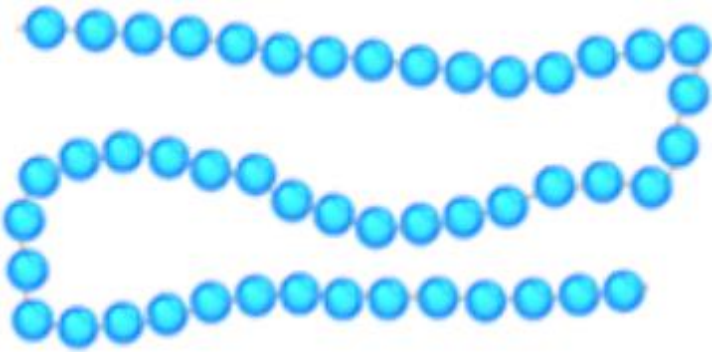

Figure 2.6. Thermoplastic polymer structure (Source: Navin Baskar 2023)

2.2.1.2.1. Polyethylene

Polyethylene is a type of thermoplastic polymer with a molecular formula $(CH_2)_n$, which includes a long chain of aliphatic hydrocarbons (Ronca 2017). Polyethylene is generally classified according to its density as high-density polyethylene (HDPE) and low-density polyethylene (LDPE). The fact that polyethylene can be developed through

many different production processes, the diversity of catalysts, and the change of comonomers have enabled it to gain a place in many different application areas such as packaging, pipes, and automotive parts (Patel 2016).

2.2.1.3. Elastomeric Polymers

Elastomers, a special classification of polymers, have an elastic and stretchable structure. Elastomers are known for their highly reversible stretchability, which means they retain their original form most of the time. The structure of the thermosetting polymer is given in Figure 2.7. The cross-links that elastomers have between chains give them their flexible and reversible properties.

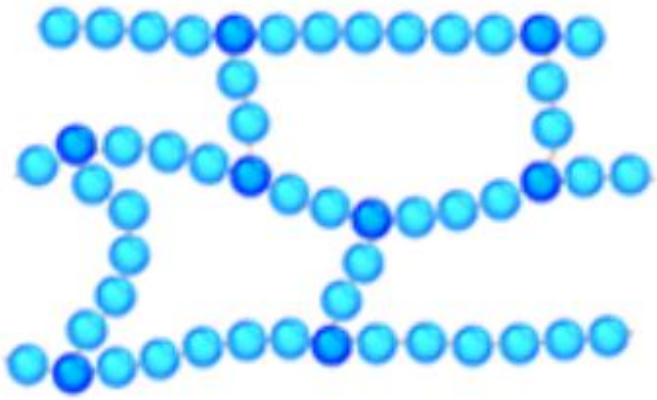

Figure 2.7. Elastomer structure (Source: Navin Baskar 2023)

Elastomers harden below the T_g due to the disorder of the polymer chains and lose their rubbery properties (Kutz 2015). Elastomers become flexible and elastic above the glass transition temperature due to the liberation of polymer chains. These properties make them extremely valuable in many industrial and consumer applications such as tires, rubbers, adhesives, automotive, and medical industries.

2.2.1.3.1. Polydimethylsiloxane

Polydimethylsiloxane (PDMS) is a promising silicone-based elastomer due to its excellent properties and diversity of use. The chemical structure of PDMS consists of flexible siloxane groups (Si-O) and repeating (Si $(CH_3)_2O$) units and is given in Figure 2.8. Si-O bonds give the PDMS its thermal and chemical stability; methyl groups (CH_3) give the hydrophobic characteristic (Ariati et al. 2021; Wolf, Salieb-Beugelaar, and Hunziker 2018). Its cross-linking reactions involving groups such as vinyl and phenyl provide versatility for different applications (Ariati et al. 2021; Seethapathy and Górecki 2012).

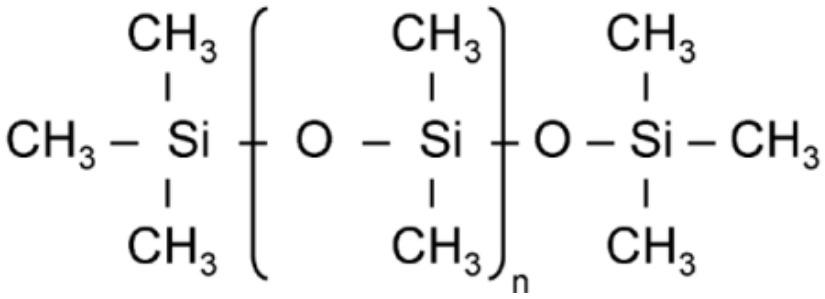

Figure 2.8. Chemical structure of PDMS (Source: Danilov et al. 2009)

Outstanding features such as simple and economic processability, excellent optical transparency (240-1100 nm), good stability to chemical, gas permeability, biocompatibility, and non-toxicity of PDMS have enabled it to be found in a wide variety of usage areas such as bio-microfluidic applications, composites, sensors, and electronic applications (Gökaltun et al. 2019; Stankova et al. 2016; Wolf et al. 2018).

2.2.2. Dispersed Phase

The dispersed phase (reinforcement) is also important for thermal, mechanical, and electrical characteristics and potential usage areas of PMCs. The reinforcement

affects directly rheological behaviors and mechanical and thermal properties. The nanoscale reinforcements can be grouped as zero-dimensional (0D), such as spherical, or dot-like particles, one-dimensional (1D), such as fiber, tube, or rod-like particles, and 2-dimensional (2D), such as sheets or flakes (Fu et al. 2019; Sahu, Boggarapu, and Sreekanth 2023). In Figure 2.9, the representative image of filler types is given.

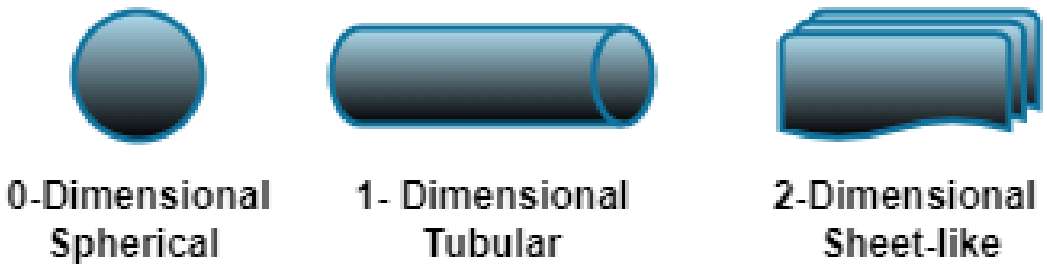

Figure 2.9. Classification of reinforcement types

Carbon black, silica nanoparticles, silver nanoparticles, and titanium dioxide are the most used examples of zero-dimensional reinforcements in the literature. Glass fibers, carbon fibers, aramid fibers, and carbon nanotubes are examples of one-dimensional reinforcement materials. The term two-dimensional structures in nanoparticles are used for structures whose two dimensions are outside the nanoscale range and the other is in the nanoscale (Sahu et al. 2023). Two-dimensional nanomaterials have attracted attention due to their surface properties and high surface area. One of the most important examples is graphene.

2.3. Semiconductor Polymer Matrix Composites

Today, interest in semiconductor polymer matrix composites (SPCs) is increasing due to their wide application areas such as electromagnetic shielding, wearable technologies such as sensors, and heating applications. SPCs can be manufactured using a conductive polymer or by combining a conductive filler material with an insulating polymer (Q. Gao, Liu, and Liu 2021; Gulrez et al. 2014; Li et al. 2012; Ren et al. 2014).

Although conductive polymers show good electrical properties, their lack of easy processability, low mechanical properties, and insoluble structure limit their use (Criado-Gonzalez et al. 2021). Metal particles/wires and carbonaceous materials such as carbon nanotube (CNT), graphene (G), graphene oxide (GO), and carbon black (CB) are frequently used as conductive fillers in the literature. Figure 2.10 shows the range of conductivities, from insulators to conductors.

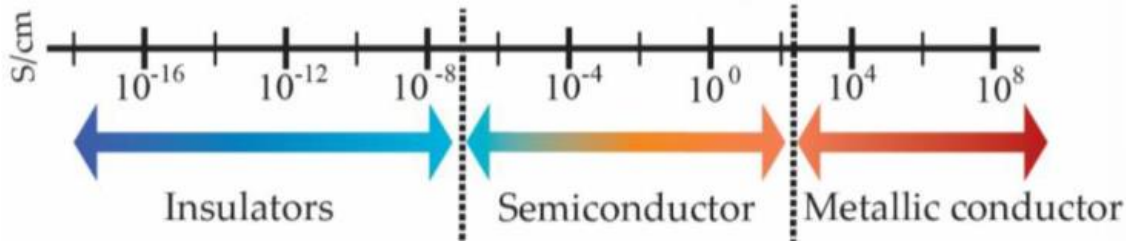

Figure 2.10. Range of conductivity (Source: Le, Kim, and Yoon 2017)

SPCs are formed by distributing a certain volume of conductive fillers within the matrix and creating a conductive network that can provide electron paths. The concentration of the material at the point where it transitions from an insulating state to a conductive state by creating conductive paths is defined as the electrical percolation threshold (Gulrez et al. 2014; Hassanabadi, Wilhelm, and Rodrigue 2014; Mysiukiewicz et al. 2018; Zhang et al. 2007).

In Figure 2.11, a schematic representation of the percolation curve according to CB content is given. Other factors that affect the electrical percolation threshold include size, porosity, shape, dispersion techniques of filler, and the polymer matrix in which it is dispersed. The network structure formed by filler particles causes rheological and mechanical effects in addition to electrical properties (Q. Gao et al. 2021; Li et al. 2012; Mysiukiewicz et al. 2018; Ren et al. 2014; Zhang et al. 2007).

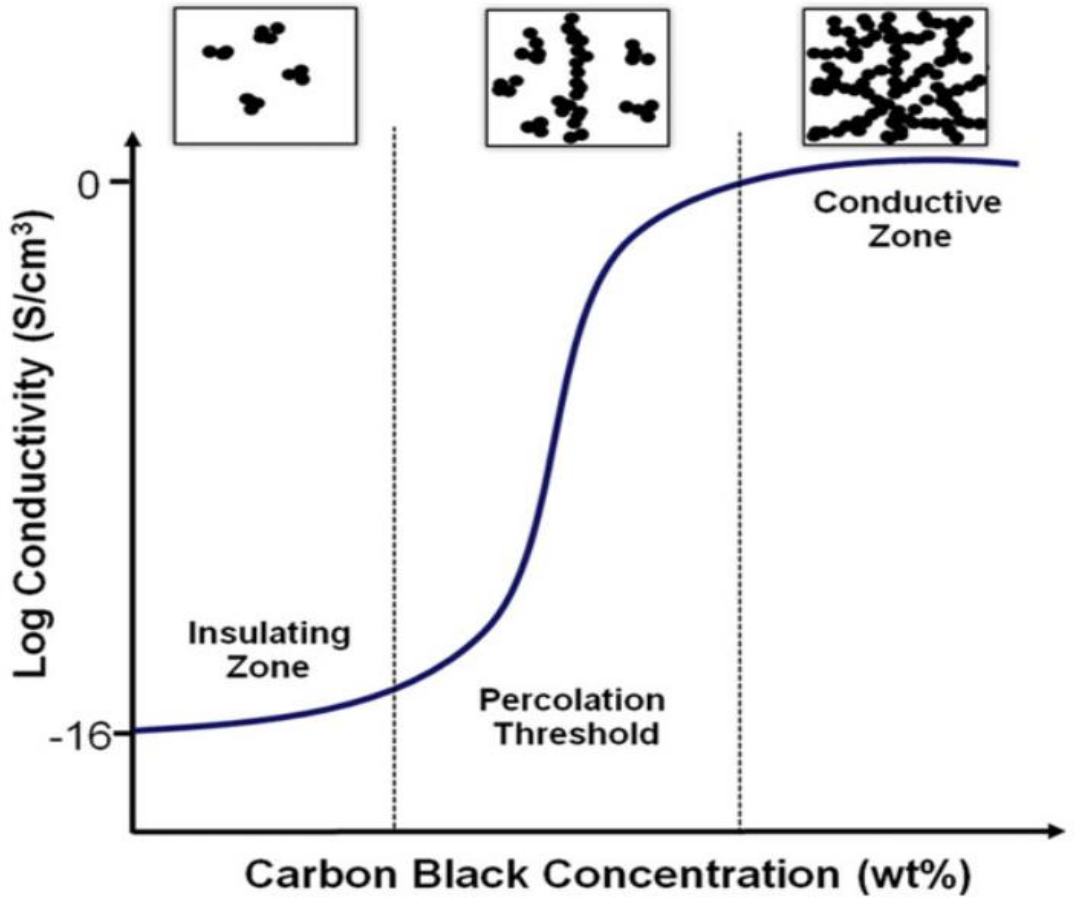

Figure 2.11. Schematic representation of percolation curve according to CB concentration (Source: Brigandi, Cogen, and Pearson 2014)

Metal materials such as silver, gold, and copper are among the materials considered to be used in developing semiconductor composites with their high electrical conductivity properties. However, carbonaceous materials have become popular due to their outstanding electrical and thermal features. One of the main reasons is that carbonaceous materials can easily create conductive network paths due to their chain structures (Zhang et al. 2007). In addition, metal materials have some disadvantages such as high weight and corrosion problems, they are easily oxidized by water and air (Ahn, Jeong, and Lee 2012; Kim et al. 2019; Mohammad, Stepashkin, and Tcherdyntsev 2022). Moreover, Hu et. al., reported that metals such as silver nanowires have difficulty adhering to the polymer surface (Hu et al. 2010). In the literature, conductive fillers used in the production of semiconductor polymer composites are given in Table 2.1.

Table 2.1. Conductivity reinforcements used in SPCs developed for different purposes

Filler	Matrix	Production method	Usage Area	References
CNT	PDMS	Solution casting	Flexible piezoresistive sensors	(Ghahramani et al. 2021)
CNT	PDMS	Solution casting	Flexible tactile sensor	(Zhu et al. 2022)
CNT	PDMS	Solution casting	Electronic skin	(Park et al. 2014)
CNT	Ethylene-vinyl acetate	Solution casting	Semiconductor composite	(Hassanabadi et al. 2014)
G	PDMS	Solution casting	Multifunctional elastomer	(Ozbas et al. 2012)
G	PDMS	Lithographic filtration	Thermistor	(Yan, Wang, and Lee 2015)
GO	Polyurethane/PEDOT: PSS	Solution casting	Wearable thermotherapy	(Zhou et al. 2017)
GO	PDMS	Solution casting	Pressure sensor	(Tian et al. 2015)
CB	Ethylene vinyl acetate/ LDPE	Melt mixing	Semiconductor composite	(Mysiukiewicz et al. 2018)
CB	Polymethylmethacrylate Polystyrene	Melt mixing	Semiconductor composite	(Q. Gao et al. 2021)
CB	PDMS	Solution casting	Elastic strain sensor	(Kong et al. 2014)

According to the table, graphene and carbon nanotubes were the most frequently used conductive additive materials. However, the high cost of these materials is

challenging for large-scale production processes. The thermal and electrical properties and the price of these materials are given in Table 2.2.

Table 2.2. Properties and prices of conductive reinforcements

Material	Thermal Conductivity (W/m.K)	Electrical Conductivity (S/m)	Price
CNT	2000-6000 (Han and Fina 2011)	$2.5x10^4$- $2x10^7$ (Tavman 2015)	$1000-2000/kg (Kim et al. 2023)
Graphene	5300 (Tavman 2015)	$1.0x10^8$ (Tavman 2015)	$90-300/kg (Y. Gao et al. 2021)
Graphite	100-400 (Tavman 2015)	$2x10^5$-$3x10^5$ (Tavman 2015)	$100/kg (Greenwood, Wentker, and Leker 2021)
CB	6-174 (Sajeel et al. 2021)	10-10^4 (Gültekin 2015)	$0.4 - 2/kg (Brändle, Schönfisch, and Schulte 2021)

This study aims to develop temperature-controlled flexible polymer composites with low-cost carbon fillers. Carbon black, which is frequently used with elastomers, is a suitable choice for the development of flexible and semiconductor composites (De Sarkar et al. 2022). It is also notable for being the most economical product among conductive carbon types, as presented in Table 2.2.

2.3.1. Conductive Reinforcements

In this section, conductive reinforcement materials that are used in polymer-based semiconductor composites are included. Considering the advantages of carbonaceous

materials, as mentioned in Section 2.3, this chapter specifically focuses on different types of carbon.

2.3.1.1. Carbon Black

Carbon black is an essential reinforcing material that is used in different areas such as pigment, anti-static coating, plastics, rubbers, and tires. CB is virtually a form of pure elemental carbon (approximately more than 90%) (Fan, Fowler, and Zhao 2020; Kausar and Taherian 2018). Figure 2.12 shows the structure of carbon black, where the functional groups are also indicated.

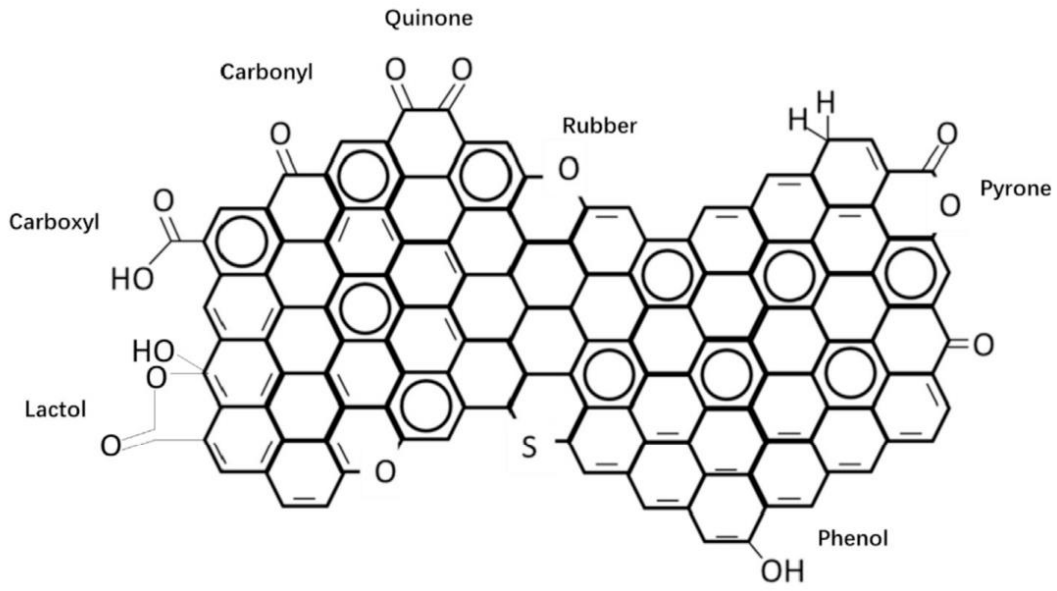

Figure 2.12. Structure of carbon black (Source: Fan et al. 2020)

Carbon black is divided into five classes according to the manufacturing method: thermal black, furnace black, channel black, lamp black, and acetylene black (Donnet 1993). Furnace blacks account for a large portion of the total carbon black market due to their frequent use in the automobile industry (Fan, Fowler, and Zhao 2020).

CB generally has primary particle sizes of 10-100 nm (Szeluga, Kumanek, and Trzebicka 2015). However, due to the structure of CB, these primary particles tend to come together and form aggregates. The sizes of these aggregates generally vary between 50-500 nm (Alam et al. 2014). Since aggregates are formed through covalent bonds, their disintegration is quite difficult. On the contrary, these aggregates tend to come together and reach sizes of 1-100 microns (Kausar and Taherian 2018). In Figure 2.13, the agglomeration step of CB is illustrated. This agglomerate structure of CB results in a high percolation threshold of approximately 15-20 wt% CB content (Li et al. 2019).

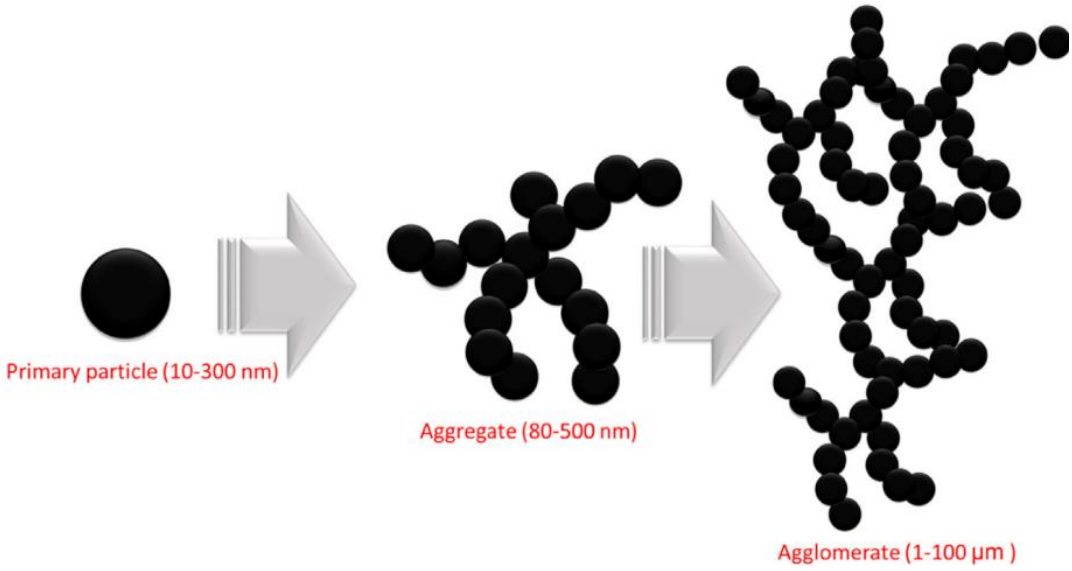

Figure 2.13. Illustration of carbon black agglomeration (Source: Kausar and Taherian 2018)

Carbon black is one of the fillers frequently used to make elastomers conductive (Choi et al. 2019; De Sarkar et al. 2022). Besides that, CBs can be used for many different purposes such as increasing material strength, UV stabilizer, coloring, and optical properties. For carbon black to show the desired properties in the matrix, it is very critical to distribute it homogeneously within the matrix, determine appropriate production techniques, and determine appropriate concentrations.

2.3.1.2. Graphite

Graphite is a carbon allotrope in crystal structure that can be found in nature or synthesized. It is the oldest known and most stable form of carbon (Saikam et al. 2023). It consists of parallel layers, one layer of which is called graphene, and these layers have a hexagonal structure (Figure 2.14) .

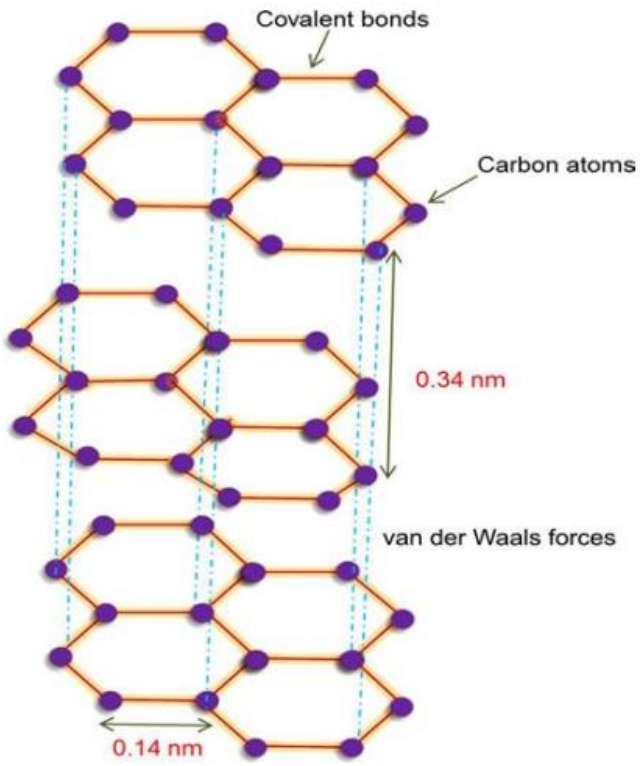

Figure 2.14. Structure of graphite (Source: Khan et al. 2016)

Graphite, which is anisotropic, has strong covalent bonds between carbon atoms in a layer, resulting in good thermal and electrical conductivity, but it shows lower thermal and electrical properties due to the weak van der Waals forces between layers (Chung 2002). One of the most important advantages of graphite is that it is abundant in nature and its cost is low (Andersen et al. 2021). Natural graphite is used in many different areas, such as pencils, lubricants, and refractoriness (Khan et al. 2016). One of the most important features of graphite is that it can be an exfoliation feature, thus it can be used

in many different applications such as electromagnetic shielding, electronics, and high thermal conductivity applications (Saikam et al. 2023).

2.3.1.3. Graphene

Graphene, a single layer of graphite, is a type of two-dimensional (sheet-like) nano-reinforcement. Due to its hexagonal structure, graphene has excellent properties like high thermal conductivity (5000 $Wm^{-1}K^{-1}$), good electrical conductivity, high surface area (2630 m^2g^{-1}), optical properties, and good mechanical features such as high modulus and stiffness (Bazylewski and Fanchini 2019; Papageorgiou, Kinloch, and Young 2017; Zhu et al. 2010) Graphene has different application technologies such as solar cells, transistors, composites, energy storage, textiles, and sensors (Mahmoudi, Wang, and Hahn 2018; Olabi et al. 2021; Razaq et al. 2022; Urban et al. 2020; Wei et al. 2021). In addition to this advantageous structure of graphene, it has been observed that it cannot achieve the expected performances as a result of studies conducted in the literature (Liu et al. 2010; Umar et al. 2023). Also, the hexagonal (2-dimensional) and semi-metallic (0-band gap) structure of graphene creates difficulties in its use in semiconductor technologies (Papageorgiou et al. 2017; Tiwari et al. 2018). Moreover, as given in Table 2.2, the cost of graphene limits its usage.

2.3.1.4. Carbon Nanotube

CNTs are one-dimensional (tubular) nanomaterials consisting of rolled sheets of graphene. Therefore, the mechanical, thermal, and electrical properties of CNTs are more advanced than graphite due to their structure (Martins-Júnior et al. 2013). CNTs are named according to the number of graphene layers. They are generally classified into multi-walled carbon nanotubes (MWCNT) and single-walled carbon nanotubes (SWCNT), as given in Figure 2.15 (Kaseem, Hamad, and Ko 2016).

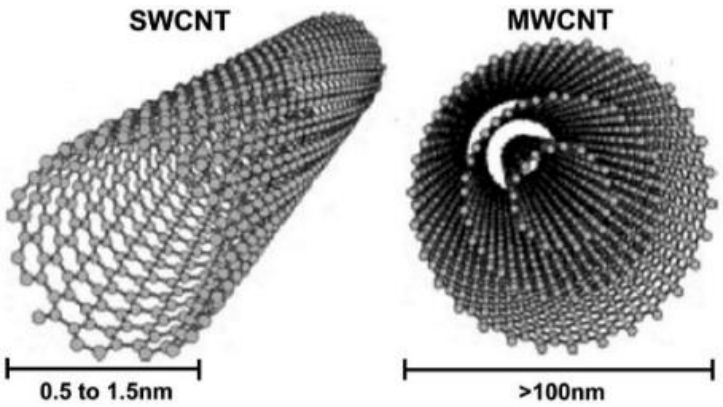

Figure 2.15. Structure and classification of CNTs (Source: Martins-Júnior et al. 2013)

CNTs are one of the prominent reinforcements for polymer matrix composites due to their outstanding thermal, mechanical, and electrical properties (Irshidat, Al-Saleh, and Al-Shoubaki 2015; Tarfaoui, Lafdi, and El Moumen 2016; Yuen et al. 2007). CNTs are also advantageous with their features such as low density, high strength, high surface area, flexibility, and chemical and thermal stability (Yuen et al. 2007). However, compared to graphite and carbon black, the high costs of CNTs are limited their use (Ali et al. 2019). Another challenge of CNT is the purification step required to remove metallic impurities (Kingston et al. 2004; Rahmat and Hubert 2011). Additionally, it is known that the environmental impacts of CNTs are 1-3 times higher compared to CB (Orozco et al. 2022).

2.4. Production Methods of Semiconductor Polymer Matrix Composites

In the development of semiconductor polymer matrix composites, determining the appropriate production technique is as important as selecting the appropriate matrix and reinforcement element. The effective use of conductive fillers is related to the homogeneous distribution of the filler in the matrix. Therefore, it is important to select the appropriate method. Three main techniques are used in the development of semiconductor composites; solution mixing, in-situ polymerization, and melt mixing (Liu et al. 2018; Pang et al. 2014). In the next section, details about the three techniques are given.

2.4.1. Solution Mixing

The solution mixing or solution blending method is a basic, economical, and effective fabrication method of PMCs. In the solution mixing process, the reinforcing element is dispersed in the appropriate solvent, which must be compatible with both phases (Takahashi et al. 2023). In the dispersion process, sonication or high-speed stirring is usually applied and then mixed with the polymer (Zhao et al. 2018). Subsequently, the solvent is evaporated from the system, usually during the mixing of the polymer and reinforcing material. By evaporating the solvent, the polymer chains can recombine and surround the nanofillers, thus forming conductive paths (Tang et al. 2019). The scheme illustrates the formation of conductive structures by the solution mixing method given in Figure 2.16. Solution mixing is generally more suitable for small-scale studies due to high solvent consumption (Sui et al. 2019; Tang et al. 2019).

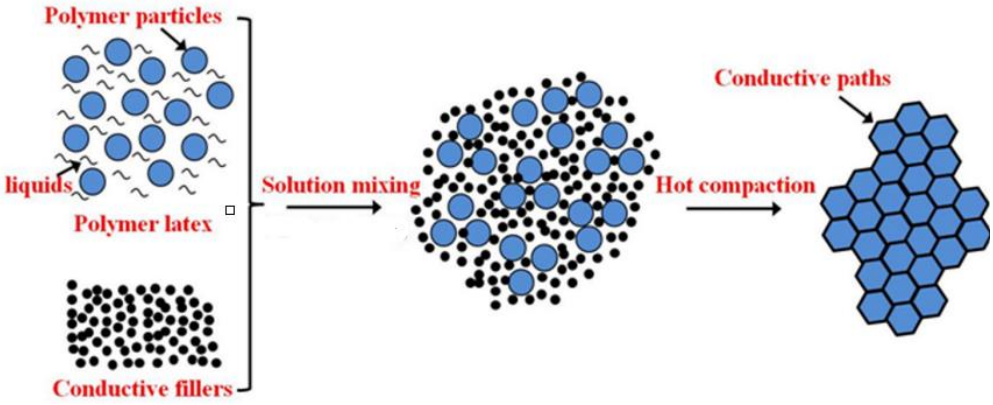

Figure 2.16. Illustration of solution mixing (Source: Li et al. 2019)

2.4.2. Melt Mixing

Melt mixing is another effective and common fabrication technique of PMCs. Melt mixing is generally preferred in large-scale manufacturing processes due to time, effectiveness, and economic reasons (Papageorgiou, Kinloch, and Young 2015). In the melt mixing method, high-shear mixing equipment such as a two or three-roll mill, single

or two-screw extruder, and ball milling is used (Pang et al. 2014; Tang et al. 2019). In the melt mixing process, viscous polymers are challenging. Increasing shear force or high temperatures can be applied to reduce viscosity. However, the increased shear force can damage the reinforcements, while high temperatures can damage polymers (Papageorgiou et al. 2015).

2.4.3. In-situ Polymerization

In-situ polymerization is another technique to produce PMCs. In this method, reinforcement materials are mixed with monomers/prepolymers in suitable solvents at appropriate temperatures, and in-situ polymerization is carried out (Shukla 2019; Tang et al. 2019). The schematic representation of in-situ polymerization is given in Figure 2.17.

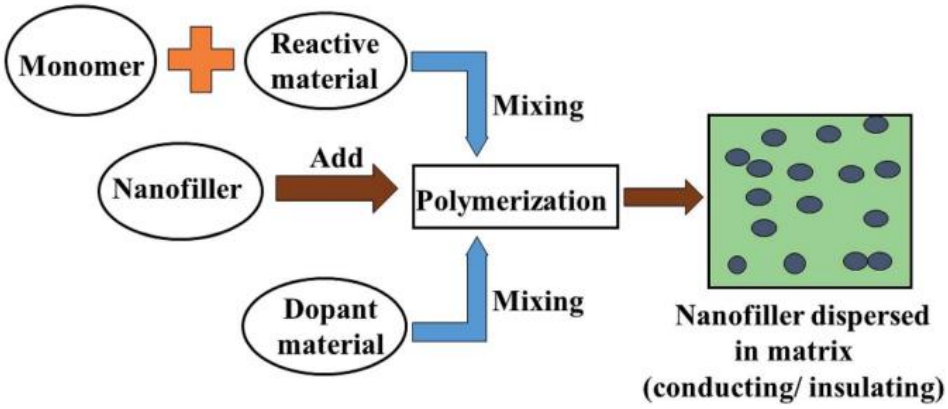

Figure 2.17. Illustration of in-situ polymerization (Source: Shukla 2019)

It has been successfully used in composites synthesized with multilayered carbon types such as graphene (Kim, Miura, and Macosko 2010; Lee et al. 2009; Papageorgiou et al. 2015; Paszkiewicz et al. 2014). However, the in-situ polymerization method is not widely used because it requires low polymer viscosity (Papageorgiou et al. 2015; Tang et al. 2019). Another important disadvantage of using this method in semiconductor composites is that it prevents the formation of conductive networks as a result of the binding of polymer chains to the filling materials (Papageorgiou et al. 2015).

2.5. Application Areas

Polymer matrix composites attract great attention from industry and researchers due to their excellent properties. One of the most important features of PMCs is that they can be developed for multiple purposes according to their intended use. With the development of technology, interest in semiconductor polymer matrix composites has increased, and different areas of use have emerged, as seen in Figure 2.18.

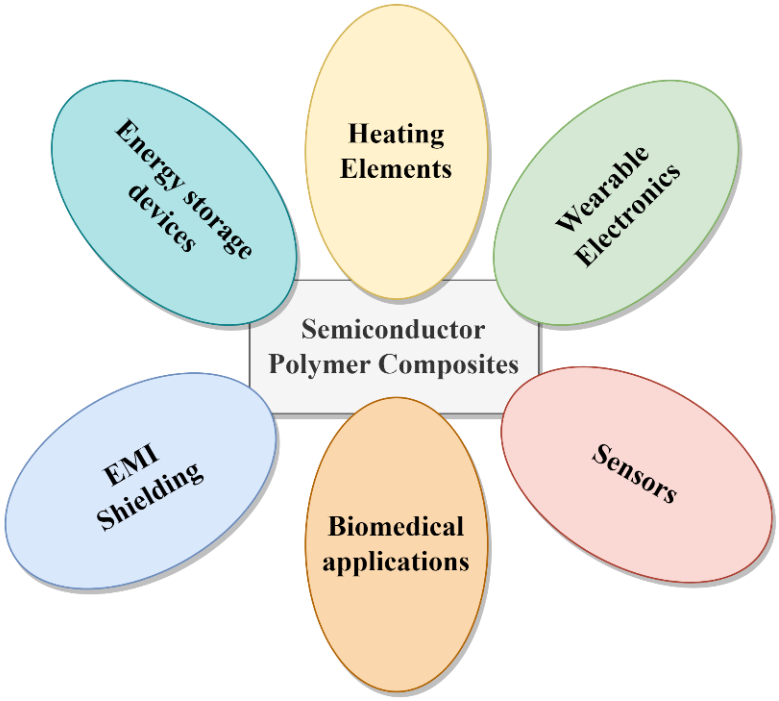

Figure 2.18. Application areas of semiconductor polymer composites

SPCs are commonly used for electromagnetic interference (EMI) shielding (Abbasi, Antunes, and Velasco 2019; Mondal et al. 2017), wearable electronic devices (Hong et al. 2015; Kim et al. 2018; Kong et al. 2014), and as heating purposes for thermotherapy, de-icing, underfloor heating, or devices used in areas such as aviation and maritime (Cheng et al. 2016; Park and Chu 2013; Sun et al. 2019; Yao, Hawkins, and Falzon 2018; Zhao et al. 2021).

CHAPTER 3

MATERIALS AND METHODS

3.1. Materials

The two types of carbon black used in the study were high-conductivity Printex XE2B and conductive Printex Kappa 70, which Orion Engineered Carbon supplied. XE2B is in bead form, with an average primary particle size of 30 nm and a BET surface area of 1000 m^2g^{-1}. Kappa 70 is in bead form with an average primary particle size of 19 nm and 245 m^2g^{-1}. natural graphite provided by Karabacak Madencilik for this study was with 85% purity and 200 mesh sizes. The polymer matrix polydimethylsiloxane (PDMS) used in this study was obtained from Dow Corning as Sylgard 184 Silicone Elastomer Kit (10:1). To ensure effective dispersion of CB in the matrix, different chemicals were used in their analytical standards, and no purification or other procedures were carried out. Methanol (Tekkim, %99.9), ethanol (Sigma Aldrich, %99.9), and n-hexane (Sigma Aldrich) were used as solvents. Surfactants such as anionic sodium dodecyl sulfate (Sigma Aldrich), cationic cetyltrimethylammonium bromide (CTAB/ Sigma Aldrich), nonionic Pluronic F-127 (Sigma Aldrich), and nonionic Triton X-100 (Sigma Aldrich) were used to improve the dispersibility of carbon blacks.

3.2. Methods

The general flow diagram of the study is given in Figure 3.1. In the method section, DLS and SEM analysis results were considered for solvent selection. Composite productions were repeated twice, and the results were presented with standard deviation values.

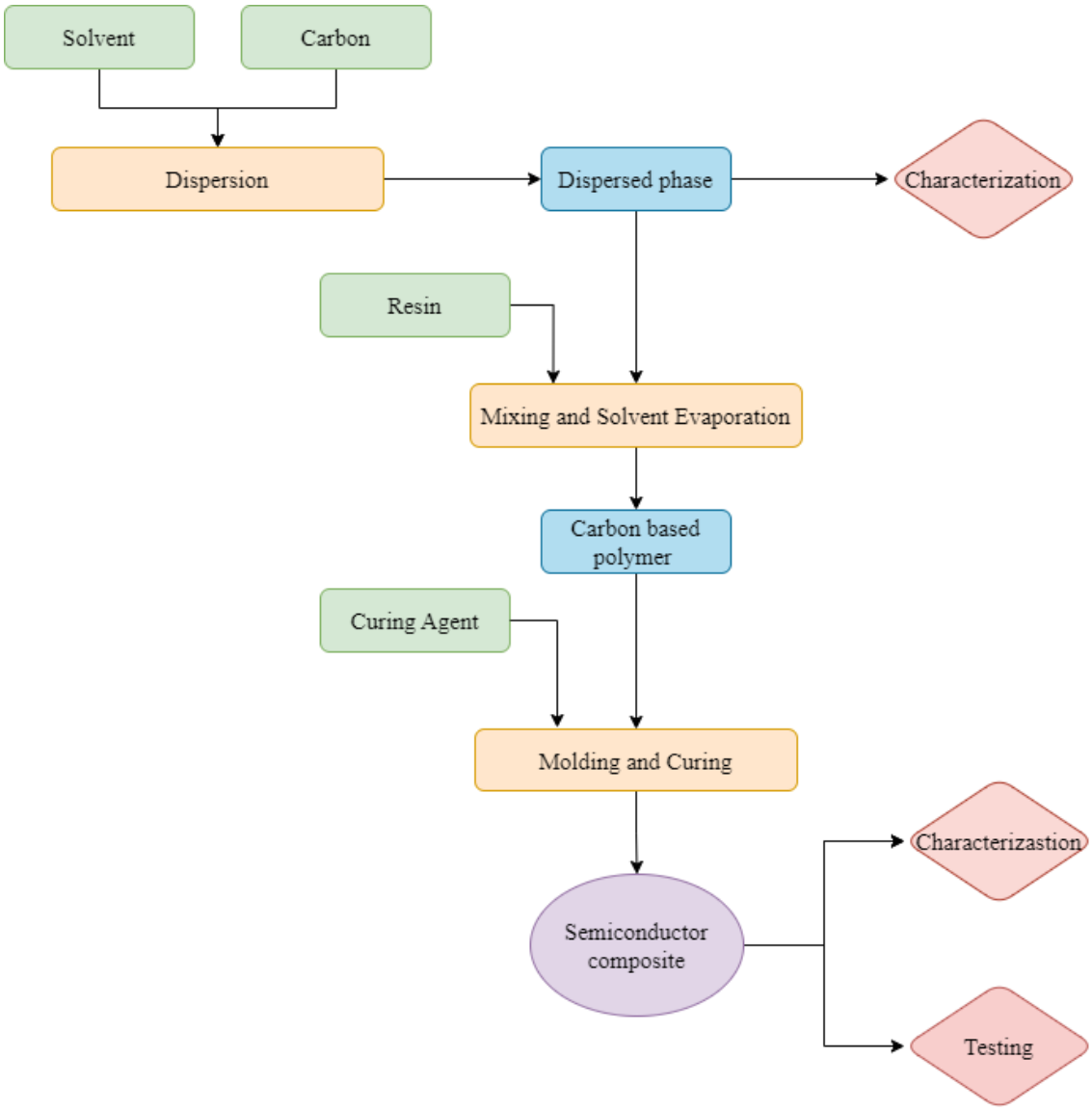

Figure 3.1. Flow diagram of the study

3.2.1. Dispersion Studies of Carbon

3.2.1.1. Effect of Solvent

In the study, three different carbons, which are Natural Graphite, Printex Kappa 70, and Printex XE2B, were dispersed in different solvents (n-hexane, methanol, and ethanol) by mechanical mixing and with and without ultrasonic treatment for better

understanding of dispersion techniques. The aim was to determine the most appropriate solvent selection for carbon dispersion in the polymer matrix.

All carbon blacks were prepared at 0.02 % in solvents. Solvent optimization was performed using characterization techniques. Then the effect of ultrasonic treatment was observed using Dynamic Light Scattering (DLS) measurements with a selected solvent (methanol) after 15 minutes of ultrasonic treatment and without ultrasonic treatment. Following the selection of the carbon dispersion technique, all types of carbon were dispersed in each solvent, and dispersion was analyzed using Scanning Electron Microscopy (SEM) and DLS.

3.2.1.2. Effect of Surfactants

Following solvent optimization, different surfactants, which are sodium dodecyl sulfate (SDS), Pluronic F-127, cetyltrimethylammonium bromide (CTAB), and Triton X-100, were used to improve the carbon dispersion. All surfactants were prepared 10^{-3} M concentrations in the optimized solvent. The carbon concentration in the surfactant-solvent mixture was prepared to be 0.1%. The effect of surfactants was examined using DLS.

3.2.2. Production of Carbon-Based Composites

The production of carbon-based semiconductor composites was carried out using the solution casting method. Experimental studies consist of three stages: i) dispersion of carbon with optimized solvent; ii) distribution of carbon in the resin and solvent evaporation; and iii) molding and curing process. The schematic representation of the experimental procedure is given in Figure 3.2.

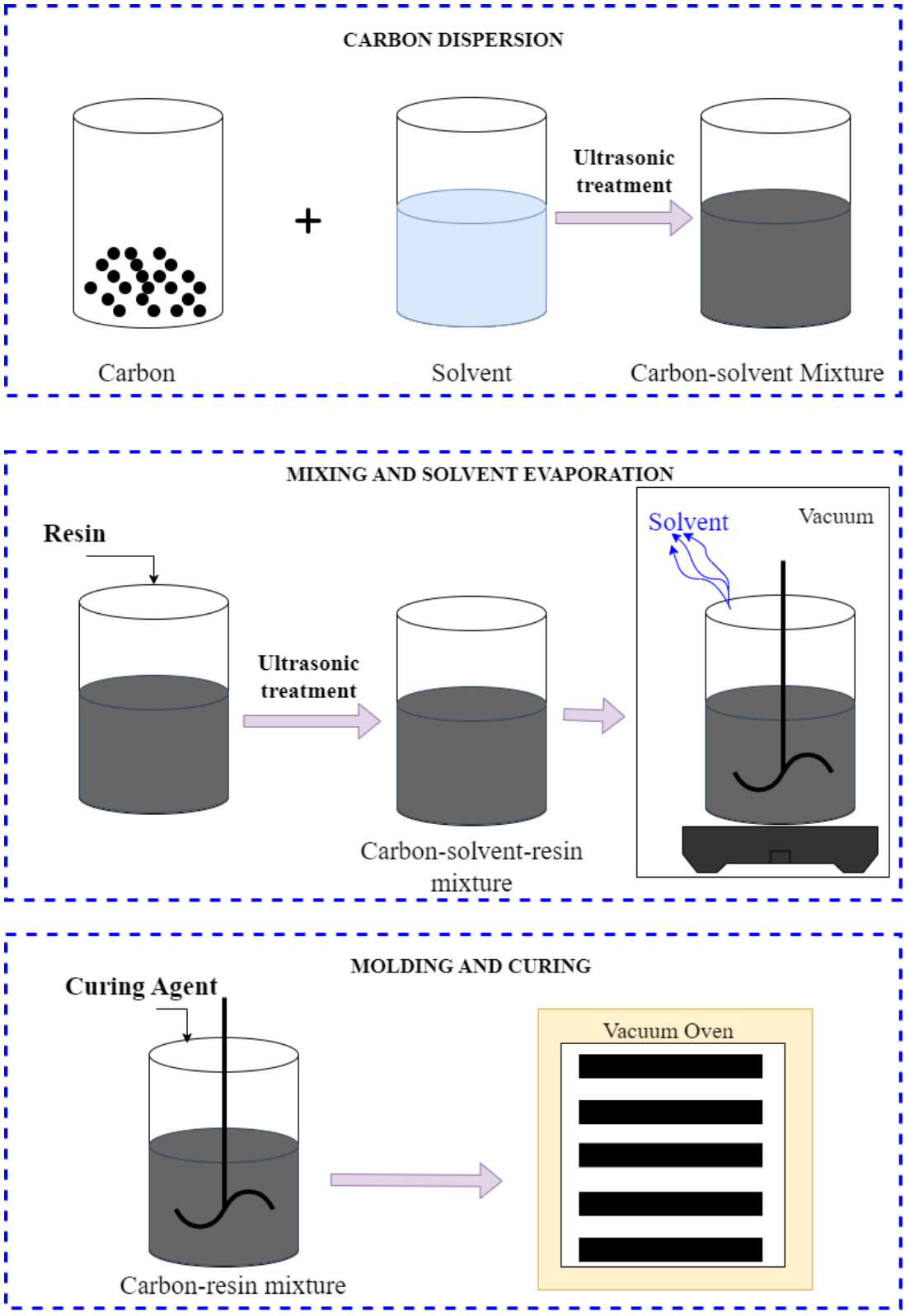

Figure 3.2. Experimental procedure

Following the solvent and carbon optimization, carbon-based composites were produced in Sylgard 184 resin at carbon weight percentages of 5%, 10%, 15%, 25%,

30%, and 35%. First, carbon was dispersed in a solvent with a 1:10 weight ratio by mechanical stirring. When necessary, carbon dispersion was achieved by adding a surfactant to the solvent to obtain a 10^{-3} M surfactant solution. Afterward, carbon-solvent mixtures were kept in an ultrasonic bath for 15 minutes to homogenize the solution. After sonication, the resin was added to the system and sonicated for 15 minutes. After the sonication, the carbon-solvent-resin mixture was stirred by mechanical stirring, and heat was applied to the system to remove all solvents before the curing agent was added. The removal of all solvents from the system was checked by weighing. After the removal of the solvent, the curing agent was added to the system and mixed with the carbon/resin mixture uniformly.

The carbon/resin/curing agent mixture was poured into the mold and a degassing process was applied to prevent bubble formation in the composites. Then the mold was cured in a vacuum oven at 100 ℃, for 30 minutes.

3.2.3. Characterization Methods for Carbon and Carbon-based Composites

In this study, different characterization techniques were used for carbon characterization and composite characterizations. Firstly, different carbon types were investigated with SEM, DLS, and FTIR analyses for morphological characterization, and BET analysis for surface area information. SEM and DLS analyses also were performed for carbon dispersion studies.

3.2.3.1. Scanning Electron Microscopy (SEM) Analysis

Scanning Electron Microscope (SEM) is an advanced imaging technique that scans the sample with focused electron beams and uses the signals from the materials to provide high-resolution images of the material surface. It is mainly used for the characterization of surface, topography, and composition of materials. The material to be

investigated must be completely dry and conductive. Therefore, the gold coating process must be applied to insulating materials before imaging.

In this study, SEM analyses were performed using the Philips XL-30S FEG device. SEM analysis was used for morphological analysis of carbons, dispersion studies, and observation of morphologies in composites. Since the carbonaceous materials used in the study have conductive properties, no gold coating was applied before the analysis of the samples. However, since carbon-free resin has insulating properties, gold plating was applied. The samples were examined in different regions and at different magnifications.

3.2.3.2. Brunauer-Emmett-Teller Analysis

Surface area is an important characteristic feature in determining the capacity of reinforcement elements. Brunauer-Emmett-Teller (BET) analysis is a common technique used to determine the specific surface area of solid materials (catalysts, nanoparticles, powders, etc.) using the principle of gas adsorption. Generally, nitrogen (N_2) was used for analysis. In this study, the Micromeritics Gemini V device was used for the characterization of each carbon and N_2 was used as an adsorptive gas.

3.2.3.3. Fourier Transform Infrared Spectroscopy

Fourier Transform Infrared Spectroscopy (FTIR) is an analytical method that uses infrared radiation (IR) and vibrations of molecules for structural, functional, and compositional characterization of the sample. The working principle of FTIR is based on converting the absorbed radiation into vibration energy by sending IR between 10000 cm^{-1} - 100 cm^{-1} to the material under examination. The signal obtained by the detector gives a spectrum from 4000 cm^{-1} to 400 cm^{-1}. The peaks that appear between these values represent the fingerprint of the material.

In this study, FTIR was used for structural characterization of each carbon. The Perkin Elmer UATR Two model was used for analysis and the carbons were characterized in powder form, without being pelletized with KBr.

3.2.3.4. Dynamic Light Scattering and Zeta Potential

Dynamic Light Scattering is an analytical method for determining the hydrodynamic size distribution of particles or molecules in a solvent. Fundamentally, the intensity and change of light scattered from particles are measured by detectors. The change in the intensity of the scattered light depends on the Brownian motion of the particles and the size of the particle is calculated using the Stokes-Einstein equation (Eq 3.1.). For zeta potential measurements, the device uses the Henry equation.

$$D = \frac{k_B T}{6\pi\eta R} \qquad Eq.\,3.1.$$

In the equation, the diffusion coefficient is represented by D, the Boltzmann constant by k_B, the viscosity of the solvent by η, the temperature by T, and the radius of the particle by R. In this study, Malvern Zeta Sizer Nano ZS is used for measuring particle size and zeta potential. For measuring particle size and zeta potential, dilute solutions were prepared. pH measurements were performed before zeta potential measurements.

3.2.3.5. Conductivity Analysis

The electrical conductivity of each carbon (XE2B, Kappa70, and Graphite) was investigated with the AZ 86031 conductivity probe. Measurements were performed by dispersing each carbon in the appropriate solvent at 0.5%, 2.5%, 5%, 10%, 20%, and 30%

by weight. Conductivity measurements of carbons were taken while the solutions were mixed.

The electrical resistivity of composites was measured with a Keithley 2400 SourceMeter with a two-point probe method. It is used for the measurement of current, voltage, and resistance. In the study, ten measurements were taken for each composite, and the average value was reported. Resistivity was calculated from the average resistance value of the composites. The length, width, and thickness have been measured to get resistivity from resistance. The formula, which is used for resistivity calculations, is given in Equation 3.2.

$$\rho = \frac{\mathrm{R} * W * t}{L} \qquad Eq.\,3.2.$$

where ρ (Ωm) is the resistivity of the sample, R (Ω) the resistance of the sample, W (m) is the width of the sample, t (m) is the thickness of the sample, and L (m) is the length of the sample. The resistivity data is used to calculate the electrical conductivity of the sample by using Equation 3.3.

$$\sigma = \frac{1}{\rho} \qquad Eq.\,3.3.$$

where σ (S/m) is the conductivity of the sample.

3.2.3.6. Thermogravimetric Analysis

Thermogravimetric analysis (TGA) analysis is to examine the change in weight of a material under an inert atmosphere depending on controlled time or temperature

(Loganathan et al. 2017). TGA provides information such as thermal stability, moisture content, volatile substance, reaction kinetics, and purity.

In this study, thermogravimetric analysis was carried out using the Perkin Elmer Diomant TG/DTA device to observe the thermal degradation behavior of composite materials produced at different carbon concentrations. Approximately 10 mg of each composite sample were prepared for the TGA analysis. Thermogravimetric analysis was carried out in an N_2 atmosphere up to 850 ℃ with a temperature increase of 10 ℃/min.

3.2.3.7. Contact Angle Measurements

Contact angle measurement is an elementary method to investigate the surface characteristics of materials, especially wettability. The wettability of a material is determined by observing the intermolecular interactions between water droplets and the surface. The contact angle of the material is measured by drawing tangent lines of the water droplet dropped on the surface, as shown in Figure 3.3.

The angle formed by drawing the tangent line to the water droplet gives information about the wettability of the surface. The fact that the angle given by the tangent curve is less than 90º indicates that the surface is a wettable surface, which is also called a hydrophilic surface. Angles greater than 90° indicate that the surface is poor wetting, that is, a hydrophobic surface.

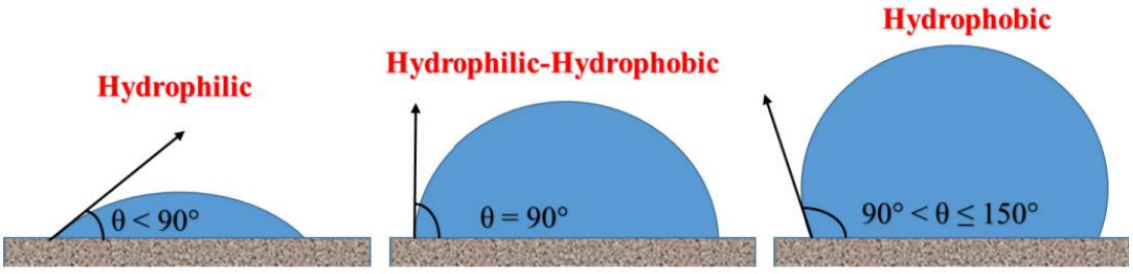

Figure 3.3. Representative image of contact angle measurements (Source: Doshi, Sillanpää, and Kalliola 2018)

In this study, contact angles of resin (Sylgard 184) and composite films with different carbon percentages were investigated with the Krüss Contact Angle Measurement System G10 device. The goniometer, LED light source, camera & zoom lens, and sample holder are the basic parts of the device. Before the measurements, all surfaces are cleaned with ethanol. All measurements were performed on the back surface of the composites to use the smooth surface. Measurements were made by dropping water drops onto the prepared surfaces. For each sample, measurements were made by taking 20 measurements from different points. A representative image of the sample is given in Figure 3.4.

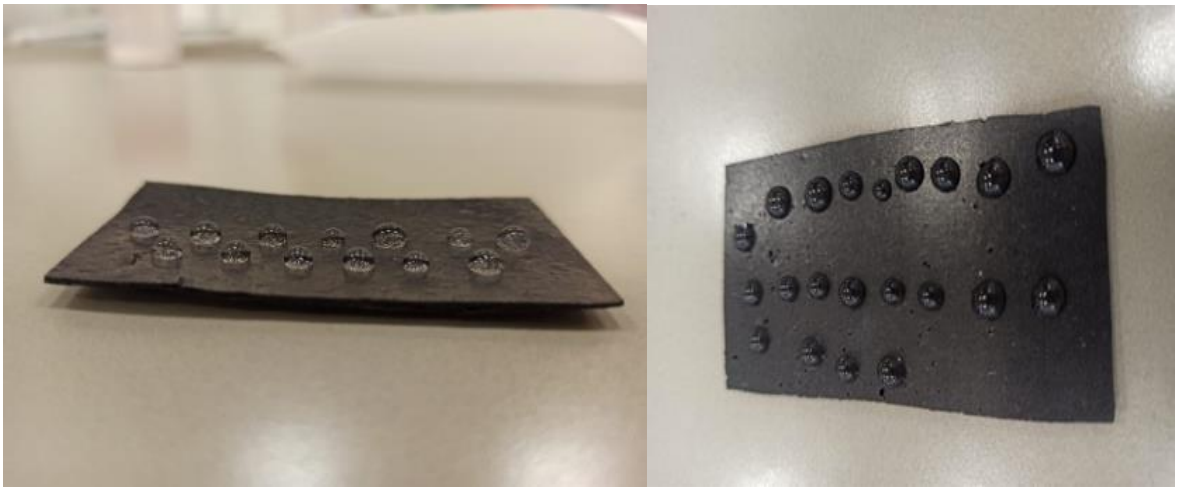

Figure 3.4. A representative image of the water droplets on the sample

The work of adhesion is an important concept used for solid-liquid interactions. The work of adhesion between solid and liquid is calculated from the following equations: Young's equation (Eq. 3.4.) and Dupré equation (Eq. 3.5). The representative image of Young's equation is given in Figure 3.5.

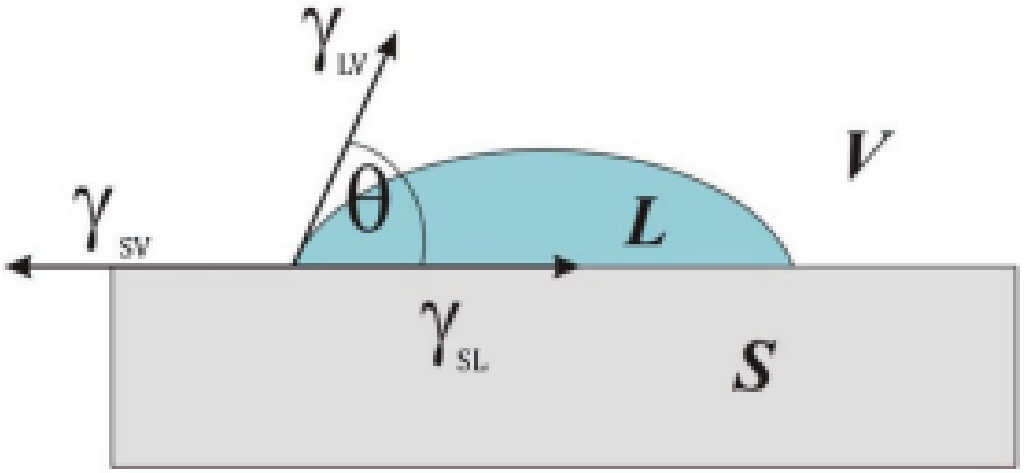

Figure 3.5. Illustration of Young's equation (Source: Altay et al. 2020)

$$\gamma_S = \gamma_{SL} + \gamma_L cos\theta \qquad Eq.3.4.$$

where,

γ_S is the solid-vapor surface free energy,

γ_{SL} is the solid-liquid interfacial free energy,

γ_L is the liquid surface free energy

$\theta$is the contact angle of the liquid on the surface.

$$\gamma_S + \gamma_L = W_{SL} + \gamma_{SL} \qquad Eq.3.5.$$

From Eq. 3.4. and Eq. 3.5., Eq. 3.6. is obtained as Young-Dupré equation, which gives the work of adhesion between solid and liquid (Tadmor et al. 2017).

$$W_{SL} = \gamma_L(1 + cos\theta) \qquad Eq.3.6.$$

3.2.3.8. Surface Free Energy Calculations: Fowkes Theory

Examining the physicochemical properties of a developed product contributes to the development and better understanding of the material. Surface characteristics (hydrophobicity/hydrophilicity) and surface free energy (SFE) are two important parameters used in material characterization. The total surface energy of solids and liquids depends on different types of molecular interactions, such as dispersive, polar, and acid/base interactions, and is considered the sum of these independent components.

There are five different approaches to calculating the SFE of solids using the contact angle measurement results: namely i)Fowkes method (Fowkes 1964), ii) Owens-Wendt method (Owens and Wendt 1969), iii)Van Oss-Chaudhury-Good method (Van Oss, Good, and Chaudhury 1986), iv) Zissman method (Fox and Zisman 1952), and v) Neumann method (Neumann et al. 1974). Most of these approaches start with Equation 3.6, which is known as Young-Dupré's equation (Altay et al. 2020; Young 1805). Different theories differ in several regards, such as derivation and convention, but most importantly they differ in the number of components or parameters which they are equipped to analyze. Some theories account for more of these phenomena than do other theories. These distinctions are to be considered when deciding which method is appropriate for the experiment at hand.

In this study, Fowkes theory was used, which is derived from the combination of Young's relation, which relates the contact angle to the surface energies of the solid and the liquid, and the surface tension and, therefore, to the polar and dispersive components of the surface energy. In the Fowkes theory, surface energy associated with the sum of these the dispersive (γ^D) and the non-dispersive (γ^{nD}) parts as given in Eq. 3.7. Fowkes theory is expressed in terms of the work of adhesion is given in Eq. 3.8.

$$\gamma_S = {\gamma_s}^D + {\gamma_s}^{nD} \qquad Eq.3.7.$$

$$W_{SL} = 2\left(\sqrt{\gamma_L^D.\gamma_s^D} + \sqrt{\gamma_L^{nD}.\gamma_s^{nD}}\right) \qquad Eq.3.8.$$

The geometric mean interprets the interactions of polar and dispersive compounds. By combining Eq. 3.6. and Eq. 3.8., the Fowkes equation which includes solid and liquid interactions with surface tension and contact angle is given in Eq. 3.9. (Fowkes 1964).

$$\left(\sqrt{\gamma_L^D.\gamma_s^D}+\sqrt{\gamma_L^{nD}.\gamma_s^{nD}}\right)=\frac{\gamma_L(1+cos\theta)}{2} \qquad Eq.\,3.9.$$

In order to calculate surface energy from Fowkes theory, it is necessary to measure the contact angle of completely dispersive liquid, which means $\gamma_L^{nD}=0$ and $\gamma_L=\gamma_L^D$, thus giving the Eq. 3.10. For this purpose, generally diiodomethane is used, since there is no polar component; $\gamma_L=\gamma_L^D=50.8\,mN/m$ (Jańczuk and Białłopiotrowicz 1989).

$$\gamma_S^D=\frac{\gamma_L(1+cos\theta)^2}{4} \qquad Eq.\,3.10.$$

Subsequently, measuring the contact angle for a liquid, which has dispersant and non-dispersant components comes. Water is generally used for this purpose, with $\gamma_L^{nD}=51.0\,mN/m$ and $\gamma_L^D=21.8\,mN/m$ (Jańczuk and Białłopiotrowicz 1989).

3.2.4. Testing of Composite Films

This study applied mechanical and thermal performance tests to examine the manufactured composites. The temperature performances of the manufactured composites were investigated under different voltages at different times. Mechanical characterization of the composites was carried out using tensile and tear tests according to the American Society for Testing and Materials (ASTM) standards. These tests will be discussed in the following paragraphs.

3.2.4.1. Temperature-Control Tests

Temperature-control tests of composites with different carbon concentrations were carried out using a Uni-t UDP6721 DC power supply, a Uni-t UTi721M model thermal camera, and a stopwatch as given in Figure 3.6.

For the tests, conductive copper tapes were applied to the edges of each composite sample to transmit energy, as seen in Figure 3.7. Tests were conducted under different voltages (5V, 10V, 15V, 20V, 24V, and 30V) for a minimum of 5 minutes each. Temperature analyses were carried out by taking measurements from three selected points along the middle surface of the samples, keeping the camera and points constant.

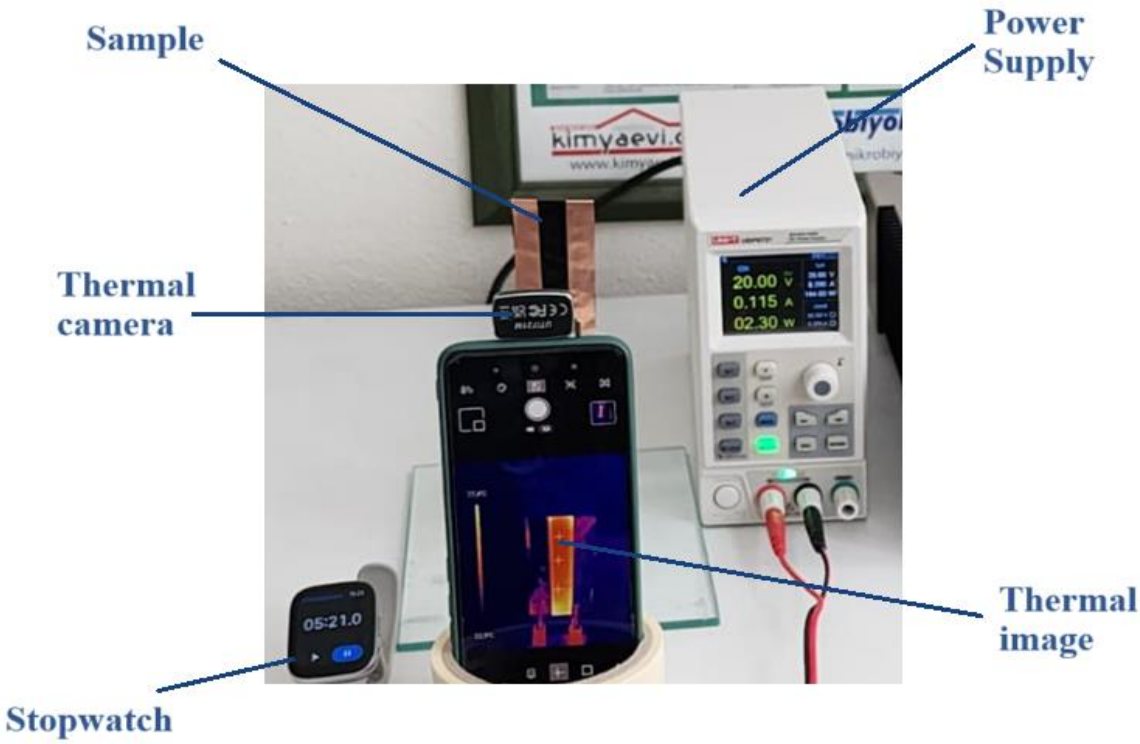

Figure 3.6. Thermal performance test setup

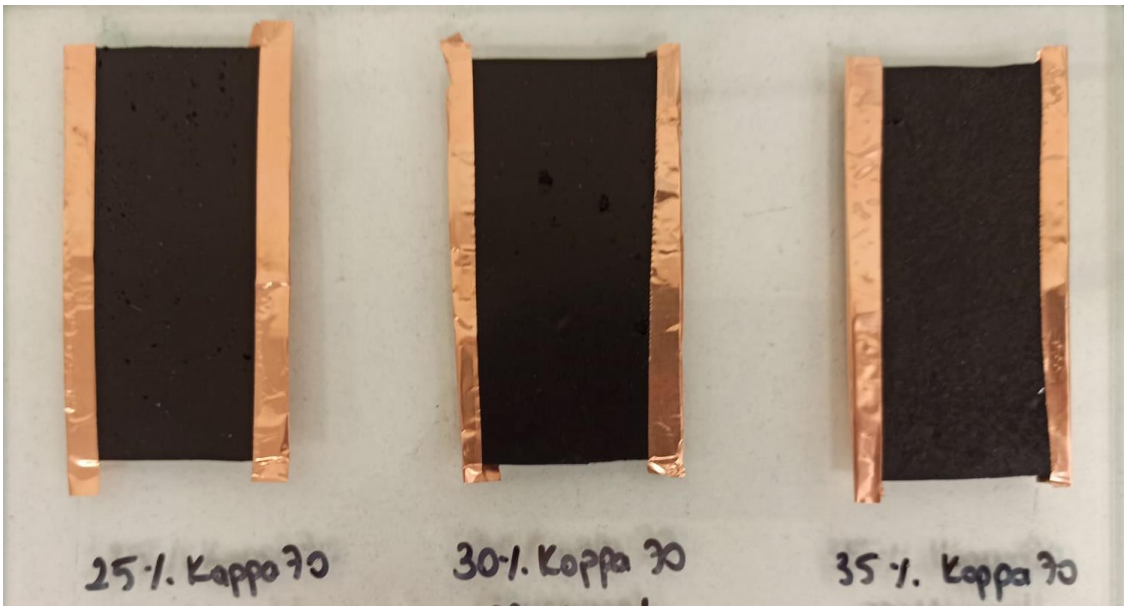

Figure 3.7. Composite samples for temperature-control tests

3.2.4.2. Mechanical Tests

Tensile and tear tests were performed for the mechanical characterization of the composites. The carbon/resin ratio with the best temperature performance was selected as the test sample. The selected composite sample was produced with dimensions of 15x15 cm and a thickness of 2 mm (Figure 3.8. a). The same procedure was applied to PDMS resin. Both tests were performed by the universal testing machine (Shimadzu AG-IC device).

ASTM D412 Type-C standard was used for the tensile strength test, and 8cm length dumbbell shape samples were cut from the 15x15 cm sample under the ASTM standard. Three test specimens were prepared for the tensile strength test (Figure 3.8. b). For tensile test measurements, firstly, the bottom and top of the composite samples were marked with white pencils, and the white areas were marked with black pencils. The extension between these two black dots was examined using a video extensometer and data monitoring software program.

The tear strength test was performed according to ASTM D 624 Type-T standard and three test specimens were prepared (Figure 3.8. c). Before the tear strength test, 4 cm preliminary cuts were made right in the middle of the samples. The tests were started by

placing each of the cut-out pieces on the upper and lower jaw as given in Figure 3.9. The test was continued until a tear occurred in the uncut area. The tear strength of the composites was calculated using Equation 3.11.

$$T = \frac{F}{t} \qquad Eq.3.11.$$

where, T defines the tear strength force per unit thickness, F defines applied force and t defines the sample thickness.

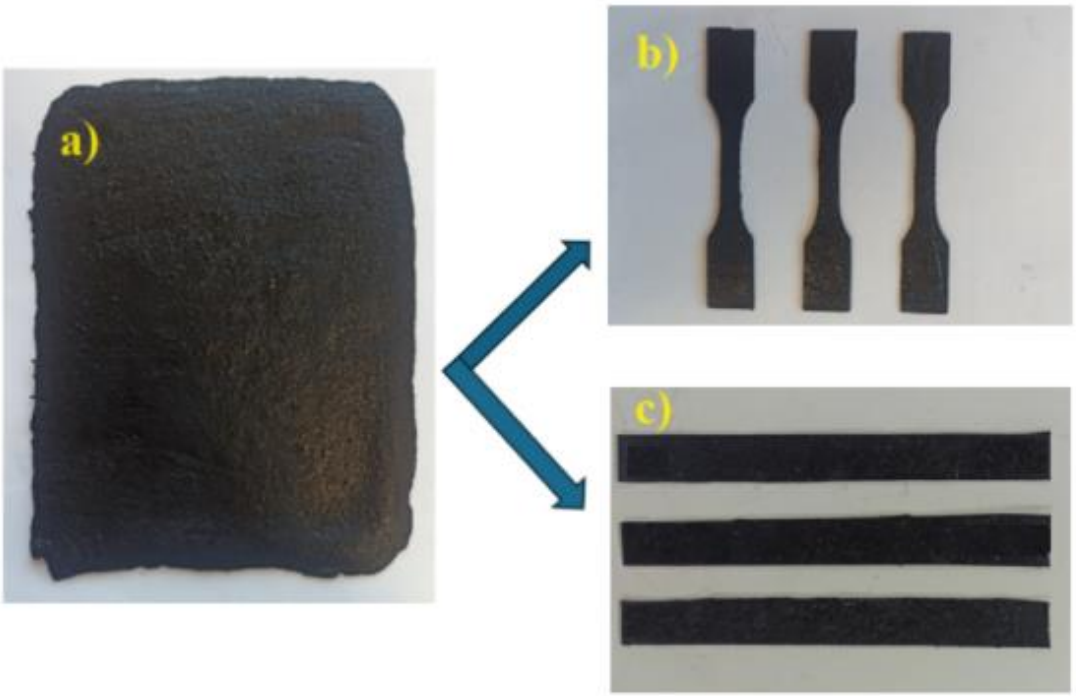

Figure 3.8. Mechanical test samples a) 15x15 cm sample b) Tensile test sample c) Tear test sample

Figure 3.9. Tear strength test placement

CHAPTER 4

RESULTS AND DISCUSSION

4.1. Characterization of Carbon Samples

In this study, different types of carbons were investigated with various characterization techniques and testing methods to select one of the samples to prepare composites. Morphological characterization of carbon was performed using SEM, size distribution and zeta potential measurements (DLS), structural analyses using FTIR, and surface area analysis using BET.

4.1.1. Scanning Electron Microscopy Analysis

SEM images of carbons, Kappa 70, XE2B, and natural graphite in powder form were obtained and are given in Figure 4.1, respectively. As expected, both carbon blacks have spherical forms, and the mean primary particle sizes are approximately 30 nm. However, the particles look strongly agglomerated and one shouldn't not use these particles as 30 nm. In the case of natural graphite, on the other hand, the structure is in a laminar form and micron size.

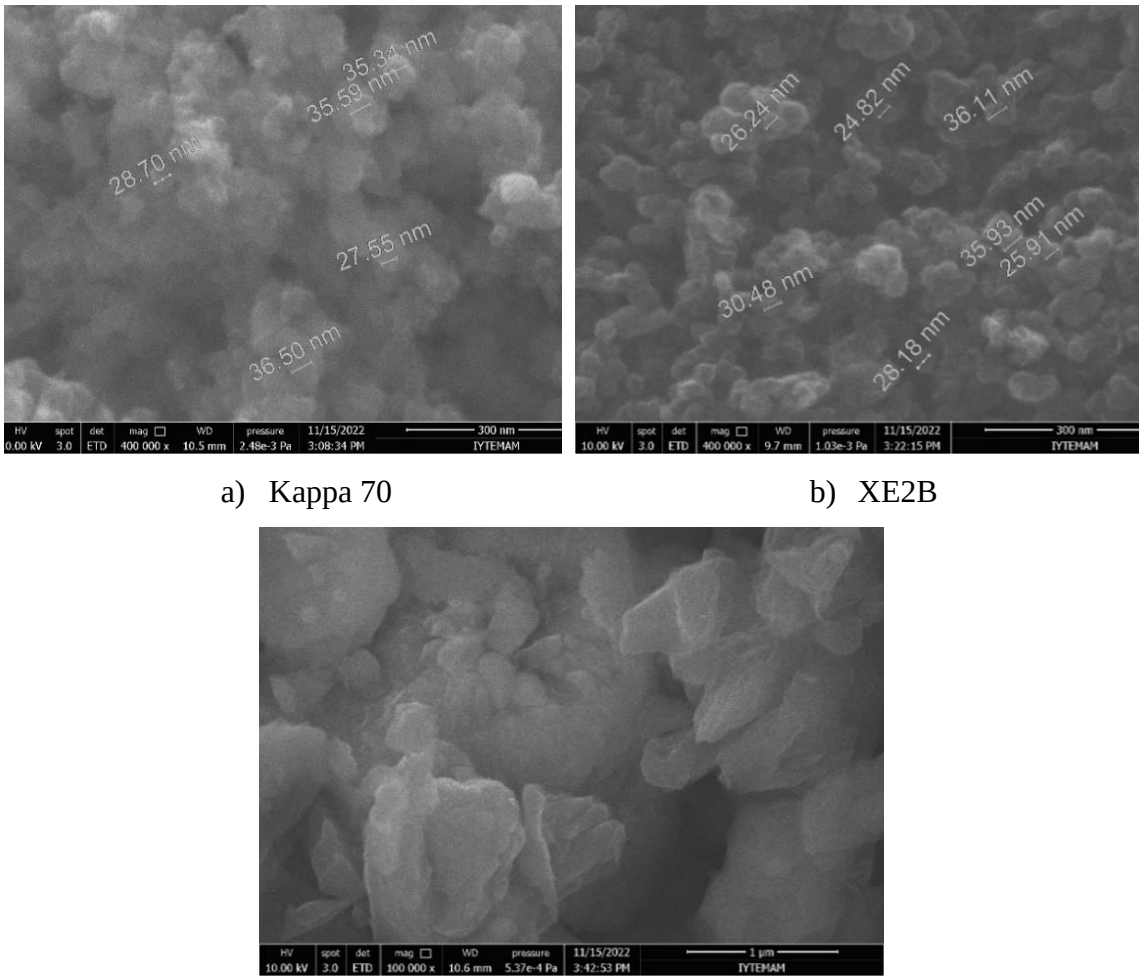

a) Kappa 70 b) XE2B

c) Natural Graphite

Figure 4.1. SEM images of a) Kappa 70, b) XE2B, and c) Natural Graphite

4.1.2. Fourier Transform Infrared Analysis

The FTIR Spectra of Natural Graphite, Kappa 70, and XE2B are given in Figure 4.2. The FTIR spectra of each carbon look similar since CB is a kind of graphite powder and parallel to the literature (Alam et al. 2014). The band around 3200-3550 cm^{-1} is described as O-H stretching of the hydroxyl groups (Sugatri et al. 2018). It is seen that there are many peak bands around 1000-2000 cm^{-1} in both carbon blacks, due to their molecular structures and functional groups like carbonyl and carboxyl groups (Figueroa Ramírez and Miranda-Hernánde 2012). The band around 1700-1720 cm^{-1} can be associated with the carbocyclic acid group (Alam et al. 2014). The aromatic C=C bond with the oxygen atom close to one of the vibrating C atoms is stretched asymmetrically

producing a peak at around 1400-1500 cm^{-1} (Hauptman et al. 2011). Asymmetric stretching vibrations of CO_2 are seen in the band at approximately 2300 cm^{-1} and can be associated with the porous structure of carbon black (González-González et al. 2020).

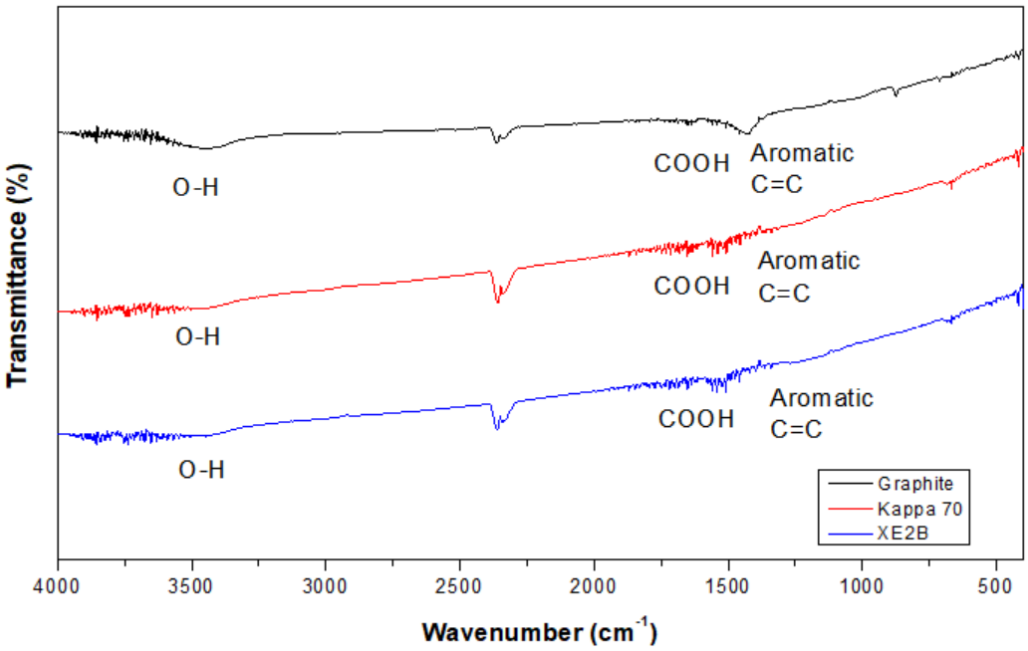

Figure 4.2. FTIR spectra of Graphite, Kappa 70 and Printex XE2B

4.1.4. Brunauer-Emmett-Teller Analysis

BET analyses of natural graphite, Kappa 70, and XE2B were presented in Table 4.1. It is seen that the surface area of carbon XE2B is large (1073.8 m^2/g) compared to graphite and other carbon. Therefore, this carbon should not be selected because of the possibility that this large surface area may cause agglomeration during the synthesis of composite structures. The surface area of graphite, on the other hand, was too low. According to BET analysis results, the homogeneous distribution of Kappa 70 in the polymer matrix was evaluated as more suitable than other carbons.

Table 4.1. BET surface area of carbons

CARBON TYPE	BET SURFACE AREA (m^2/g)
Graphite	2.9
Kappa 70	224.3
XE2B	1073. 8

4.1.4. Conductivity Measurements

In order to better understand the electrical conductivity performances of the carbons to be used in the study, conductivity analyses of each carbon in appropriate solvents were carried out using an AZ 86031 model probe. 0.5%, 2.5%, 5%, 10%, 15%, 20%, and 30% carbon by weight were dispersed in the solvent with the help of an ultrasonic bath, and conductivity measurements were performed while the solutions were mixed. The electrical conductivity values of each carbon in response to varying concentrations are given in Table 4.2.

Table 4.2 shows that the electrical conductivity of graphite is much lower than both carbon blacks. Up to 5% concentration, the electrical conductivity of Kappa70 was observed to be approximately twice that of XE2B carbon black. XE2B achieved the highest conductivity value at 10% concentration. However, since XE2B could not be dispersed at concentrations higher than 10%, conductivity measurements could not be taken. This is due to the high surface area that XE2B has, as mentioned in section 4.1.3. It was observed that Kappa70 reached the highest conductivity value with 12.05 mS at 20% concentration.

According to the characterization results, it was evaluated that kappa70 carbon black came to the fore in terms of usability in semiconductor composites. However, in the next section, dispersion studies of all carbon types in different solvents will be carried out and their use in composite production will be determined.

Table 4.2. Conductivity measurements of carbons according to varying concentrations

Concentration	Graphite	Kappa70	XE2B
0.5 %	66.0 µS	43.7 µS	20.04 µS
2.5 %	125.8 µS	334.0 µS	199.9 µS
5. 0 %	166.7 µS	1344.0 µS	694 µS
10.0 %	291.0 µS	5.63 mS	6.82 mS
15.0 %	376.0 µS	10.24 mS	-
20.0 %	506.0 µS	12.05 mS	-
30.0 %	721.0 µS	-	-

4.2. Carbon Dispersion in Different Solvents

Since the homogeneous and uniform distribution of carbons in composite materials will directly affect the conductivity performance, therefore the heating performance, the dispersion of carbon was studied. These studies were conducted under different conditions, as will be discussed in the following paragraphs. The details of the methods applied are given in Chapter 3, in the Methods section. Samples were prepared with and without ultrasonic treatment. First of all, the effects of ultrasonic treatment were observed. For this reason, some amount of carbon (Kappa 70) was dispersed in methanol with and without ultrasonic treatment and analyzed by DLS, and the results are presented in Figure 4.3.

It is seen that the effect of ultrasonic treatment is significant. The average particle size was around 700 nm when there was no ultrasonic treatment and around 200 nm when there was an ultrasonic treatment. Therefore, it was decided to apply an ultrasonic treatment for carbon dispersion in the composite production process.

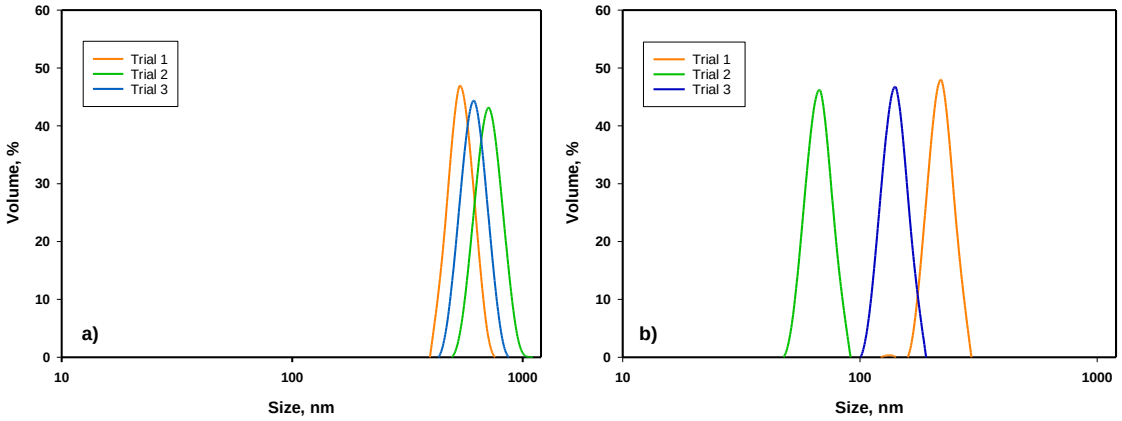

Figure 4.3. Effect of ultrasonic treatment of 0.02% Kappa70 in methanol: a)without sonication, b)with sonication

4.2.1. Effect of Solvent Type

The selection of solvent is very critical for carbon dispersion. Therefore, in this study, different solvents were tested for each carbon black and graphite dispersion. The solvents tested were ethanol, methanol, and hexane (Borah, Rajitha, and Dash 2018; Chen et al. 2010; Ghanbari and Ehsani 2018; Yan and Jeong 2014). The same amount of carbon samples was dispersed in these solvents using mechanical mixing and sonication for 15 minutes. Then, the dispersion behavior of carbon samples was characterized using DLS and SEM.

The DLS size distributions and SEM images of dispersed particles were presented in Figures 4.4, 4.5, and 4.6 for Printex XE2B, Kappa 70, and natural graphite, respectively. It can be seen that the smallest particle size distribution obtained from the DLS results is methanol, n-hexane, and ethanol for both carbon blacks, respectively, while it is n-hexane, methanol, and ethanol for graphite, respectively. However, only DLS results are not sufficient to make this interpretation, because it has been observed that the settling of carbons is within a few minutes in all solvents during analysis. Therefore, carbon distribution needs to be examined with a different technique such as SEM. In the study, SEM analyses were performed to support DLS results. SEM images, on the other hand, show not much difference between ethanol and methanol dispersions for all carbon

types. In the case of hexane, it was observed that particles show a fume structure for both carbon blacks not for graphite dispersions.

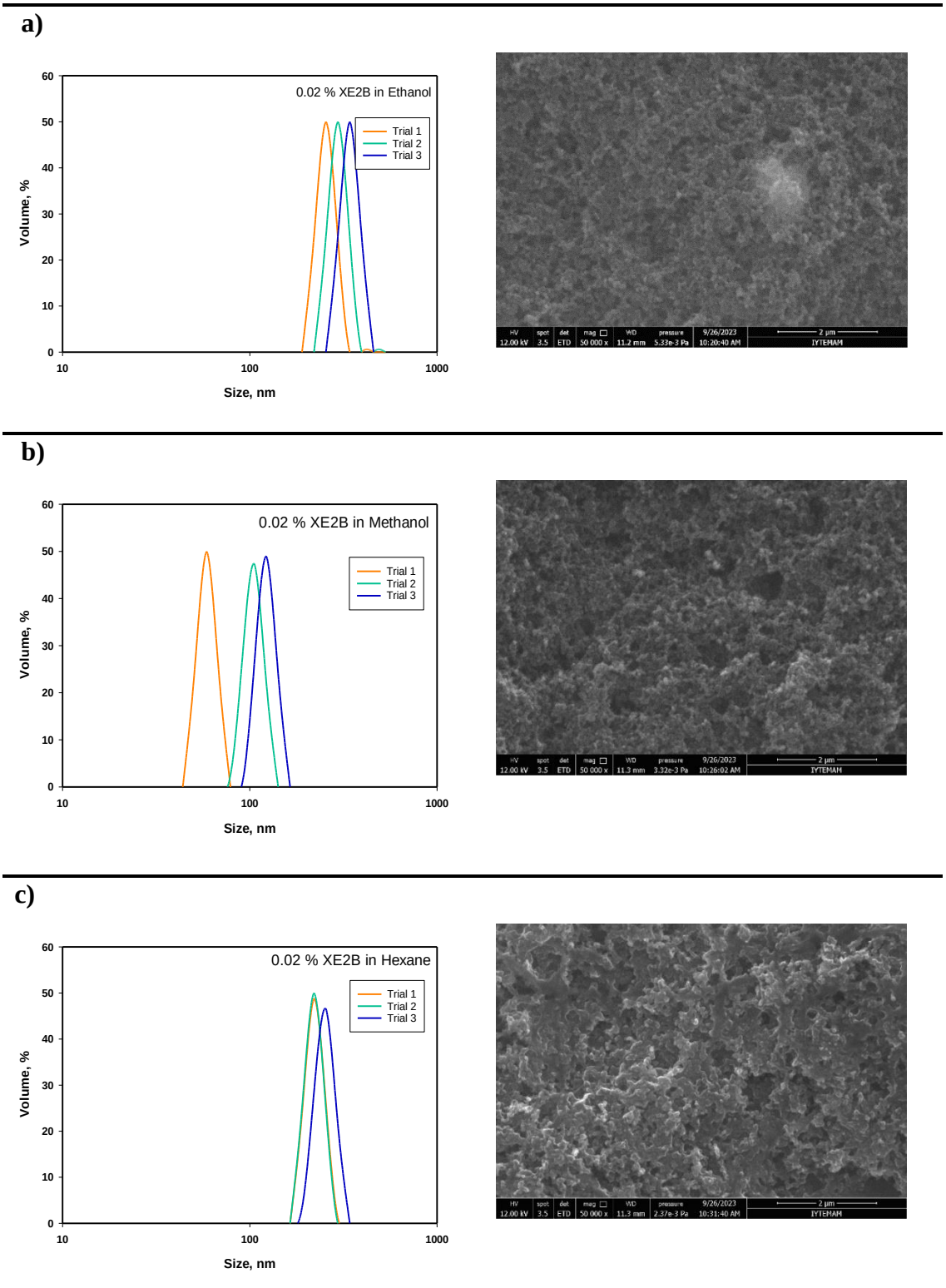

Figure 4.4. Dispersion studies of Printex XE2B in a) ethanol, b) methanol, and c)hexane

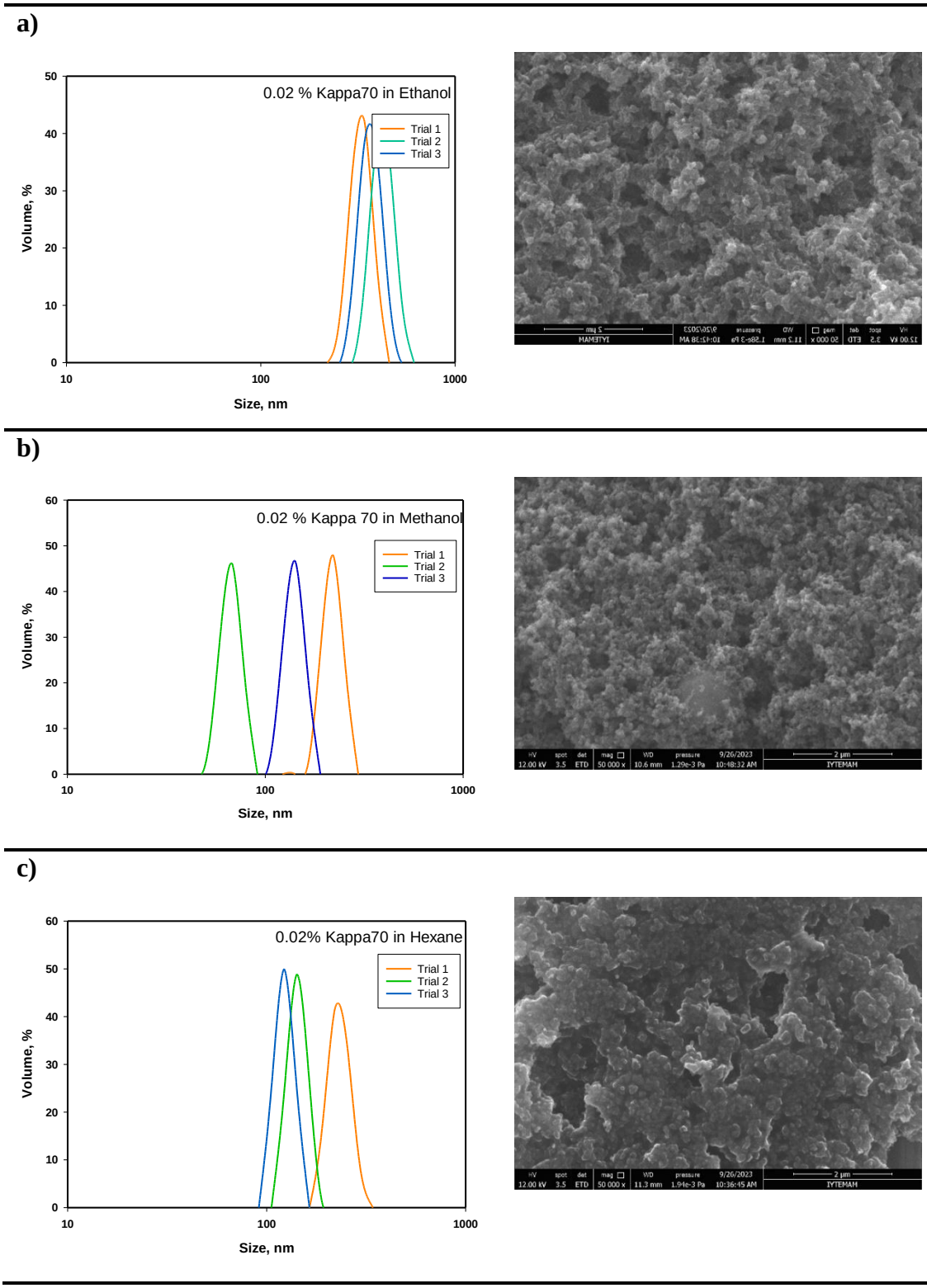

Figure 4.5. Dispersion studies of Printex Kappa 70 in a) ethanol, b) methanol, and c)hexane

a)

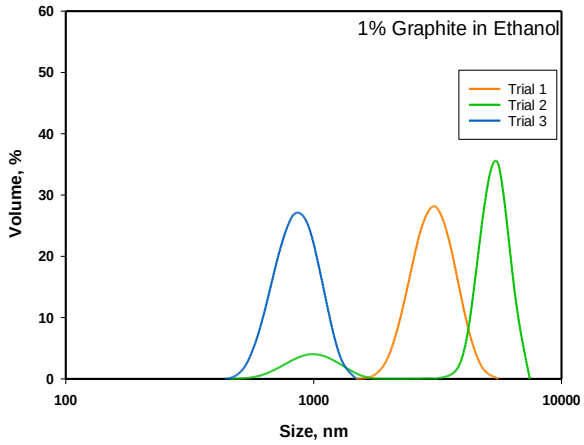

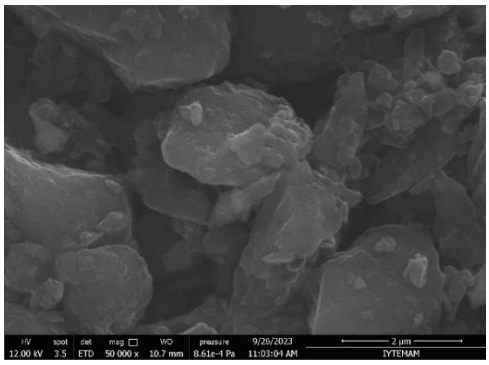

b)

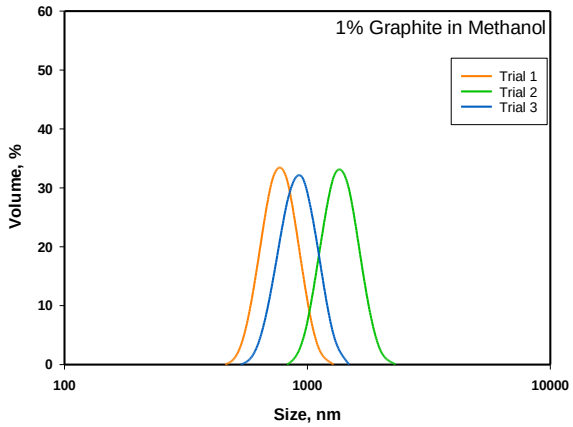

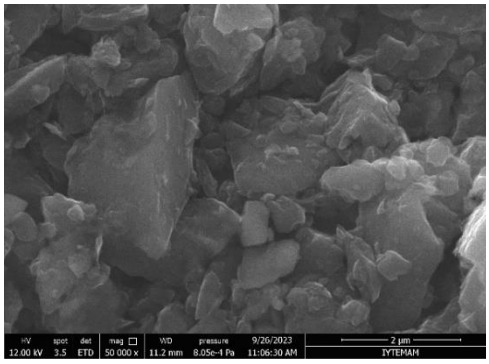

c)

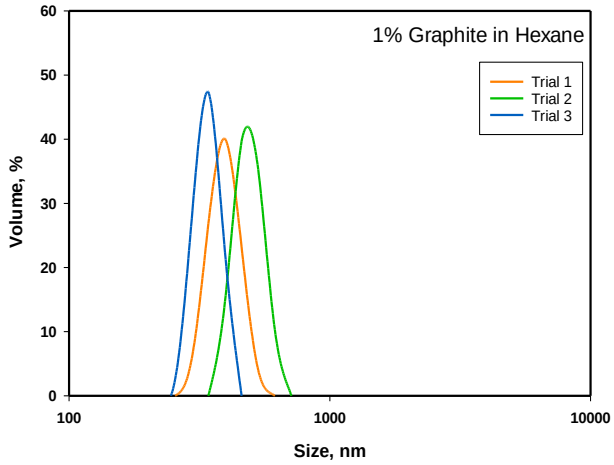

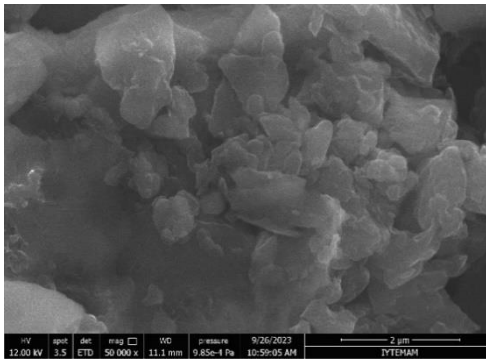

Figure 4.6. Dispersion studies of Graphite in a) ethanol, b) methanol, and c)hexane

Based on these dispersion studies of carbon, methanol was chosen as the solvent for the rest of the study. In addition, the fact that methanol has the lowest boiling temperature has been considered an advantage in the composite production process. The zeta potential of selected carbon black (Kappa 70) and methanol solution was also examined, and given in Figure 4.7.

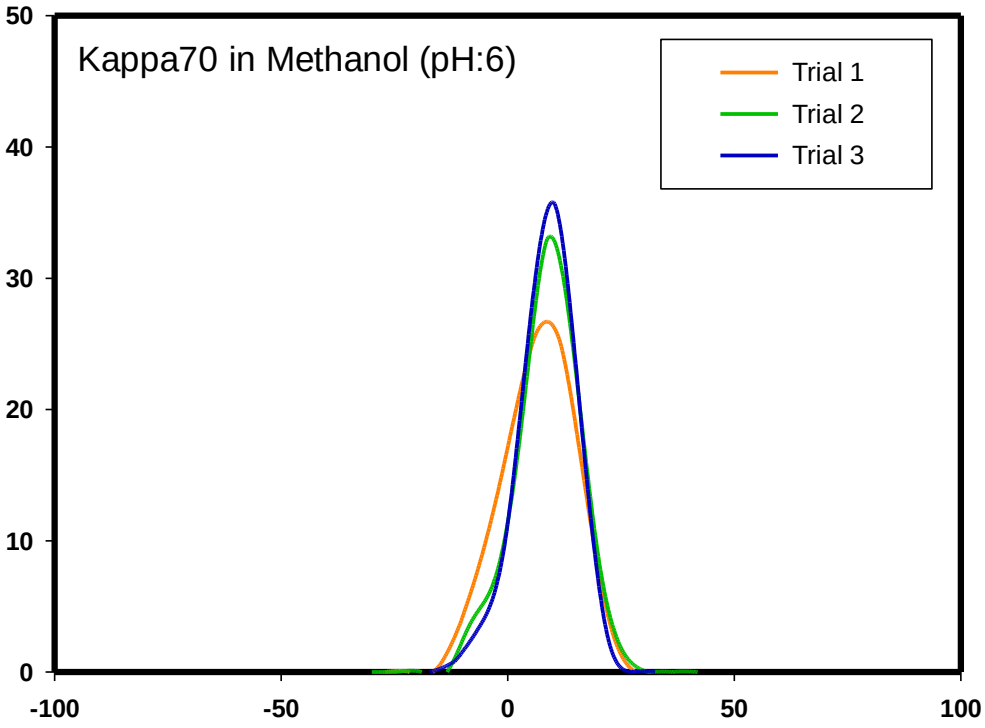

Figure 4.7. Zeta potential of Kappa70-methanol solution (pH:6)

4.2.2. Effect of Surfactants

The dispersion behavior of carbon sample Kappa70 was tested using some simple and polymeric surfactants with different characteristic structures, such as anionic (Sodium Dodecyl Sulfate-SDS), cationic (CTAB), and nonionic surfactants (T-X100 and F-127). The detailed properties of these surfactants are given above in Chapter 3, in Material Section. DLS size distribution measurements were conducted to study the

dispersion behavior of Kappa70 in the presence of surfactants, and the results are presented in Figure 4.8.

It is seen from Figure 4.8 that the presence of surfactants with positive, negative, and no charges seem not to improve dispersion behavior positively. When the settling behavior of dispersions was also observed, ionic surfactants caused quick agglomeration and settling behavior. The presence of nonionic surfactants (simple, T-X-100, or polymeric, F-127), on the other hand, the settling took a much longer time. They seem to affect the dispersion of particles up to a certain degree. To explain these results, the patches that the carbon surface may most likely have and the attraction of surfactants on these surface parts with different charges were simulated by a simple physical model in Figure 4.9. The functional groups of a carbon surface (See Figure 2.12.) due to its oxidation are well known and expecting different types of carbon surfaces together at the same time for a given carbon dispersion system is logical (Fan et al. 2020). As seen there may be positive and negative charged parts of the carbon surface (Fan et al. 2020), and ionic surfactants may attract to these parts and may adsorb such that the hydrophobic part of their structure may oriented through into the solution side which may cause agglomeration due to the hydrophobic attraction between the particles with similar conditions. However, the non-ionic surfactants may prefer the hydrophobic parts of the surface and provide dispersion of particles. Both size and zeta potential distributions of carbon particles support this hypothesis (Figure 4.8, and Figure 4.10). The narrower size distribution obtained in the case of ionic surfactants may belong to certain sizes of particles due to the presence of settling in the size measurement cell of the device.

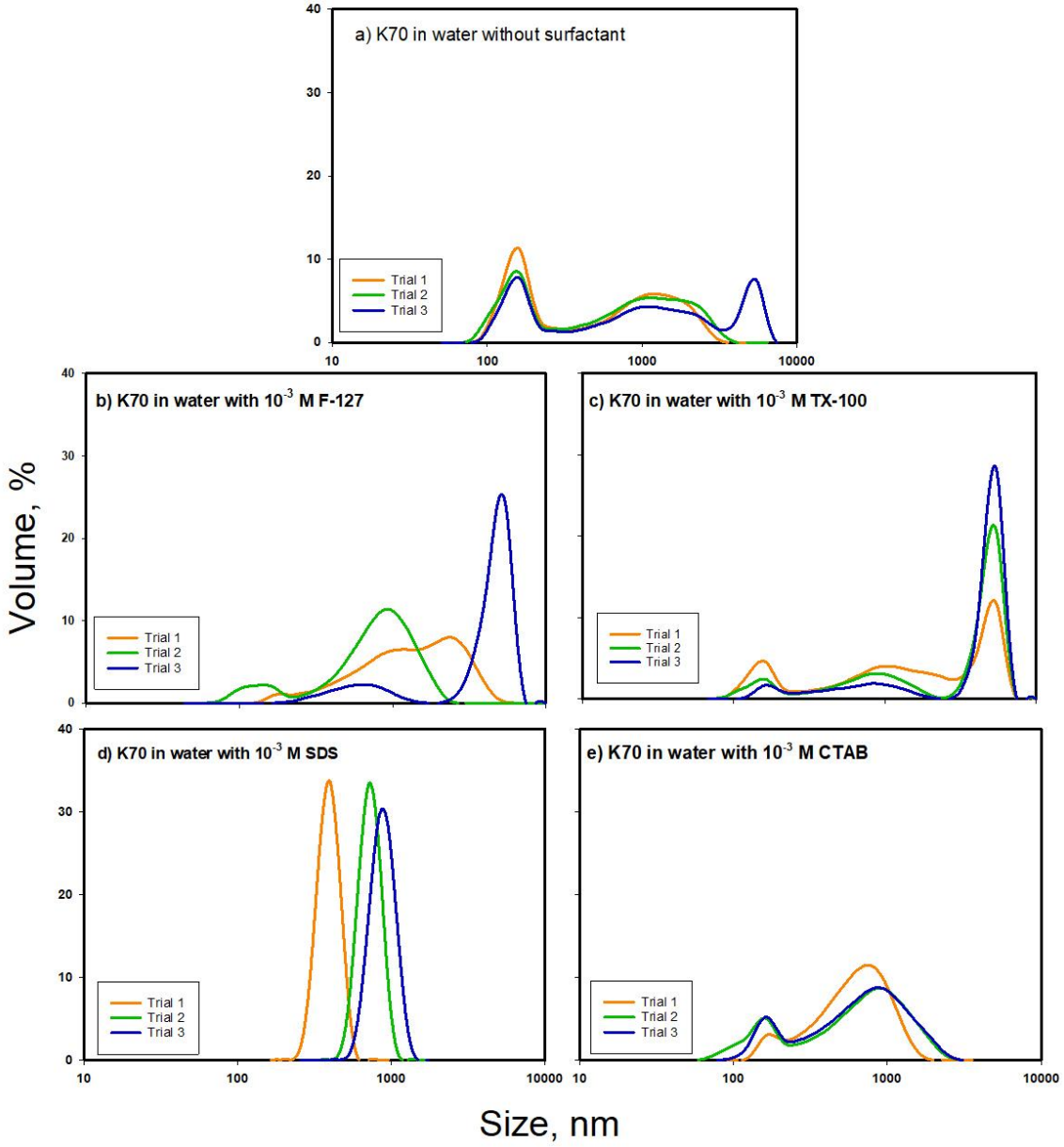

Figure 4.8. Size distribution of Kappa 70 in water a) without surfactant b) 10^{-3} M F-127, c) 10^{-3} M TX-100, d)10^{-3} M SDS, and e) 10^{-3} M CTAB

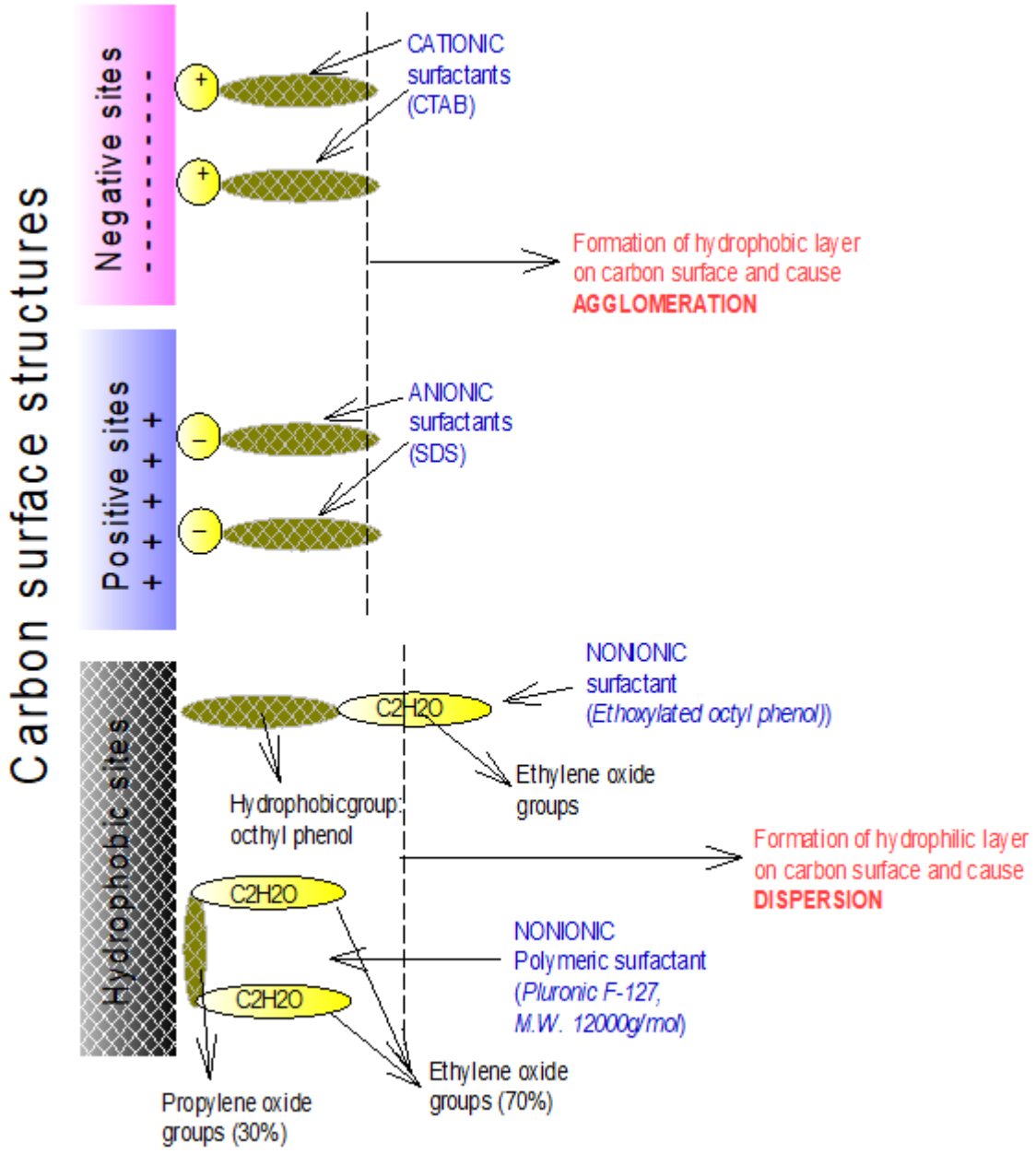

Figure 4.9. Surfactant attachment mechanisms of the carbon surface

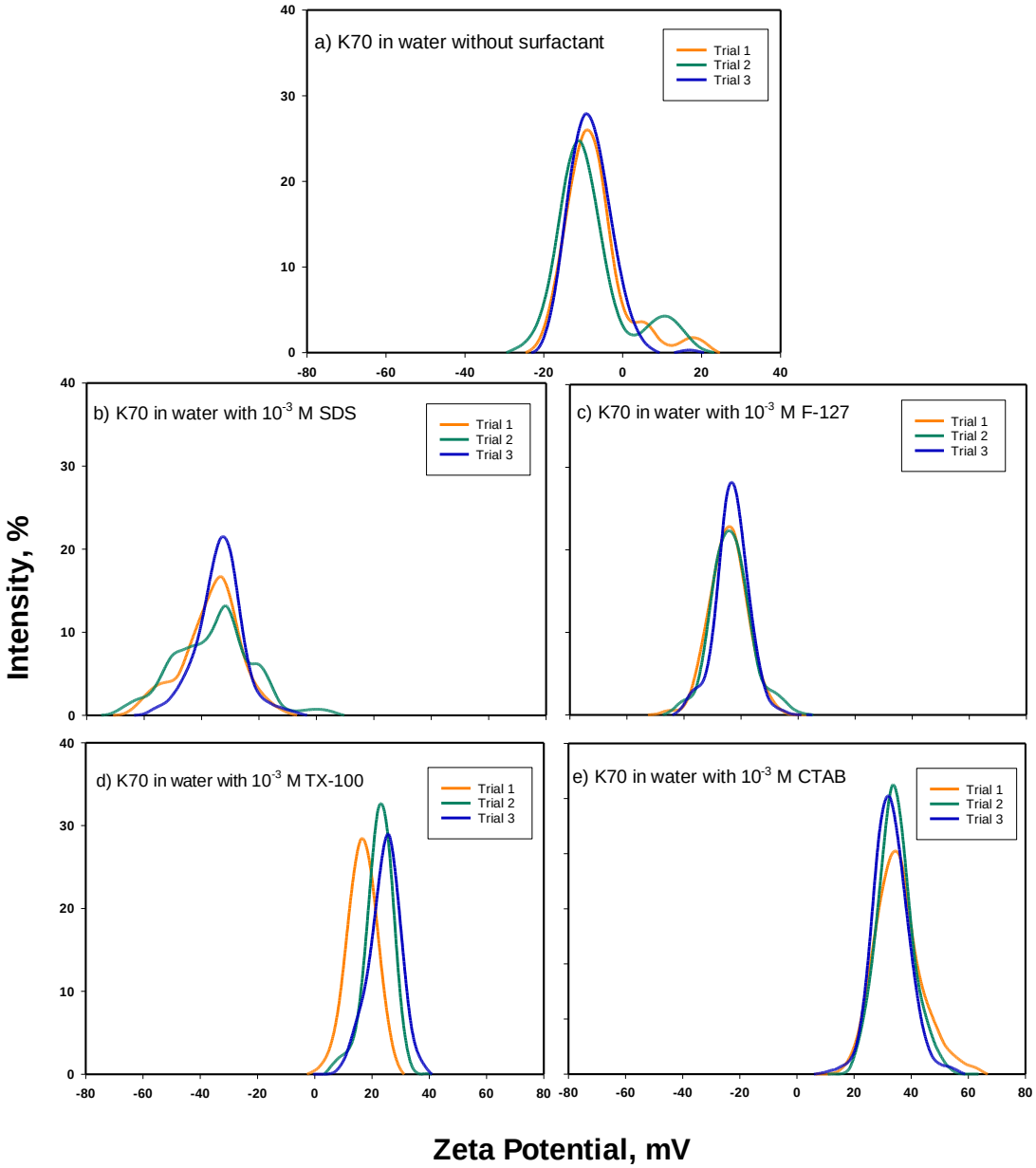

Figure 4.10. Zeta Potential of Kappa 70 in water a) without surfactant b) with 10^{-3} M SDS, c) 10^{-3} M F-127, d) 10^{-3} M TX-100, and e) 10^{-3} M CTAB (pH:7)

Similar types of size and charge measurements were also conducted in methanol since the solvent used for the dispersion of carbon was methanol (Figure 4.11, and Figure 4.12). As seen from the figures, the carbon surfaces become less charged, and similar in methanol, even in the cases of surfactants, and they seem to be agglomerated. The SEM images of these particles are given below to clarify the observations (Figure 4.13).

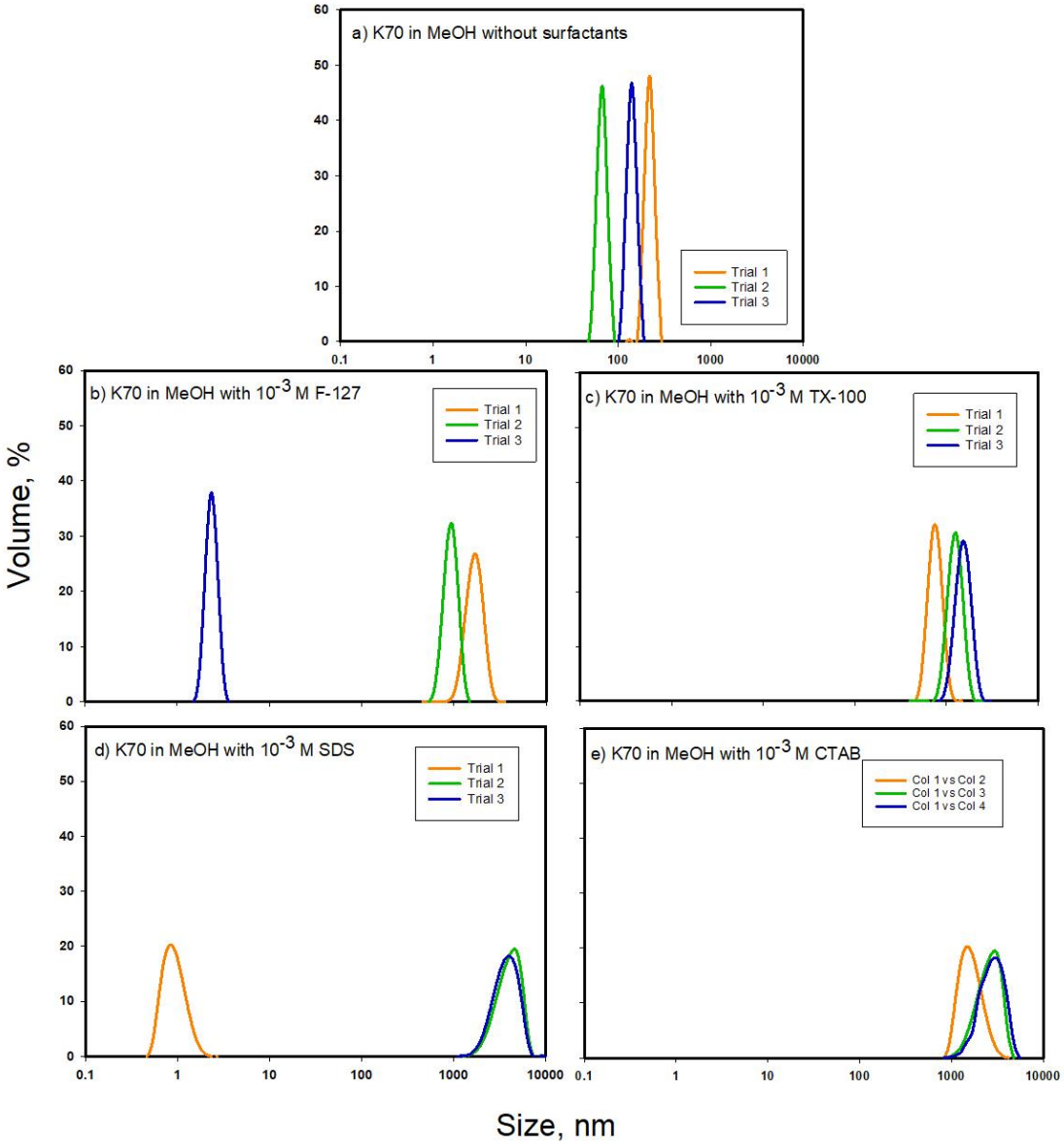

Figure 4.11. Size distribution of Kappa 70 in Methanol a) without surfactant b) 10^{-3} M F-127, c) 10^{-3} M TX-100, d)10^{-3} M SDS, and e) 10^{-3} M CTAB

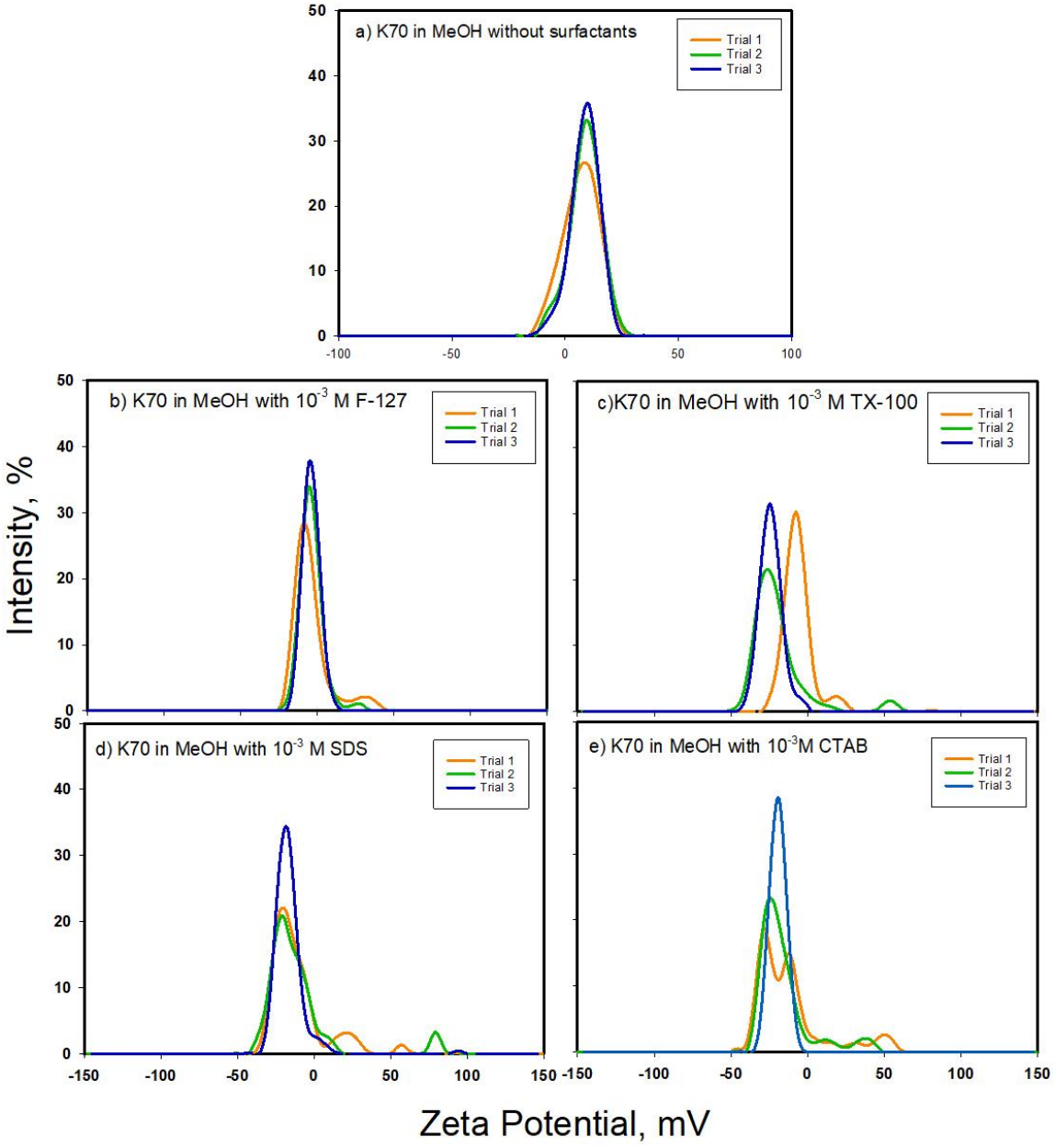

Figure 4.12. Zeta Potential of Kappa 70 in Methanol a) without surfactant, b) 10^{-3} M F-127, c) 10^{-3} M TX-100, d)10^{-3} M SDS, and e) 10^{-3} M CTAB

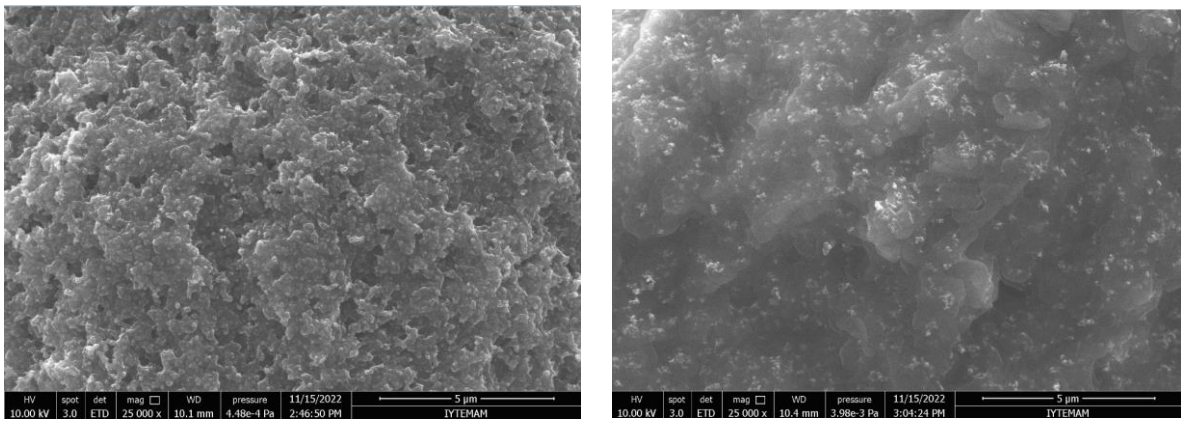

Figure 4.13. SEM images of carbon dispersed in MeOH in the presence of surfactants a)T-X100 and b)CTAB:

4.3. Preparation and Characterization of Carbon-based Composites

In the study, the production of semiconductor composites was carried out using the solution casting method. Based on the characterization studies conducted above, Kappa70 (K70) was chosen to be used in the production of semiconductor composites by evaluating the BET surface area, conductivity, and dispersibility results. As agreed in Section 4.2.1., methanol was used as the solvent.

The mass of Kappa 70 was used at concentrations of 15%, 20%, 25%, 30%, and 35% by weight in the resin. The minimum carbon black concentration was determined as 15 wt% according to the literature (Li et al. 2019). Since the dispersion of Kappa70 is not possible after 35%, the carbon concentration limit was accepted as 35%. Carbon Kappa70 was dispersed using sonication at relevant concentrations in methanol at a weight ratio of 1:10. Then, the calculated mass of PDMS was added to the system and sonicated for 15 minutes. After this process, the solvent was evaporated by heat while mechanical mixing was applied under vacuum. The experimental stage is given in Figure 4.14. After all the solvent evaporated, the curing agent was added and mixed for 5 minutes, and poured onto the panels. After the degassing process, it was left to cure in a vacuum oven at 100 ℃ for 30 minutes.

Figure 4.14. Experimental stage

The Kappa70/PDMS composites manufactured are given in Figure 4.15. It has been observed that the addition of carbon after 25% greatly affects rheology. Carbon blacks at high concentrations tended to agglomerate and porous composite structures were obtained. Roughnesses were observed on the surface of the 35% K70/PDMS composite.

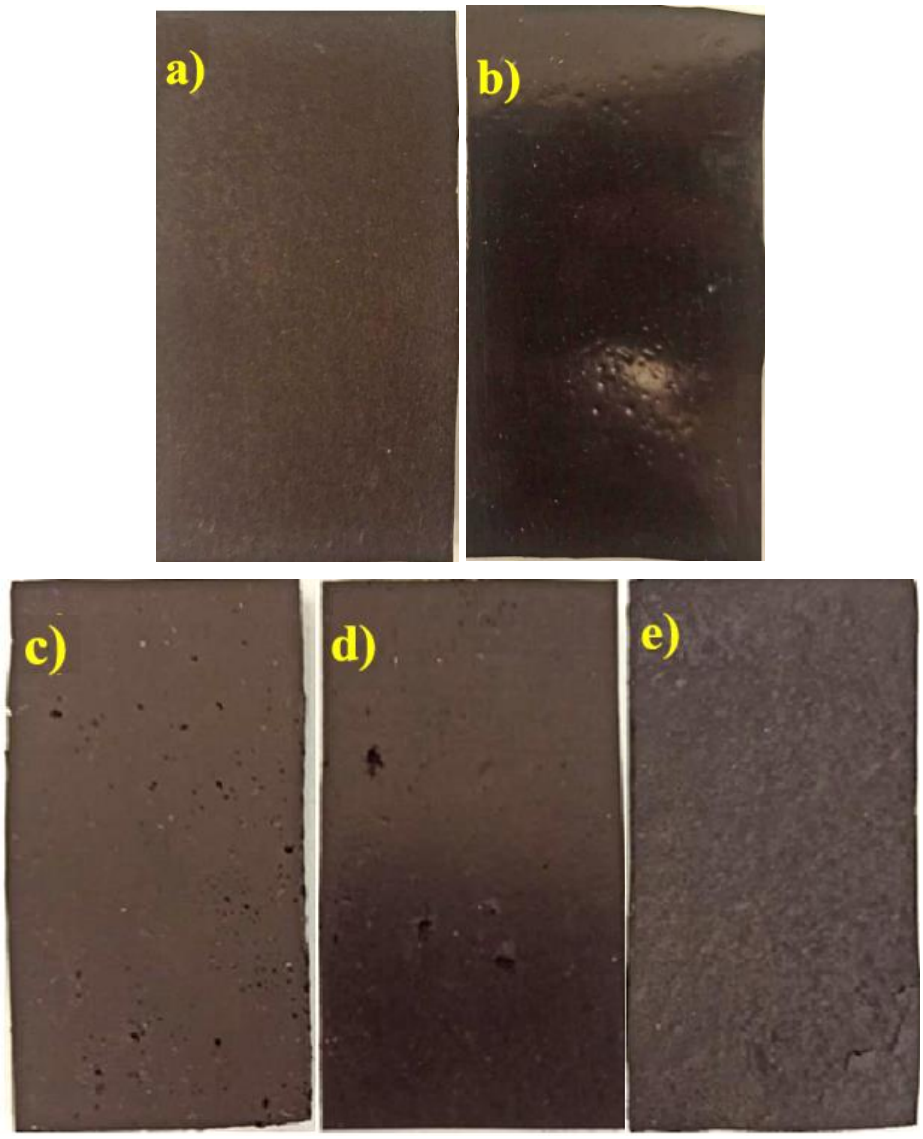

Figure 4.15. Images of manufactured Kappa70/PDMS composites: a) 15 wt.% K70/PDMS, b)20 wt% K70/PDMS, c)25 wt.% Kappa70/PDMS, d) 30 wt.% Kappa70/PDMS, and e)35 wt.% Kappa70/PDMS

In the study, as discussed above, surfactants do not make any significant contribution to carbon dispersion. However, composite production was also carried out using different surfactants according to the above-mentioned procedure in order to observe the effect within the polymer. Additionally, composite production was carried out using a similar procedure using 10% and 15% XE2B carbon black by weight. Since it was not possible to increase XE2B above 15 wt%, higher carbon concentrations were not studied.

4.3.1. Conductivity Measurements

The electrical resistivity of composite samples produced by adding different amounts of carbons Kappa70 and XE2B reinforcement to the PDMS matrix structure was examined. The length, width, thickness, and electrical resistivity values of manufactured composite samples are given in Appendix A.1. Table 4.3 shows the average electrical resistivity, average conductivity, and standard deviation of composite samples. All composites measured were seen to be in the semiconductor range, according to the literature (Le et al. 2017). Since the resistivity values of 15% and 20% Kappa70/PDMS composites exceeded the device's measurement range, resistivity measurements could not be taken in these composites.

Table 4.3. Electrical resistivity and conductivity of composite samples

Sample	Average Resistivity (Ω)	Average Conductivity (S/m)
15% K70/PDMS	-	-
20% K70/PDMS	-	-
25% K70/PDMS	9831	0.14 ±0.02
30% K70/PDMS	340	3.17 ±0.49
35% K70/PDMS	122	10.79 ±2.24
10% XE2B/PDMS	11022	0.0087 ± 0.01
15% XE2B/PDMS	275	2.57 ± 0.20

The highest conductivity value calculated was for 35 wt.% composites as 10.79x10 S/m. That is expected, as it contains less PDMS than other composites, that is the insulator part. However, high carbon concentration greatly affected the rheology, making composite production quite difficult. Therefore, it will not be a suitable and economical solution for industrial applications. 30% K70/PDMS and 15% XE2B/PDMS composites have close electrical conductivity values. However, production problems were experienced in the 15% XE2B/PDMS composite due to increased rheology like 35%K70/PDMS. In the case of resistance values, however, one has to be careful, as in

the case of a 15% XE2B composite with lower resistance, the electrical conductivity was lower. This is because the resistance measurements of the materials are also affected by parameters such as thickness, width, and length. For this reason, the evaluations were made just on electrical conductivity values.

Figure 4.16. shows the resistance and conductivity relationship of K70/PDMS composites with respect to increasing carbon concentration. As expected, with decreasing resistivity, an increase in conductivity can be seen for all types of composites with different weight percentages.

In the study, composite production was also carried out using surfactants to improve the distribution of 30% K70 carbon, which was found to be the most suitable in terms of rheology and conductivity, in PDMS. Table 4.4 shows the effect of surfactant addition on the conductivity of the composite. The detailed results of these composites are given in Appendix A, Table A.2. As mentioned in Chapter 4.2.2, surfactants had no significant effect on carbon distribution. It has been observed that composites with the same carbon concentration, to which different surfactants are added, have similar electrical conductivity values.

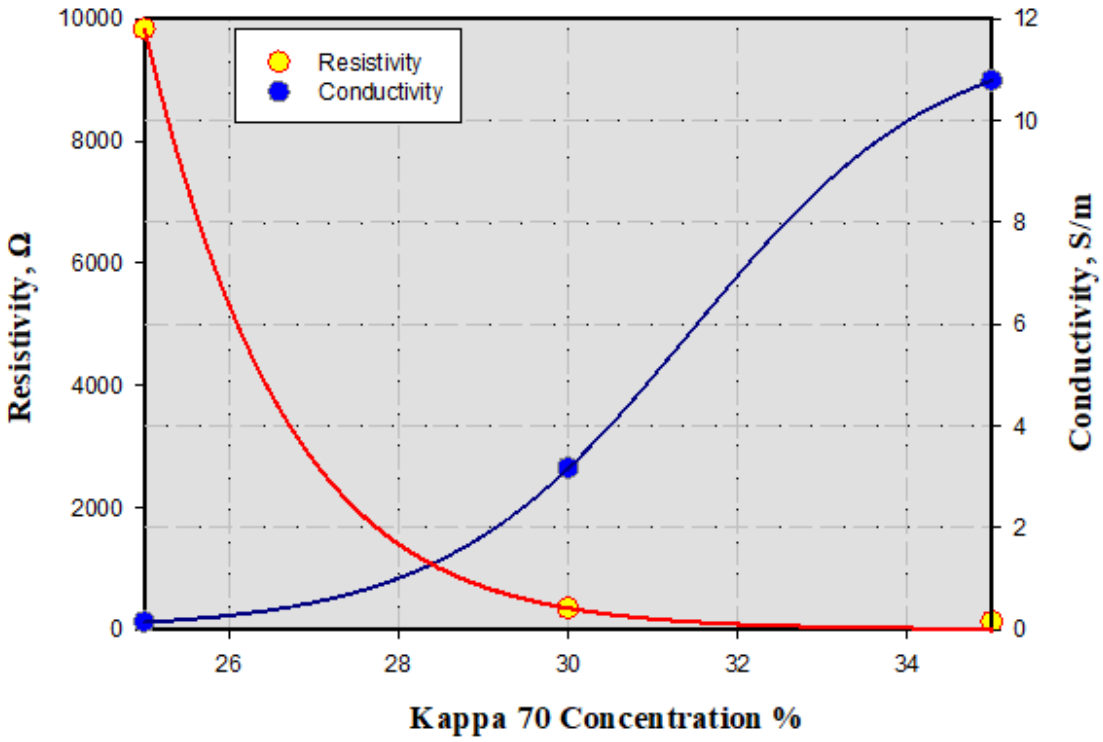

Figure 4.16. Resistance and conductivity in response to carbon concentration

Table 4.4. Effect of surfactants on the electrical conductivity of 30 wt.% K70 composite samples

Sample	Average Conductivity (S/cm)
30% K70/PDMS	3.17
30% K70/PDMS/TX-100	2.96
30% K70/PDMS/SDS	3.11
30% K70/PDMS/F-127	3.09
30% K70/PDMS/CTAB	3.00

In the literature, there are results in which similar conductivity values are obtained by using high-cost reinforcements such as MWCNT in the PDMS matrix. Some of these studies included 1 to 15 wt% MWCNT or MWCNT/GNP in the PDMS matrix, and the conductivity values of these composites ranged from 1.0 to 6.3 S/m (Kim et al. 2016; Liu and Choi 2009; Norkhairunnisa et al. 2012; Oh et al. 2016; Yan and Jeong 2015). However, in this study, comparable conductivity results were obtained economically. Considering the values given in Table 2.2, the carbon cost in composites containing 1% CNT by weight, which is the lowest value, is approximately $20, while the carbon cost in the production of 30% carbon black added composites will be around $0.002.

Additionally, it has been observed in the literature that the electrical conductivity of composites produced using 10%, 30%, and 60 wt% CB and high-density polyethylene is $1x10^{-10}$, $1x10^{-7}$, and $1x10^{-5}$ S/cm, respectively (Sajeel et al. 2021). In the study, the composites developed using Kappa 70 have higher electrical conductivity values compared to the literature by almost 1000%.

4.3.2. Scanning Electron Microscopy

Cross-sectional areas of bare PDMS and semi-conductive composites (25% K70/PDMS, 30% K70 /PDMS, 35% K70/PDMS) were examined using SEM analyses. Figure 4.17., shows the carbon (K70) distribution in the resin (PDMS). Figure 4.17.a. shows the cross-sectional area of bare PDMS for a better understanding of carbon

distribution. According to Figure 4.17., it was seen that agglomerations increased as the carbon content increased, as expected. Agglomerations were observed even in the 25% K70/PDMS composite with the lowest carbon concentration. These agglomerations directly affect the properties of composites, such as electrical and thermal conductivity, surface characteristics, and mechanical properties. As seen in Figure 4.17.b., although K70 is mostly spread on the PDMS surface, it is seen that it is not distributed homogeneously. In the 30% K70/PDMS sample (Figure 4.17.c.), it was observed that carbon spread over the entire PDMS and agglomerations increased. Notably, in the 35% K70/PDMS sample (Figure 4.17.d.), although the carbon was spread over the entire surface, the agglomerations formed were quite large.

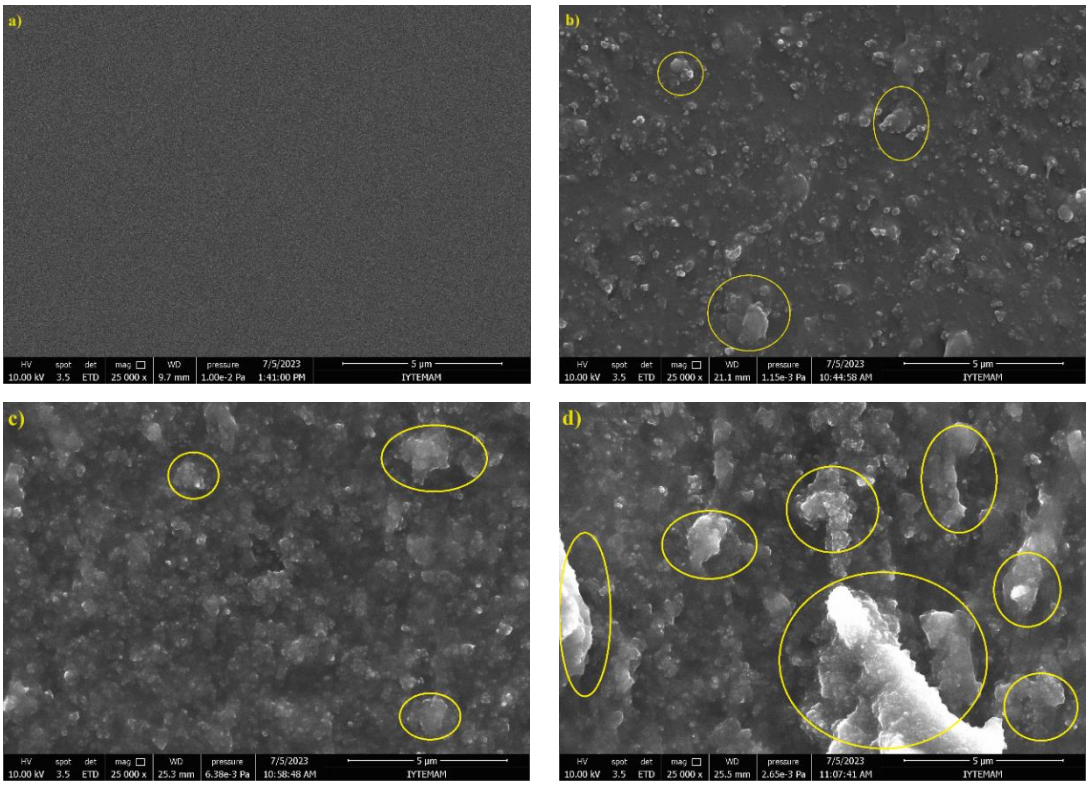

Figure 4.17. Cross-sectional areas of a) bare PDMS, b) 25%K70/PDMS c)30% K70/PDMS, and d) 35% K70/PDMS

4.3.3. FTIR Analysis

FTIR analyses of composite samples were performed to study any relationship or bonding between K70 and PDMS. The FTIR spectra of K70, PDMS, and K70/PDMS composites are presented in Figure 4.18. The results of Carbon K70 were already discussed in Chapter 4.2.3. PDMS showed the Si-CH_3 symmetric bending peak around 1262 cm^{-1} and 800 cm^{-1} (Al-Oweini and El-Rassy 2009; Ruan et al. 2023). Around 1049 cm^{-1} wavelength Si-O-Si stretching peaks were observed (Krenczkowska et al. 2019). The peaks around 2960 cm^{-1} and 2908 cm^{-1} show symmetrical and asymmetrical CH_3 stretching (Yetisgin et al. 2020). The main peaks of K70 are O-H stretching at around 3200-3550 cm^{-1} and COOH at around 1700-1720 cm^{-1}. After combining CB with PDMS, the composites did not show any new chemical bands.

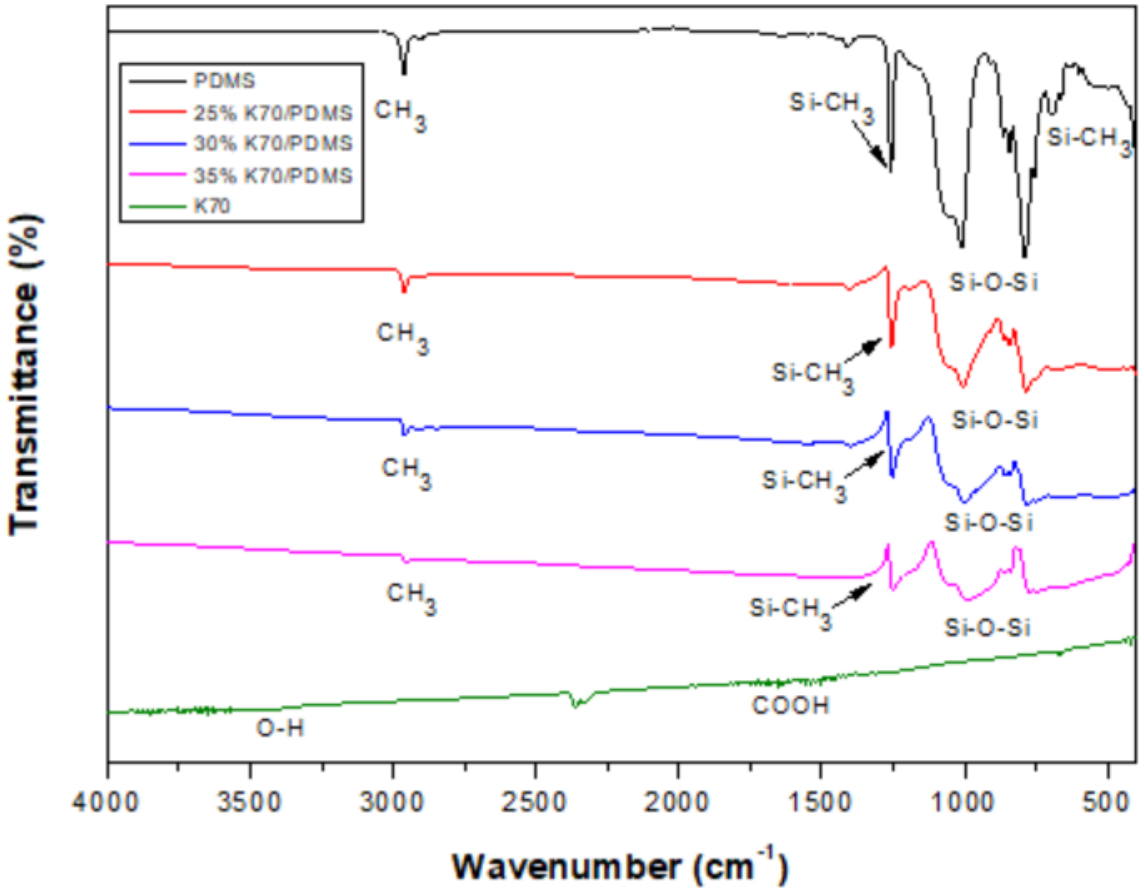

Figure 4.18. FTIR spectra of Kappa 70, PDMS, and K70/PDMS composites

4.3.4. Thermogravimetric Analysis

Thermogravimetric analyses were carried out for bare PDMS and 25%, 30%, and 35% K70/PDMS composites in an N_2 atmosphere at a temperature increase of 10 ℃/min up to 850 ℃, and presented in Figure 4.19.

It is seen that the bare PDMS resin was observed to decompose with a sharp weight loss of 29% between 400 and 600 °C, and 13.79% between 600 and 670 °C. In the end, 46% of the PDMS weight was remained. All K70/PDMS composites were found to have thermal stability. With increasing carbon concentration, the weight losses of the composites were found to be 50.5%, 47.7%, and 42.6% in the range of 480 and 510 °C, respectively. The composite with the highest carbon concentration has the least weight loss at 50.4%.

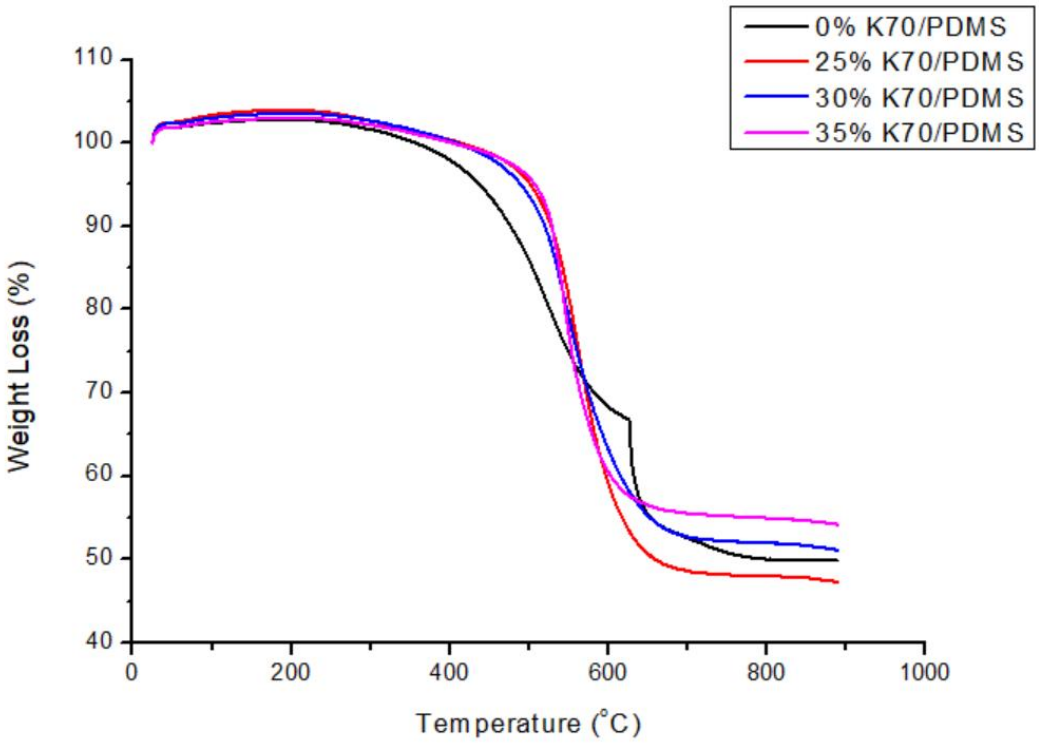

Figure 4.19. Thermogravimetric analysis of composite samples in terms of weight loss

4.3.5. Contact Angle Measurements

Contact angle measurements were conducted to test the surface characteristics (hydrophobic or hydrophilic behavior) of composite films prepared with different carbon percentages. First of all, the contact angle of the resin (Sylgard 184) that contains 0% carbon was measured and the characteristic feature of the matrix was determined. Figure 4.20 shows the contact angle measurement of the water droplet on the resin surface.

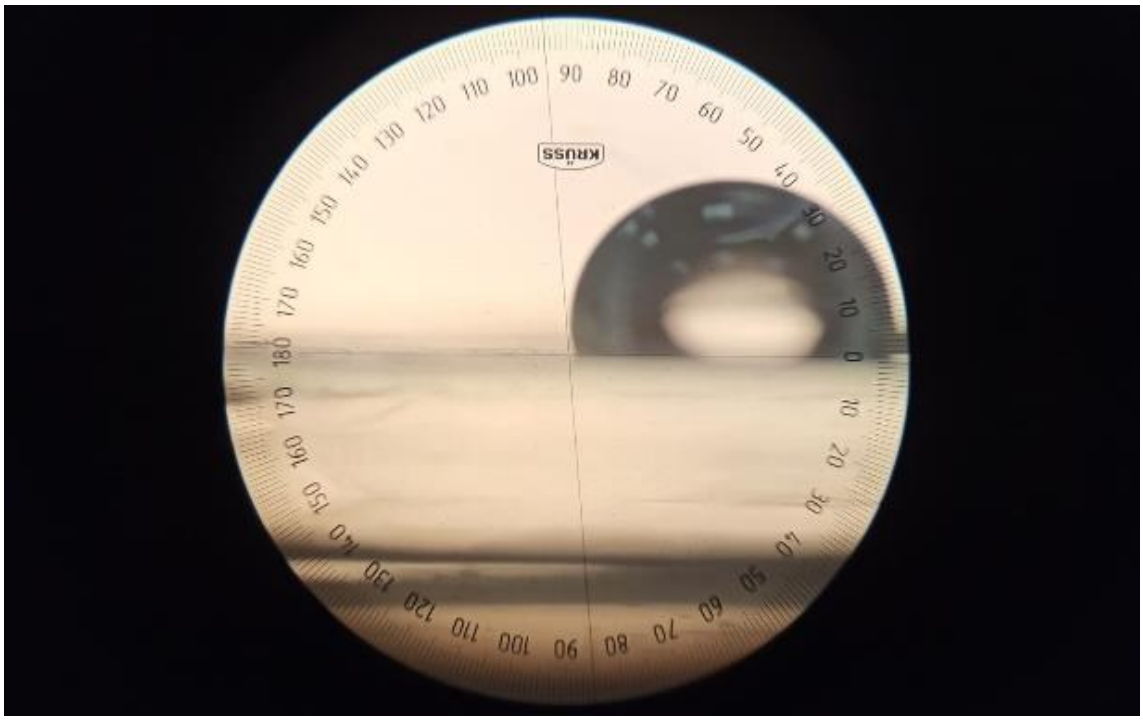

Figure 4.20. Representative image of contact angle measurement of water droplets on resin without carbon

Figure 4.21 represents the results of contact angle measurements obtained in composite surface/water/air systems. First of all, the hydrophobic characteristic of PDMS, which has a surface tension value of 20.4 nM/m, as stated in the literature (Akther et al. 2020; Ariati et al. 2021; Colas and Curtis 2013) was confirmed. The results show that the wetting properties of surfaces are not homogenous and there is a distribution of

different surface structures. But on average, the carbon-added composite surfaces seem still hydrophobic and are non-wettable.

The work of adhesion ($W_{ad} = \gamma_{LG}$ (1+Cosθ)) of these surfaces was calculated as W_{ad} = 72 J/m^2 also shows that these surfaces do not wet simultaneously.

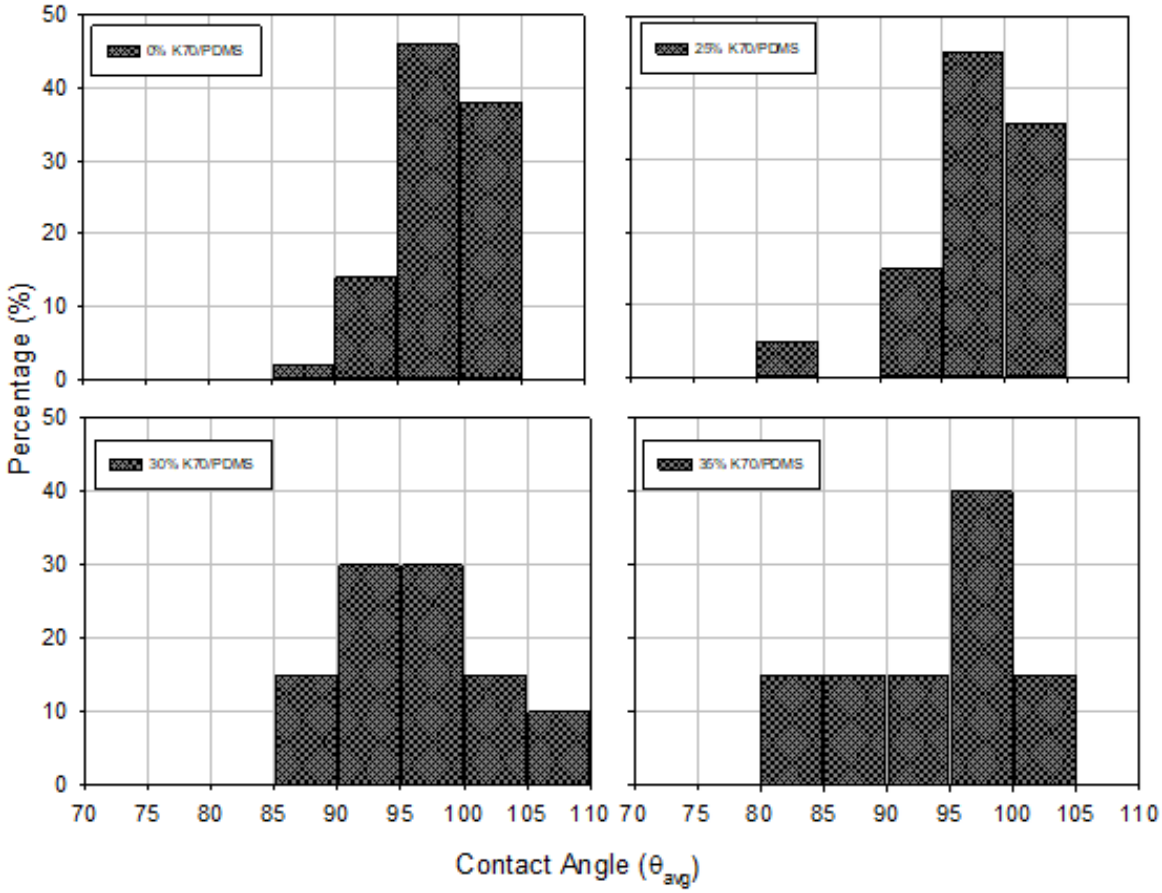

Figure 4.21. Contact angle measurement of a) 0% Kappa70/PDMS, b) 25% Kappa70/PDMS, c) 30% Kappa70/PDMS, d) 35% Kappa70/PDMS

Since contact angle values are known to depend on surface roughness, these measurements were also conducted and listed in the following table (Table 4.5). The details of the surface roughness measurements are given in Chapter 3. It is measured along the x and y planes of the composite samples. As expected, surface roughness increased with increasing carbon concentration, most probably due to an increase in agglomeration among carbon particles in high amounts.

Table 4.5. Surface roughness of composite samples

0% K70/PDMS		25% K70/PDMS		30% K70/PDMS		35% K70/PDMS	
x (µm)	**y (µm)**	**x (µm)**	**y (µm)**	**x (µm)**	**y (µm)**	**x (µm)**	**y (µm)**
0.17	0.17	1.52	1.46	1.28	0.98	4.74	4.64
0.14	0.16	1.37	1.56	1.10	1.21	4.07	3.76
0.13	0.15	1.82	1.50	1.01	1.40	4.30	6.51
0.11	0.24	1.44	1.41	2.66	1.13	4.31	6.55
0.14	0.26	2.01	2.00	3.17	0.96	5.95	5.11
0.14	0.18	1.77	1.45	2.88	1.24	4.67	3.36
0.22	0.12	1.69	2.20	2.86	0.92	4.35	4.96
0.17	0.15	1.79	1.82	2.68	1.10	4.03	4.04
0.10	0.18	1.91	1.14	3.07	1.64	3.85	3.21
0.13	0.13	1.81	1.93	2.31	1.14	3.60	2.36

4.3.6. Surface Free Energy Calculations

In this study, Fowkes theory was used for surface energy calculations. For this purpose some contact angle measurements with some special liquids as discussed in Chapter 3. First contact angle measurements were done using diiodomethane, a completely dispersible liquid, and the result was recorded as an average of 69° (1.20 radians) for 30% K70/PDMS composite. Since there is no polar component in diiodomethane, Equation 3.1. was used and the dispersive part of solid surface free energy was calculated as $23.44\ mN/m$ as given in Eq. 4.1.

$$\gamma_S^D = \frac{50.8\ mN/m\ (1+\cos\ (1.20)^2}{4} = 23.44\ mN/m \qquad Eq.\ 4.1.$$

Then, using water, that has dispersing and non-dispersing components, the contact angle was measured as 92° (1.60 radians) for 30%K70/PDMS. Using Eq. 3.9., the solid

surface free energy of the polar component was calculated as $3.08\ mN/m$ as given in Eq. 4.2.

$$\gamma_s^{nD} = \left(\frac{\gamma_L(1+cos\theta)}{2 * (\gamma_L^{nD})^{0.5}} - \frac{(\gamma_L^D . \gamma_s^D)^{0.5}}{(\gamma_L^{nD})^{0.5}} \right)^2 = 3.08\ mN/m \qquad Eq.\ 4.2.$$

where,

$\gamma_{L,water}$=72.8 mN/m (Vargaftik, Volkov, and Voljak 1983)

$\gamma_{L,water}^{nD}$=51 mN/m (Jańczuk and Białlopiotrowicz 1989)

$\gamma_{L,water}^{D}$=21.8 mN/m (Jańczuk and Białlopiotrowicz 1989)

By applying Eq. 3.7., the average surface energy of the composite material surfaces produced in this study was around 26.52 mN/m as given in Eq. 4.3. This value shows that the materials prepared in this study have low energy, hydrophobic surfaces, and are not wettable by water.

$$\gamma_s = 23.44 \frac{mN}{m} + \frac{3.08 mN}{m} = 26.52 \frac{mN}{m} \qquad Eq.\ 4.3.$$

The same procedure was applied to film surfaces made of PDMS resin only. The contact angle measurements with diiodomethane and water were measured as 62º and 96º, respectively. The estimated average surface energy of these bare PDMS surfaces was found to be around 28.72 mN/m. It is seen that the bare PDMS and composite surface-free energies are quite similar. The addition of carbon decreased the surface energy of composites little and surfaces became slightly more hydrophobic (less water wettable).

4.4. Testing of Composites

4.4.1. Temperature-Control Tests

Temperature control tests were performed for only semiconductor composites which are 25%, 30%, and 35% K70/PDMS. Temperature control tests were performed for only semiconductor composites, which are 25%, 30%, and 35% K70/PDMS. Composite samples were energized at different voltages for 5 minutes, and then temperature changes were examined using a thermal camera. The average temperature of the composite was obtained by using the temperature values of three fixed points marked on the surface of the composites, as given in Figure 4.22.

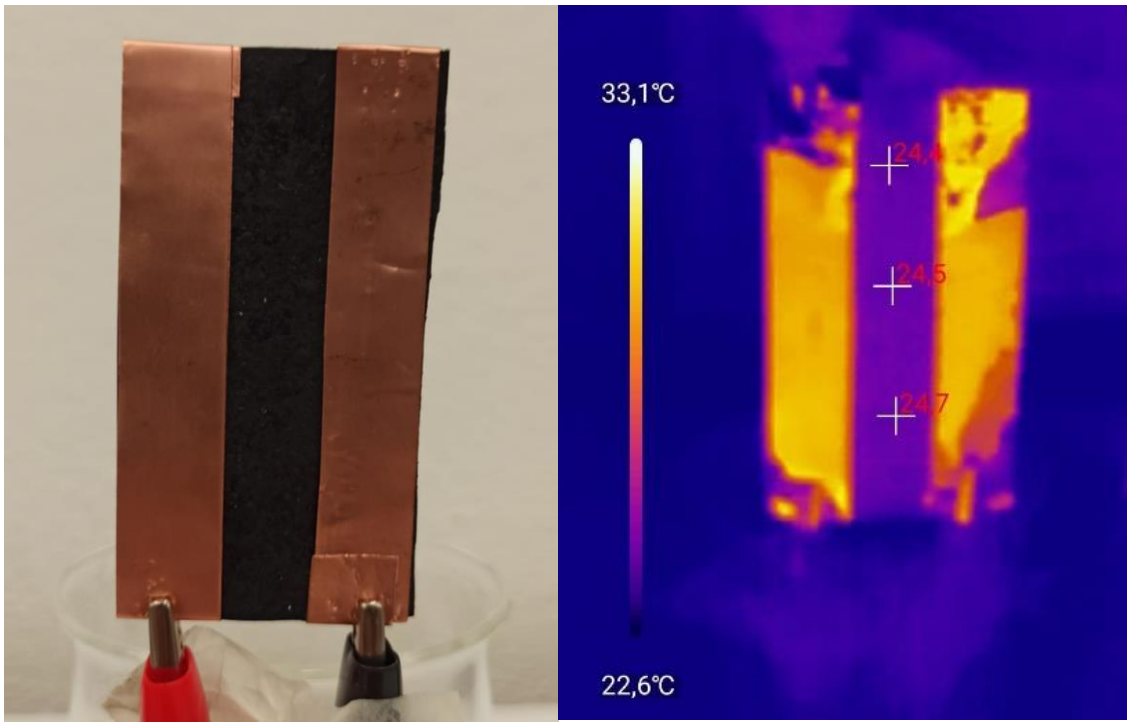

Figure 4.22. Composite sample thermal performance test

Figure 4.23 shows the average temperature values for all the composites under different voltages. As seen from the figure, the 25% K70/PDMS composite could not provide resistive heating under any voltages; that is, there was no temperature change. In

the case of 30 and 35%K70/PDMS composites, on the other hand, there was an increase with an increase in voltage and they both reached to 38 ºC at 20 volts. Then the effect of an increase in voltage on temperature starts to decrease in the case of 35% K70/PDMS composite and slows down compared to the 30% K70/PDMS composite with the highest temperature performance of 46.8 and 49.7 ℃. This was contrary to expectations, the composite with lower conductivity reached higher temperatures as the voltage increased. This was attributed to the surface roughness due to the high carbon concentration of the system containing 35% K70. The high surface roughness of the composite seems to affect the adhesion of the copper tapes that are used in this study, to the surface, and therefore the energy flow to provide the desired performance. The other reason could be the agglomeration of carbon particles among themselves at high concentrations due to their hydrophobic character.

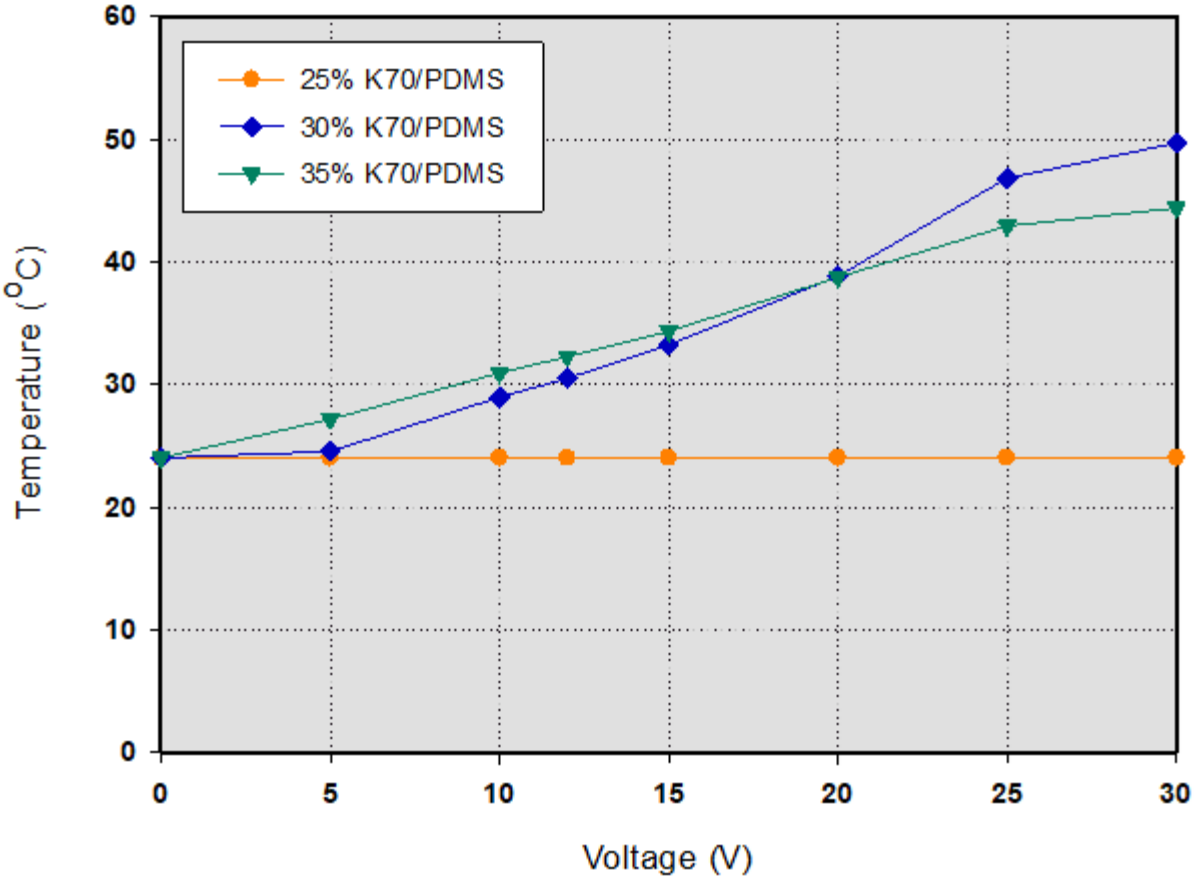

Figure 4.23. Composites maximum temperatures under different voltages

Figure 4.24 shows the temperature changes in both composites under 25V. It can be seen from the figure that the 30% K70/PDMS composite provides a much more homogeneous heating performance. It has been observed that a 35% K70/PDMS composite has local cold areas under 25 V. Additionally, it was also observed that the temperatures along the edges of the copper bands where energy transfer was achieved in 30% and 35% K70/PDMS composites reached 91.9 and 122.2 ℃, respectively. Since these temperature values are the energy starting points, higher temperatures were obtained at the edges than at the composite surfaces.

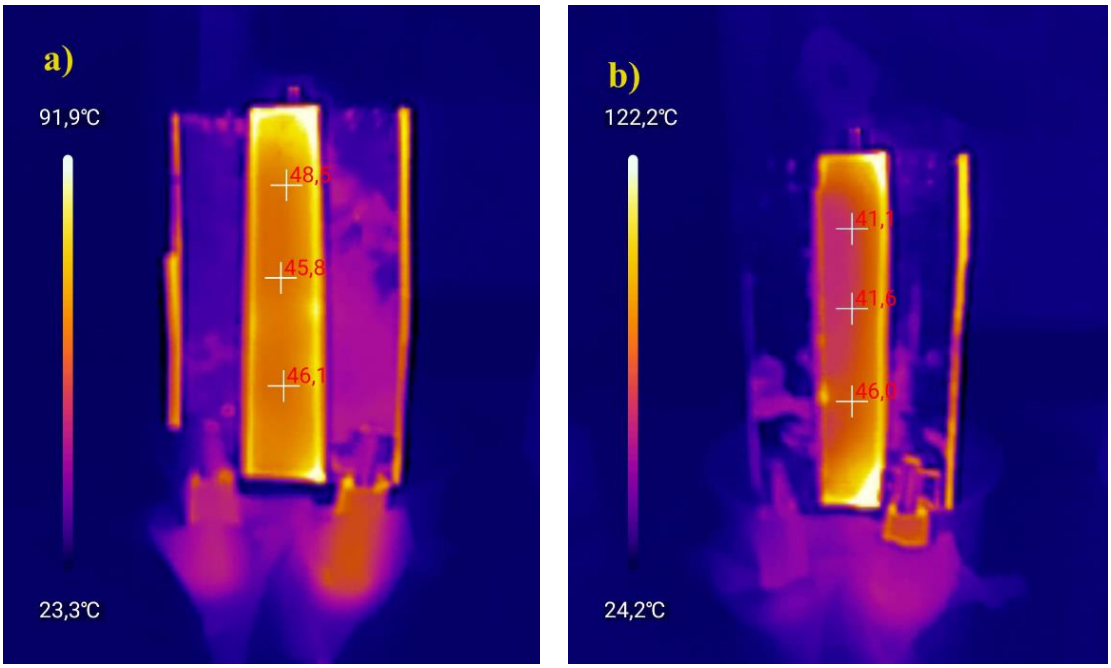

Figure 4.24. Composites temperatures performance under 25 V a) 30% K70/PDMS, and b) 35% K70/PDMS

As a result of the thermal performance tests, the 30% K70/PDMS composite, which achieved the highest and most homogeneous temperatures, was evaluated as the most suitable composite for the carbon type studied and the conditions of this study. For this reason, the time-dependent temperature change of the 30% K70/PDMS composite under 20 V was also examined and is given in Figure 4.25. The composite showed a temperature increase of approximately 12 ℃ in 2 minutes and reached steady-state conditions at 45 ℃ in 22 minutes.

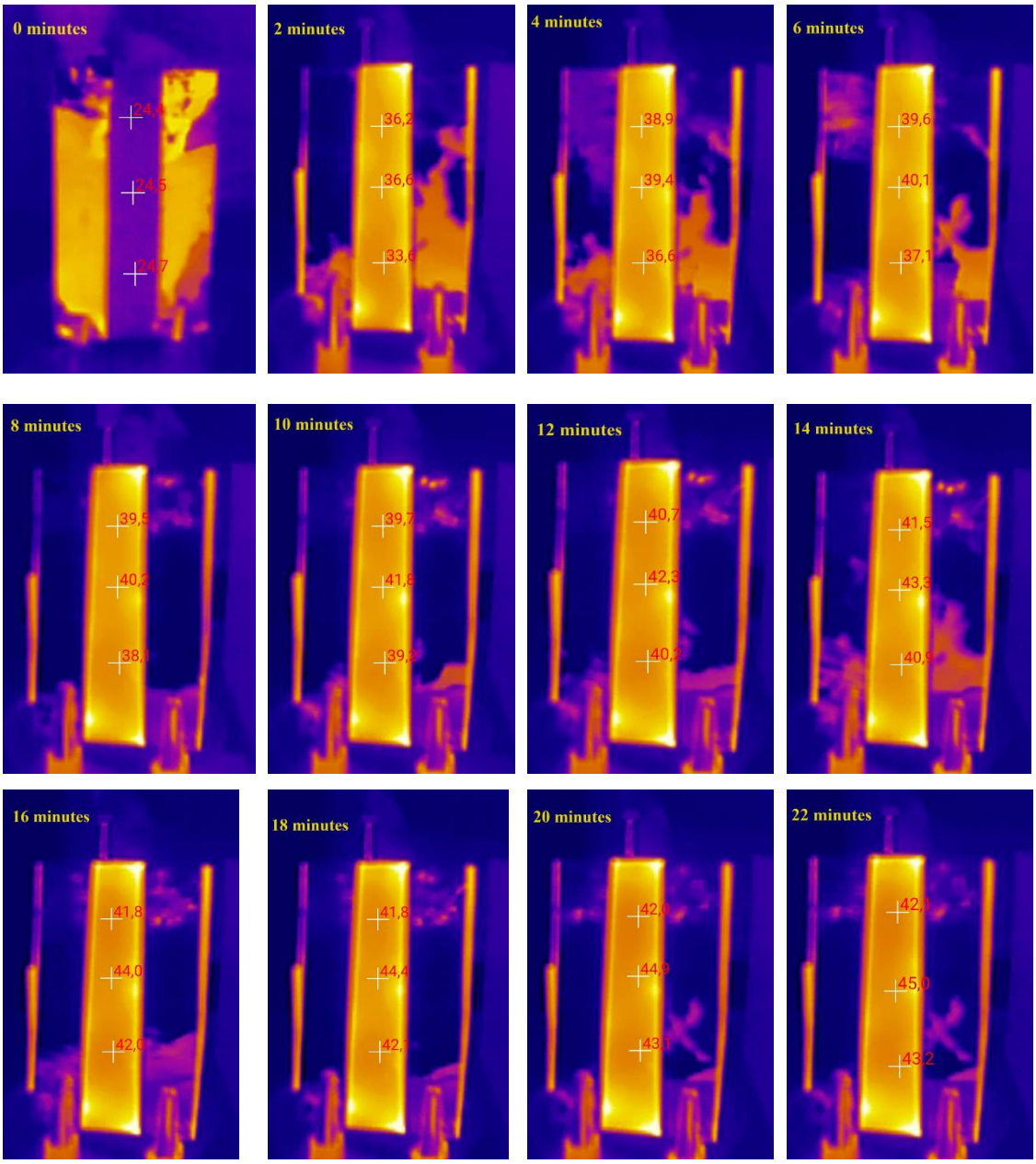

Figure 4.25. Temperature change of 30% K70/PDMS composite under 20 V with respect to time

4.4.2. Mechanical Performance Tests

In this study, tensile strength tests were performed for bare PDMS and 30% K70/PDMS composites, according to ASTM D412 Type-C. The stress/strain curve of three samples of bare PDMS and 30% K70/PDMS composites is given in Figure 4.26.

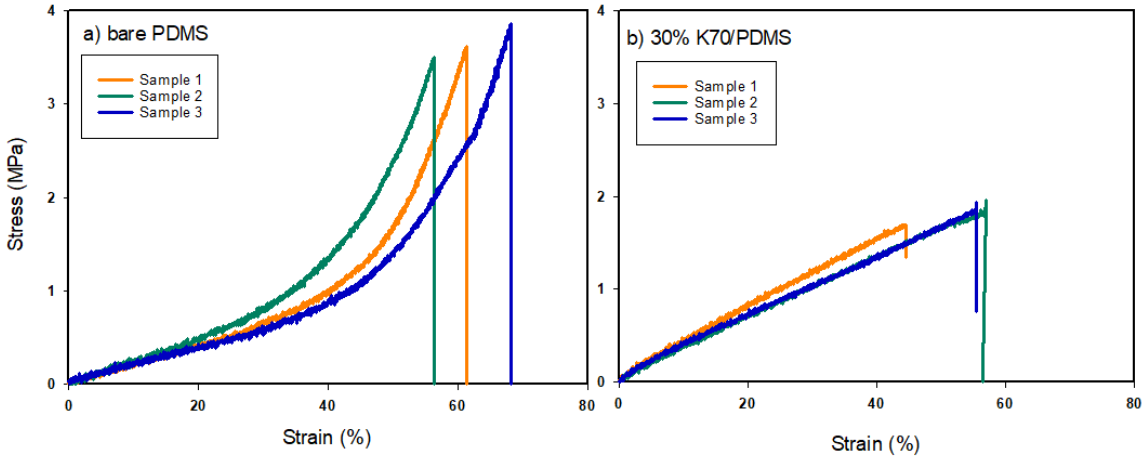

Figure 4.26. Stress-strain curve of a) bare PDMS, and b) 30% K70/PDMS

Up to a quite remarkable strain level, both specimens exhibited elastic behavior. In the stress versus strain graphs, 10% to 20% strain was determined as the linear elastic region for bare PDMS and composite samples. The elastic modulus of the bare PDMS and 30% K70/PDMS composite samples was determined in these linear elastic fields using Hooke's law and is given in Table 4.6.

In the literature, the elastic modulus of PDMS varies from 1.3 to 3.0 MPa and the tensile strength differs between 3.5 and 5.1 MPa (Ariati et al. 2021; Shivashankar, Sangamesh, and Kulkarni 2019). The tensile strength and elastic modulus results of bare PDMS are similar in the literature as given in Table 4.6. According to the table, with the addition of 30% carbon, the elastic modulus of bare PDMS was improved by 97.8%; however, the tensile strength decreased by 50.4%. The decrease in tensile strength can be associated with the carbon aggregation in the PDMS matrix, production defects such as porous structure (air bubbles), and the interfacial relations between resin and carbon such as weak bonding. As seen in Figure 4.17. c, agglomerations were observed at the carbon concentration where this desired conductivity was achieved, which could cause a decrease in tensile strength. In addition, the literature has concluded that high carbon concentrations for elastomers cause a reduction in tensile strength (Alam et al. 2014; Sun et al. 2019; Wang et al. 2014).

Table 4.6. Tensile Test Results of bare PDMS and composite samples

a) Bare PDMS	**Max. Force (N)**	**Tensile Strength (MPa)**	**Elastic Modulus (MPa)**	**Elongaiton at Break (%)**
Sample 1	35.79	3.62	1.86	31,49
Sample 2	32.94	3.49	1.76	37,77
Sample 3	36.52	3.78	1.72	38,55
Avg	**35.08**	**3.63**	**1.78**	**38,94**
Std. Dev.	**1.89**	**0.15**	**0.07**	**3,87**
b) 30 % K70 /PDMS	**Max. Force (N)**	**Tensile Strength (MPa)**	**Elastic Modulus (MPa)**	**Elongaiton at Break (%)**
Sample 1	24.47	1.69	3.79	20.03
Sample 2	29.09	1.86	3.35	27,63
Sample 3	27.84	1.85	3.08	23.21
Avg	**27.14**	**1.80**	**3.52**	**23.63**
Std. Dev.	**2.39**	**0.09**	**0.24**	**3.81**

The increase in elastic modulus is due to the addition of carbon black, which has a hard and strong nature, giving hardness to the composite material. This means that the material will deform less under a certain stress. The percentage of elongation at break decreased with the addition of carbon black, which was also associated with an increase in stiffness. Figure 4.27 shows before and after the bare PDMS and 30%K70/PDMS tensile test samples.

Figure 4.27. Bare PDMS tensile test samples a)before the test, b) after the test; 30% K70/PDMS tensile test samples c) before the test d)after the test

The tear test graphs of bare PDMS and 30% K70/PDMS samples are given in Figure 4.28. The maximum peak force value was considered in the test, and tear strength was calculated using Equation 3.11; the results are presented in Table 4.7. According to the table, with the addition of 30% carbon, the tear strength of bare PDMS was improved by 197%. Figure 4.29 Figure 4.27 shows before and after the bare PDMS and 30%K70/PDMS tear test samples.

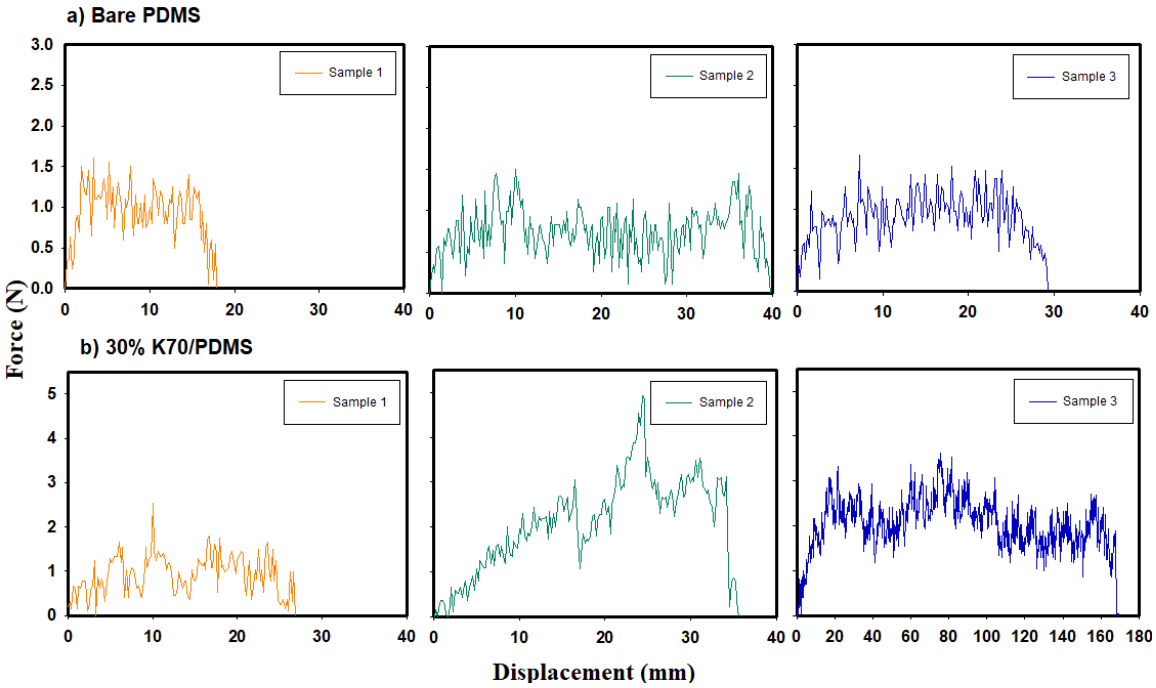

Figure 4.28. Tear test results of a) bare PDMS, and b) 30% K70/PDMS

Table 4.7. Tear test results of a) bare PDMS and b) 30% K70/PDMS

a)Bare PDMS	Max. Force (N)	Tear Strength (N/mm)
Sample 1	1.60	0.86
Sample 2	1.51	0.93
Sample 3	1.66	1.01
Avg	**0.99**	**0.93**
Std. Dev.	**0.08**	**0.07**
b)30% K70/PDMS	**Max. Force (N)**	**Tear Strength (N/mm)**
Sample 1	4.34	2.66
Sample 2	4.94	3.05
Sample 3	3.63	2.63
Avg	**4.30**	**2.78**
Std. Dev.	**0.66**	**0.23**

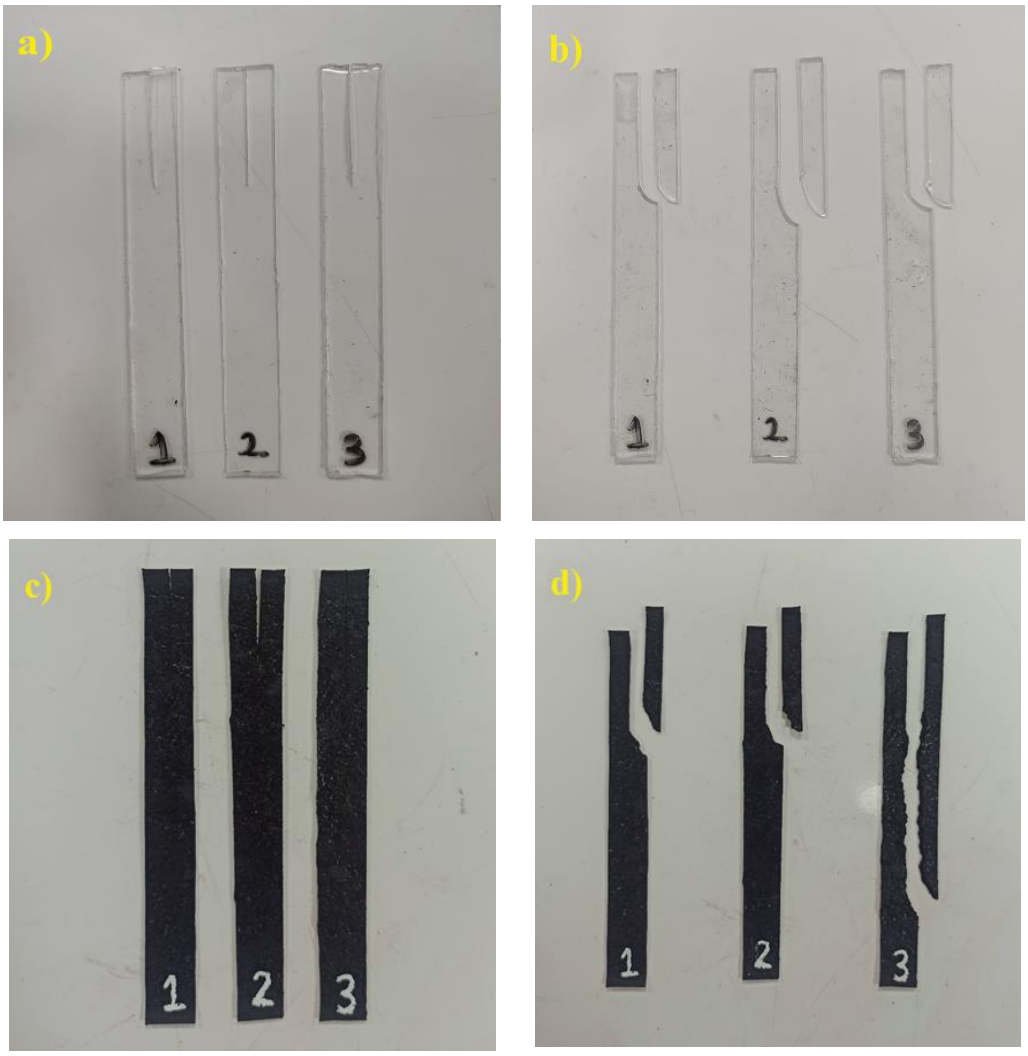

Figure 4.29. Bare PDMS tear test samples a)before the test, b) after the test; 30% K70/PDMS tear test samples c) before the test d) after the test

CHAPTER 5

CONCLUSION

This study aimed to produce carbon-based semiconductor polymeric composites for heating film applications that can be used individually or in industrial areas such as space and automobiles, using economically available materials. Commercially available carbon blacks (XE2B, Kappa70) and natural graphite were used as additives in the study. Carbons were characterized by techniques such as size, electrical conductivity, BET surface area measurements, and dispersion/settling behavior studies. As a result of these characterization studies, Kappa70 and methanol were selected as the additives and solvents. The effect of surfactants with different properties (ionic, nonionic, and polymeric) was also tested. However, their effect in the composite mixture was complex and depended very much on the structure of the surfactant and the surface characteristics of carbon.

Composites with conductivity in the range of 0 to 10.8 S/m were able to be produced by varying the carbon content between 15% and 35% by weight of Kappa70/PDMS composite. The 30% K70/PDMS composite had the highest temperature performance at 49.7 ℃ under 30 Volts. This also shows that composites can be produced with the desired conductivity and temperature according to their usage areas.

The morphological characterization of composites by scanning electron microscope (SEM) showed that carbon nanoparticles start to agglomerate at high concentrations. Thermogravimetric analysis (TGA) showed similar multistage weight loss in the composites; this showed that the composites had parallel thermal degradation mechanisms. While bare PDMS can withstand temperatures up to 400°C, the resulting composites can withstand temperatures up to 500°C. This showed that the composites were mechanically more durable at high temperatures. Mechanical characterization of the composites shows that the addition of 30% Kappa70 improved the elastic modulus by 97.8%, but the tensile strength decreased by 50.4%. This decrease in tensile strength has been associated with agglomerations and production-related problems due to the high carbon concentration of the composites.

In conclusion, it has been seen that composites can be designed according to their usage areas in terms of electrical, thermal, surface, and mechanical properties, and the study could continue in industry by improving production techniques.

REFERENCES

Abbasi, Hooman, Marcelo Antunes, and José Ignacio Velasco. 2019. "Recent Advances in Carbon-Based Polymer Nanocomposites for Electromagnetic Interference Shielding." *Progress in Materials Science* 103.

Ahn, Yumi, Youngjun Jeong, and Youngu Lee. 2012. "Improved Thermal Oxidation Stability of Solution-Processable Silver Nanowire Transparent Electrode by Reduced Graphene Oxide." *ACS Applied Materials and Interfaces* 4(12). doi: 10.1021/am301913w.

Akaluzia, R. O., F. O. Edoziuno, A. A. Adediran, B. U. Odoni, S. Edibo, and T. M. A. Olayanju. 2021. "Evaluation of the Effect of Reinforcement Particle Sizes on the Impact and Hardness Properties of Hardwood Charcoal Particulate-Polyester Resin Composites." Pp. 570–77 in *Materials Today: Proceedings*. Vol. 38. Elsevier Ltd.

Akther, Fahima, Shazwani Binte Yakob, Nam Trung Nguyen, and Hang T. Ta. 2020. "Surface Modification Techniques for Endothelial Cell Seeding in PDMS Microfluidic Devices." *Biosensors* 10(11).

Alam, M. K., M. T. Islam, M. F. Mina, and M. A. Gafur. 2014. "Structural, Mechanical, Thermal, and Electrical Properties of Carbon Black Reinforced Polyester Resin Composites." *Journal of Applied Polymer Science* 131(13). doi: 10.1002/app.40421.

Ali, Sharafat, Syed Aziz Ur Rehman, Hong Yan Luan, Muhammad Usman Farid, and Haiou Huang. 2019. "Challenges and Opportunities in Functional Carbon Nanotubes for Membrane-Based Water Treatment and Desalination." *Science of the Total Environment* 646.

Almushaikeh, Alaa M., Saleh O. Alaswad, Mohammed S. Alsuhybani, Bandar M. AlOtaibi, Ibrahim M. Alarifi, Naif B. Alqahtani, Salem M. Aldosari, Sami S. Alsaleh, Ahmed S. Haidyrah, Alanood A. Alolyan, and Basheer A. Alshammari. 2023. "Manufacturing of Carbon Fiber Reinforced Thermoplastics and Its Recovery of Carbon Fiber: A Review." *Polymer Testing* 122.

Al-Oweini, Rami, and Houssam El-Rassy. 2009. "Synthesis and Characterization by FTIR Spectroscopy of Silica Aerogels Prepared Using Several Si(OR)4 and R″Si(OR′)3 Precursors." *Journal of Molecular Structure* 919(1–3). doi: 10.1016/j.molstruc.2008.08.025.

Altay, Bilge Nazli, Ruoxi Ma, Paul D. Fleming, Michael J. Joyce, Adarsh Anand, Ting Chen, Bekir Keskin, Dinesh Maddipatla, Vikram S. Turkani, Prashant R. Kotkar, Alexander Fleck, Rasheed Rasheed, and Duo He. 2020. "Surface Free Energy Estimation: A New Methodology for Solid Surfaces." *Advanced Materials Interfaces* 7(6). doi: 10.1002/admi.201901570.

Altera, Abdelwahab Z. a., Oğuzhan Yavuz Bayraktar, Burak Bodur, and Gökhan Kaplan. 2021. "Investigation of the Usage Areas of Different Fiber Reinforced Concrete." *Kastamonu University Journal of Engineering and Sciences* 7(1).

Andersen, Henrik Lyder, Lisa Djuandhi, Uttam Mittal, and Neeraj Sharma. 2021. “Strategies for the Analysis of Graphite Electrode Function.” *Advanced Energy Materials* 11(48).

Ariati, Ronaldo, Flaminio Sales, Andrews Souza, Rui A. Lima, and João Ribeiro. 2021. “Polydimethylsiloxane Composites Characterization and Its Applications: A Review.” *Polymers* 13(23).

Bazylewski, Paul, and Giovanni Fanchini. 2019. “Graphene: Properties and Applications.” Pp. 287–304 in *Comprehensive Nanoscience and Nanotechnology*. Vols. 1–5. Elsevier.

Bîrca, Alexandra, Oana Gherasim, Valentina Grumezescu, and Alexandru Mihai Grumezescu. 2019. “Introduction in Thermoplastic and Thermosetting Polymers.” Pp. 1–28 in *Materials for Biomedical Engineering: Thermoset and Thermoplastic Polymers*. Elsevier.

Borah, Bikash, Gunda Rajitha, and Raj Kishora Dash. 2018. “Correlation between the Thickness and Properties of the Ethanol Treated GO–PDMS Based Composite Materials.” *Journal of Materials Science: Materials in Electronics* 29(23). doi: 10.1007/s10854-018-0154-2.

Brändle, Gregor, Max Schönfisch, and Simon Schulte. 2021. “Estimating Long-Term Global Supply Costs for Low-Carbon Hydrogen.” *Applied Energy* 302. doi: 10.1016/j.apenergy.2021.117481.

Brigandi, Paul J., Jeffrey M. Cogen, and Raymond A. Pearson. 2014. “Electrically Conductive Multiphase Polymer Blend Carbon-Based Composites.” *Polymer Engineering and Science* 54(1).

Campbell, F. C. 2010. *Structural Composite Materials*. United States of America: ASM International.

Chawla, Krishan K. 2012. “Ceramic Matrix Composites.” Pp. 249–92 in *Composite Materials*. New York, NY: Springer New York.

Chawla, Krishan K. 2019. *Composite Materials: Science and Engineering*.

Chen, Hao, Ionel Botef, Babu Guduri, and V. V. Srinivasu. 2010. “Thermal and Bonding Properties of Nano Size Carbon Black Filled PDMS.” in *AIP Conference Proceedings*. Vol. 1276.

Cheng, Yin, Hange Zhang, Ranran Wang, Xiao Wang, Haitao Zhai, Tao Wang, Qinghui Jin, and Jing Sun. 2016. “Highly Stretchable and Conductive Copper Nanowire Based Fibers with Hierarchical Structure for Wearable Heaters.” *ACS Applied Materials and Interfaces* 8(48):32925–33. doi: 10.1021/acsami.6b09293.

Choi, Hyun Jung, Moo Sung Kim, Damiro Ahn, Sang Young Yeo, and Sohee Lee. 2019. “Electrical Percolation Threshold of Carbon Black in a Polymer Matrix and Its Application to Antistatic Fibre.” *Scientific Reports* 9(1). doi: 10.1038/s41598-019-42495-1.

Chung, D. D. L. 2002. “Review: Graphite.” *Journal of Materials Science* 37(8).

Colas, André, and Jim Curtis. 2013. *Handbook of Polymer Applications in Medicine and Medical Devices*.

Criado-Gonzalez, Miryam, Antonio Dominguez-Alfaro, Naroa Lopez-Larrea, Nuria Alegret, and David Mecerreyes. 2021. "Additive Manufacturing of Conducting Polymers: Recent Advances, Challenges, and Opportunities." *ACS Applied Polymer Materials* 3(6).

Danilov, V., C. Dölle, M. Ott, H-e Wagner, and J. Meichsner. 2009. "Plasma Treatment of Polydimethylsiloxane Thin Films Studied by Infrared Reflection Absorption Spectroscopy." *29th ICPIG* (June).

Dinu, Roxana, Ugo Lafont, Olivier Damiano, and Alice Mija. 2022. "High Glass Transition Materials from Sustainable Epoxy Resins with Potential Applications in the Aerospace and Space Sectors." *ACS Applied Polymer Materials* 4(5). doi: 10.1021/acsapm.2c00183.

Donnet, J. B. 1993. *Carbon Black: Science and Technology, Second Edition*. Vol. 36.

Doshi, Bhairavi, Mika Sillanpää, and Simo Kalliola. 2018. "A Review of Bio-Based Materials for Oil Spill Treatment." *Water Research* 135.

Fan, Yiran, Geoff D. Fowler, and Ming Zhao. 2020. "The Past, Present and Future of Carbon Black as a Rubber Reinforcing Filler – A Review." *Journal of Cleaner Production* 247.

Figueroa Ramírez, S. J., and M. Miranda-Hernánde. 2012. "Carbon Film Electrodes as Support of Metallic Particles." *International Journal of Electrochemical Science* 7(1). doi: 10.1016/s1452-3981(23)13327-x.

Fowkes, Frederick M. 1964. "ATTRACTIVE FORCES AT INTERFACES." *Industrial & Engineering Chemistry* 56(12). doi: 10.1021/ie50660a008.

Fox, H. W., and W. A. Zisman. 1952. "The Spreading of Liquids on Low-Energy Surfaces. III. Hydrocarbon Surfaces." *Journal of Colloid Science* 7(4). doi: 10.1016/0095-8522(52)90008-1.

Fu, Shaoyun, Zheng Sun, Pei Huang, Yuanqing Li, and Ning Hu. 2019. "Some Basic Aspects of Polymer Nanocomposites: A Critical Review." *Nano Materials Science* 1(1). doi: 10.1016/j.nanoms.2019.02.006.

Gao, Qingsen, Jingguang Liu, and Xianhu Liu. 2021. "Electrical Conductivity and Rheological Properties of Carbon Black Based Conductive Polymer Composites Prior to and after Annealing." *Polymers and Polymer Composites* 29(9_suppl). doi: 10.1177/09673911211001277.

Gao, Yuan, Hongwen Jing, Guangping Fu, Zhenlong Zhao, and Xinshuai Shi. 2021. "Studies on Combined Effects of Graphene Oxide-Fly Ash Hybrid on the Workability, Mechanical Performance and Pore Structures of Cementitious Grouting under High W/C Ratio." *Construction and Building Materials* 281. doi: 10.1016/j.conbuildmat.2021.122578.

Gergely, András, Imre Bertóti, Tamás Török, Éva Pfeifer, and Erika Kálmán. 2013. "Corrosion Protection with Zinc-Rich Epoxy Paint Coatings Embedded with

Various Amounts of Highly Dispersed Polypyrrole-Deposited Alumina Monohydrate Particles." *Progress in Organic Coatings* 76(1). doi: 10.1016/j.porgcoat.2012.08.005.

Ghahramani, Pardis, Kamran Behdinan, Rasool Moradi-Dastjerdi, and Hani E. Naguib. 2021. "Theoretical and Experimental Investigation of MWCNT Dispersion Effect on the Elastic Modulus of Flexible PDMS/MWCNT Nanocomposites." *Nanotechnology Reviews* 11(1):55–64. doi: 10.1515/ntrev-2022-0006.

Ghanbari, Khashayar, and Morteza Ehsani. 2018. "Change in Surface Properties of Polydimethylsiloxane/Polyurethane/Carbon Nanotubes Elastomeric Coatings." *Progress in Organic Coatings* 125. doi: 10.1016/j.porgcoat.2018.09.022.

Gökaltun, Aslıhan, Young Bok (Abraham) Kang, Martin L. Yarmush, O. Berk Usta, and Ayse Asatekin. 2019. "Simple Surface Modification of Poly(Dimethylsiloxane) via Surface Segregating Smart Polymers for Biomicrofluidics." *Scientific Reports* 9(1). doi: 10.1038/s41598-019-43625-5.

González-González, Reyna Berenice, Lucy T. González, Sigfrido Iglesias-González, Everardo González-González, Sergio O. Martinez-Chapa, Marc Madou, Mario Moisés Alvarez, and Alberto Mendoza. 2020. "Characterization of Chemically Activated Pyrolytic Carbon Black Derived from Waste Tires as a Candidate for Nanomaterial Precursor." *Nanomaterials* 10(11). doi: 10.3390/nano10112213.

Greenwood, Matthew, Marc Wentker, and Jens Leker. 2021. "A Bottom-up Performance and Cost Assessment of Lithium-Ion Battery Pouch Cells Utilizing Nickel-Rich Cathode Active Materials and Silicon-Graphite Composite Anodes." *Journal of Power Sources Advances* 9. doi: 10.1016/j.powera.2021.100055.

Gulrez, Syed K. H., M. E. Ali Mohsin, Hamid Shaikh, Arfat Anis, Anesh Manjaly Pulose, Mukesh K. Yadav, Eng Hau P. Qua, and S. M. Al-Zahrani. 2014. "A Review on Electrically Conductive Polypropylene and Polyethylene." *Polymer Composites* 35(5).

Gültekin, Nergis Demirel. 2015. "Investigation of Thermal and Electrical Conductivity Properties of Carbon Black Coated Cotton Fabrics." *Marmara University Journal Of Science* 27(3). doi: 10.7240/mufbed.67752.

Hamidi, Youssef K., and Cengiz M. Altan. 2017. "Process-Induced Defects in Resin Transfer Molded Composites." Pp. 95–106 in *Comprehensive Composite Materials II*. Elsevier.

Han, Zhidong, and Alberto Fina. 2011. "Thermal Conductivity of Carbon Nanotubes and Their Polymer Nanocomposites: A Review." *Progress in Polymer Science (Oxford)* 36(7).

Hassanabadi, Hojjat Mahi, Manfred Wilhelm, and Denis Rodrigue. 2014. "A Rheological Criterion to Determine the Percolation Threshold in Polymer Nano-Composites." *Rheologica Acta* 53(10–11). doi: 10.1007/s00397-014-0804-0.

Hauptman, Nina, Marta Klanjšek Gunde, Matjaž Kunaver, and Marija Bešter-Rogač. 2011. "Influence of Dispersing Additives on the Conductivity of Carbon Black

Pigment Dispersion." *Journal of Coatings Technology and Research* 8(5). doi: 10.1007/s11998-011-9330-5.

Hong, Sukjoon, Habeom Lee, Jinhwan Lee, Jinhyeong Kwon, Seungyong Han, Young D. Suh, Hyunmin Cho, Jaeho Shin, Junyeob Yeo, and Seung Hwan Ko. 2015. "Highly Stretchable and Transparent Metal Nanowire Heater for Wearable Electronics Applications." *Advanced Materials* 27(32):4744–51. doi: 10.1002/adma.201500917.

Hsissou, Rachid, Rajaa Seghiri, Zakaria Benzekri, Miloudi Hilali, Mohamed Rafik, and Ahmed Elharfi. 2021. "Polymer Composite Materials: A Comprehensive Review." *Composite Structures* 262.

Hu, Liangbing, Han Sun Kim, Jung Yong Lee, Peter Peumans, and Yi Cui. 2010. "Scalable Coating and Properties of Transparent, Flexible, Silver Nanowire Electrodes." *ACS Nano* 4(5). doi: 10.1021/nn1005232.

Irshidat, Mohammad R., Mohammed H. Al-Saleh, and Mahmoud Al-Shoubaki. 2015. "Using Carbon Nanotubes to Improve Strengthening Efficiency of Carbon Fiber/Epoxy Composites Confined RC Columns." *Composite Structures* 134. doi: 10.1016/j.compstruct.2015.08.108.

Jańczuk, Bronisław, and Tomasz Białłopiotrowicz. 1989. "Surface Free-Energy Components of Liquids and Low Energy Solids and Contact Angles." *Journal of Colloid And Interface Science* 127(1). doi: 10.1016/0021-9797(89)90019-2.

Jin, Fan Long, Xiang Li, and Soo Jin Park. 2015. "Synthesis and Application of Epoxy Resins: A Review." *Journal of Industrial and Engineering Chemistry* 29.

Jojibabu, Panta, Y. X. Zhang, and B. Gangadhara Prusty. 2020. "A Review of Research Advances in Epoxy-Based Nanocomposites as Adhesive Materials." *International Journal of Adhesion and Adhesives* 96. doi: 10.1016/j.ijadhadh.2019.102454.

Kaseem, Mosab, Kotiba Hamad, and Young Gun Ko. 2016. "Fabrication and Materials Properties of Polystyrene/Carbon Nanotube (PS/CNT) Composites: A Review." *European Polymer Journal* 79.

Kausar, Ayesha. 2017. "Role of Thermosetting Polymer in Structural Composite." *Issue 1 Kausar A. American Journal of Polymer Science & Engineering* 5:1–12.

Kausar, Ayesha, and Reza Taherian. 2018. "Electrical Conductivity Behavior of Polymer Nanocomposite with Carbon Nanofillers." in *Electrical Conductivity in Polymer-Based Composites: Experiments, Modelling, and Applications*.

Khan, Zaheen Ullah, Ayesha Kausar, and Hidayat Ullah. 2016. "A Review on Composite Papers of Graphene Oxide, Carbon Nanotube, Polymer/GO, and Polymer/CNT: Processing Strategies, Properties, and Relevance." *Polymer - Plastics Technology and Engineering* 55(6):559–81.

Kim, Hyunmin, Minjeong Seo, Jong Woo Kim, Do Kyun Kwon, Song Ee Choi, Jin Woong Kim, and Jae Min Myoung. 2019. "Highly Stretchable and Wearable Thermotherapy Pad with Micropatterned Thermochromic Display Based on Ag Nanowire–Single-Walled Carbon Nanotube Composite." *Advanced Functional Materials* 29(24). doi: 10.1002/adfm.201901061.

Kim, Hyunwoo, Yutaka Miura, and Christopher W. MacOsko. 2010. “Graphene/Polyurethane Nanocomposites for Improved Gas Barrier and Electrical Conductivity.” *Chemistry of Materials* 22(11). doi: 10.1021/cm100477v.

Kim, Jeong Hun, Ji Young Hwang, Ha Ryeon Hwang, Han Seop Kim, Joong Hoon Lee, Jae Won Seo, Ueon Sang Shin, and Sang Hoon Lee. 2018. “Simple and Cost-Effective Method of Highly Conductive and Elastic Carbon Nanotube/Polydimethylsiloxane Composite for Wearable Electronics.” *Scientific Reports* 8(1). doi: 10.1038/s41598-017-18209-w.

Kim, Jin Hee, Sumin Kim, Jong Hun Han, Sol Bin Seo, Yu Rim Choi, Jinsub Lim, and Yoong Ahm Kim. 2023. “Perspective on Carbon Nanotubes as Conducting Agent in Lithium-Ion Batteries: The Status and Future Challenges.” *Carbon Letters* 33(2).

Kim, Taehoon, Junyong Park, Jongmoo Sohn, Donghwi Cho, and Seokwoo Jeon. 2016. “Bioinspired, Highly Stretchable, and Conductive Dry Adhesives Based on 1D-2D Hybrid Carbon Nanocomposites for All-in-One ECG Electrodes.” *ACS Nano* 10(4). doi: 10.1021/acsnano.6b01355.

Kingston, Christopher T., Zygmunt J. Jakubek, Stéphane Dénommée, and Benoit Simard. 2004. “Efficient Laser Synthesis of Single-Walled Carbon Nanotubes through Laser Heating of the Condensing Vaporization Plume.” *Carbon* 42(8–9). doi: 10.1016/j.carbon.2004.02.020.

Kong, Jeong Ho, Nam Su Jang, Soo Hyung Kim, and Jong Man Kim. 2014. “Simple and Rapid Micropatterning of Conductive Carbon Composites and Its Application to Elastic Strain Sensors.” *Carbon* 77:199–207. doi: 10.1016/j.carbon.2014.05.022.

Krenczkowska, Dominika, Krystyna Mojsiewicz-Pieńkowska, Bartosz Wielgomas, Krzysztof Cal, Rafał Bartoszewski, Sylwia Bartoszewska, and Zbigniew Jankowski. 2019. “The Consequences of Overcoming the Human Skin Barrier by Siloxanes (Silicones) Part 1. Penetration and Permeation Depth Study of Cyclic Methyl Siloxanes.” *Chemosphere* 231. doi: 10.1016/j.chemosphere.2018.09.154.

Kutz, Myer. 2015. *Mechanical Engineers Handbook. Volume 1 : Materials and Engineering Mechanics*. Vol. 1.

Le, Thanh Hai, Yukyung Kim, and Hyeonseok Yoon. 2017. “Electrical and Electrochemical Properties of Conducting Polymers.” *Polymers* 9(4).

Lee, Yu Rok, Anjanapura V. Raghu, Han Mo Jeong, and Byung Kyu Kim. 2009. “Properties of Waterborne Polyurethane/Functionalized Graphene Sheet Nanocomposites Prepared by an in Situ Method.” *Macromolecular Chemistry and Physics* 210(15). doi: 10.1002/macp.200900157.

Li, Wenlin, Yaqiong Zhang, Jingjing Yang, Jun Zhang, Yanhua Niu, and Zhigang Wang. 2012. “Thermal Annealing Induced Enhancements of Electrical Conductivities and Mechanism for Multiwalled Carbon Nanotubes Filled Poly(Ethylene-Co-Hexene) Composites.” *ACS Applied Materials and Interfaces* 4(12). doi: 10.1021/am302597f.

Li, Yichao, Xianrong Huang, Lijian Zeng, Renfu Li, Huafeng Tian, Xuewei Fu, Yu Wang, and Wei Hong Zhong. 2019. “A Review of the Electrical and Mechanical

Properties of Carbon Nanofiller-Reinforced Polymer Composites." *Journal of Materials Science* 54(2).

Liew, Kai Bin, Choon Fu Goh, Sajid Asghar, and Haroon K. Syed. 2021. "Overview of Mechanical and Physicochemical Properties of Polymer Matrix Composites." in *Encyclopedia of Materials: Composites*. Vol. 1.

Liu, Chao Xuan, and Jin Woo Choi. 2009. "Patterning Conductive PDMS Nanocomposite in an Elastomer Using Microcontact Printing." *Journal of Micromechanics and Microengineering* 19(8). doi: 10.1088/0960-1317/19/8/085019.

Liu, Chenguang, Zhenning Yu, David Neff, Aruna Zhamu, and Bor Z. Jang. 2010. "Graphene-Based Supercapacitor with an Ultrahigh Energy Density." *Nano Letters* 10(12). doi: 10.1021/nl102661q.

Liu, Hu, Qianming Li, Shuaidi Zhang, Rui Yin, Xianhu Liu, Yuxin He, Kun Dai, Chongxin Shan, Jiang Guo, Chuntai Liu, Changyu Shen, Xiaojing Wang, Ning Wang, Zicheng Wang, Renbo Wei, and Zhanhu Guo. 2018. "Electrically Conductive Polymer Composites for Smart Flexible Strain Sensors: A Critical Review." *Journal of Materials Chemistry C* 6(45).

Loganathan, Sravanthi, Ravi Babu Valapa, Raghvendra Kumar Mishra, G. Pugazhenthi, and Sabu Thomas. 2017. "Thermogravimetric Analysis for Characterization of Nanomaterials." in *Thermal and Rheological Measurement Techniques for Nanomaterials Characterization*. Vol. 3.

Mahmoudi, Tahmineh, Yousheng Wang, and Yoon Bong Hahn. 2018. "Graphene and Its Derivatives for Solar Cells Application." *Nano Energy* 47.

Martins-Júnior, P. A., C. E. Alcântara, R. R. Resende, and A. J. Ferreira. 2013. "Carbon Nanotubes: Directions and Perspectives in Oral Regenerative Medicine." *Journal of Dental Research* 92(7).

Mishra, Munmaya. 2018. *Encyclopedia of Polymer Applications, 3 Volume Set*.

Mohammad, Hussam, Andrey A. Stepashkin, and Victor V. Tcherdyntsev. 2022. "Effect of Graphite Filler Type on the Thermal Conductivity and Mechanical Behavior of Polysulfone-Based Composites." *Polymers* 14(3). doi: 10.3390/polym14030399.

Mohd Radzuan, Nabilah Afiqah, Abu Bakar Sulong, and Jaafar Sahari. 2017. "A Review of Electrical Conductivity Models for Conductive Polymer Composite." *International Journal of Hydrogen Energy* 42(14):9262–73. doi: 10.1016/j.ijhydene.2016.03.045.

Mondal, Subhadip, Sabyasachi Ghosh, Sayan Ganguly, Poushali Das, Revathy Ravindren, Subhashis Sit, Goutam Chakraborty, and Narayan Ch Das. 2017. "Highly Conductive and Flexible Nano-Structured Carbon-Based Polymer Nanocomposites with Improved Electromagnetic-Interference-Shielding Performance." *Materials Research Express* 4(10). doi: 10.1088/2053-1591/aa9032.

Mysiukiewicz, Olga, Bartosz Gospodarek, Paweł Ławniczak, and Tomasz Sterzyński. 2018. "Influence of the Conductive Network Creation on Electrical, Rheological, and Mechanical Properties of Composites Based on LDPE and EVA Matrices." *Advances in Polymer Technology* 37(8). doi: 10.1002/adv.22138.

Navin Baskar. 2023. “Thermoplastics vs Thermoset Plastics: What’s The Difference?” *Https://Skill-Lync.Com/Blogs/Technical-Blogs/Cae-Thermoplastics-vs-Thermoset-Plastics-What-the-Difference*.

Neumann, A. W., R. J. Good, C. J. Hope, and M. Sejpal. 1974. “An Equation-of-State Approach to Determine Surface Tensions of Low-Energy Solids from Contact Angles.” *Journal of Colloid And Interface Science* 49(2). doi: 10.1016/0021-9797(74)90365-8.

Norkhairunnisa, M., A. Azizan, M. Mariatti, H. Ismail, and L. C. Sim. 2012. “Thermal Stability and Electrical Behavior of Polydimethylsiloxane Nanocomposites with Carbon Nanotubes and Carbon Black Fillers.” *Journal of Composite Materials* 46(8). doi: 10.1177/0021998311412985.

Ogbonna, V. E., A. P. I. Popoola, and O. M. Popoola. 2023. “A Review on Recent Advances on the Mechanical and Conductivity Properties of Epoxy Nanocomposites for Industrial Applications.” *Polymer Bulletin* 80(4).

Oh, Jae Young, Gwang Hoon Jun, Sunghwan Jin, Ho Jin Ryu, and Soon Hyung Hong. 2016. “Enhanced Electrical Networks of Stretchable Conductors with Small Fraction of Carbon Nanotube/Graphene Hybrid Fillers.” *ACS Applied Materials and Interfaces* 8(5). doi: 10.1021/acsami.5b11205.

Olabi, A. G., Mohammad Ali Abdelkareem, Tabbi Wilberforce, and Enas Taha Sayed. 2021. “Application of Graphene in Energy Storage Device – A Review.” *Renewable and Sustainable Energy Reviews* 135.

Oladele, I. O., I. O. Ibrahim, A. A. Adediran, A. D. Akinwekomi, Y. V. Adetula, and T. M. A. Olayanju. 2020. “Modified Palm Kernel Shell Fiber/Particulate Cassava Peel Hybrid Reinforced Epoxy Composites.” *Results in Materials* 5. doi: 10.1016/j.rinma.2019.100053.

Oliveira, Thainá A., Rosimery R. Oliveira, Renata Barbosa, Joyce B. Azevedo, and Tatianny S. Alves. 2017. “Effect of Reprocessing Cycles on the Degradation of PP/PBAT-Thermoplastic Starch Blends.” *Carbohydrate Polymers* 168. doi: 10.1016/j.carbpol.2017.03.054.

Orozco, Felipe, Alex Salvatore, Anchista Sakulmankongsuk, Diego Ribas Gomes, Yutao Pei, Esteban Araya-Hermosilla, Andrea Pucci, Ignacio Moreno-Villoslada, Francesco Picchioni, and Ranjita K. Bose. 2022. “Electroactive Performance and Cost Evaluation of Carbon Nanotubes and Carbon Black as Conductive Fillers in Self-Healing Shape Memory Polymers and Other Composites.” *Polymer* 260. doi: 10.1016/j.polymer.2022.125365.

Van Oss, C. J., R. J. Good, and M. K. Chaudhury. 1986. “The Role of van Der Waals Forces and Hydrogen Bonds in ‘Hydrophobic Interactions’ between Biopolymers and Low Energy Surfaces.” *Journal of Colloid And Interface Science* 111(2). doi: 10.1016/0021-9797(86)90041-X.

Owens, D. K., and R. C. Wendt. 1969. “Estimation of the Surface Free Energy of Polymers.” *Journal of Applied Polymer Science* 13(8). doi: 10.1002/app.1969.070130815.

Ozbas, Bulent, Christopher D. O'Neill, Richard A. Register, Ilhan A. Aksay, Robert K. Prud'Homme, and Douglas H. Adamson. 2012. "Multifunctional Elastomer Nanocomposites with Functionalized Graphene Single Sheets." *Journal of Polymer Science, Part B: Polymer Physics* 50(13). doi: 10.1002/polb.23080.

Pang, Huan, Ling Xu, Ding Xiang Yan, and Zhong Ming Li. 2014. "Conductive Polymer Composites with Segregated Structures." *Progress in Polymer Science* 39(11).

Papageorgiou, Dimitrios G., Ian A. Kinloch, and Robert J. Young. 2015. "Graphene/Elastomer Nanocomposites." *Carbon* 95.

Papageorgiou, Dimitrios G., Ian A. Kinloch, and Robert J. Young. 2017. "Mechanical Properties of Graphene and Graphene-Based Nanocomposites." *Progress in Materials Science* 90.

Park, Jonghwa, Youngoh Lee, Jaehyung Hong, Youngsu Lee, Minjeong Ha, Youngdo Jung, Hyuneui Lim, Sung Youb Kim, and Hyunhyub Ko. 2014. "Tactile-Direction-Sensitive and Stretchable Electronic Skins Based on Human-Skin-Inspired Interlocked Microstructures." *ACS Nano* 8(12). doi: 10.1021/nn505953t.

Park, S. H., and K. M. Chu. 2013. "Highly Conducting Carbon Nanotube Composite for Electric Heating Unit Applications." *Electronics Letters* 49(2):133–35. doi: 10.1049/el.2012.3811.

Pascault, Jean-Pierre, and Roberto J. J. Williams. 2013. "THERMOSETTING POLYMERS." edited by E. Sald´ıvar-Guerra and E. Vivaldo-Lima. John Wiley & Sons, Inc.

Paszkiewicz, Sandra, Anna Szymczyk, Zdenko Špitalský, Jaroslav Mosnáček, Konrad Kwiatkowski, and Zbigniew Rosłaniec. 2014. "Structure and Properties of Nanocomposites Based on PTT-Block-PTMO Copolymer and Graphene Oxide Prepared by in Situ Polymerization." *European Polymer Journal* 50(1). doi: 10.1016/j.eurpolymj.2013.10.031.

Patel, Rajen M. 2016. "Polyethylene." in *Multilayer Flexible Packaging: Second Edition*.

Radlmaier, V., C. Heckel, M. Winnacker, A. Erber, and H. Koerber. 2017. "Effects of Thermal Cycling on Polyamides during Processing." *Thermochimica Acta* 648. doi: 10.1016/j.tca.2016.12.011.

Rahmat, Meysam, and Pascal Hubert. 2011. "Carbon Nanotube-Polymer Interactions in Nanocomposites: A Review." *Composites Science and Technology* 72(1). doi: 10.1016/j.compscitech.2011.10.002.

Ratna Prasad, A. V., and K. Mohana Rao. 2011. "Mechanical Properties of Natural Fibre Reinforced Polyester Composites: Jowar, Sisal and Bamboo." *Materials and Design* 32(8–9):4658–63. doi: 10.1016/j.matdes.2011.03.015.

Razaq, Aamir, Faiza Bibi, Xiaoxiao Zheng, Raffaello Papadakis, Syed Hassan Mujtaba Jafri, and Hu Li. 2022. "Review on Graphene-, Graphene Oxide-, Reduced Graphene Oxide-Based Flexible Composites: From Fabrication to Applications." *Materials* 15(3).

Ren, Danqi, Shaodi Zheng, Feng Wu, Wei Yang, Zhengying Liu, and Mingbo Yang. 2014. "Formation and Evolution of the Carbon Black Network in Polyethylene/Carbon Black Composites: Rheology and Conductivity Properties." *Journal of Applied Polymer Science* 131(7). doi: 10.1002/app.39953.

Robinson, Paul., Emile S. Greenhalgh, and Silvestre. Pinho. 2012. *Failure Mechanisms in Polymer Matrix Composites : Criteria, Testing and Industrial Applications*. Woodhead Publishing.

Ronca, Sara. 2017. "Chapter 10 - Polyethylene." in *Brydson's Plastics Materials (Eighth Edition)*.

Ruan, Shengqian, Shikun Chen, Yi Liu, Yajun Zhang, Dongming Yan, and Mingzhong Zhang. 2023. "Early-Age Deformation of Hydrophobized Metakaolin-Based Geopolymers." *Cement and Concrete Research* 169. doi: 10.1016/j.cemconres.2023.107168.

Sahu, Santosh Kumar, Vasavi Boggarapu, and P. S. Rama Sreekanth. 2023. "Improvements in the Mechanical and Thermal Characteristics of Polymer Matrix Composites Reinforced with Various Nanofillers: A Brief Review." *Materials Today: Proceedings*. doi: 10.1016/j.matpr.2023.07.032.

Saikam, Leelakrishna, P. Arthi, Bakthavatchalam Senthil, and Mahalingam Shanmugam. 2023. "A Review on Exfoliated Graphite: Synthesis and Applications." *Inorganic Chemistry Communications* 152.

Sajeel, N. K., Houkan Mohammad, Karthik Kannan, Mohammed Ismail Saleh, and Kishor Kumar Sadasivuni. 2021. "Thermal, Electrical, and Sensing Properties of Recycled HDPE/Carbonaceous Industrial Waste Composites." *Macromolecular Symposia* 400(1). doi: 10.1002/masy.202100146.

De Sarkar, Mousumi, Takashi Sunada, Seiya Tomizawa, and Atsunori Kondo. 2022. "Effect of Carbon Black on Properties of Acrylonitrile-Chloroprene Rubber." *Journal of Applied Polymer Science* 139(5). doi: 10.1002/app.51588.

Seethapathy, Suresh, and Tadeusz Górecki. 2012. "Applications of Polydimethylsiloxane in Analytical Chemistry: A Review." *Analytica Chimica Acta* 750.

Sharma, Arun Kumar, Rakesh Bhandari, Amit Aherwar, Ruta Rimašauskiene, and Camelia Pinca-Bretotean. 2020. "A Study of Advancement in Application Opportunities of Aluminum Metal Matrix Composites." Pp. 2419–24 in *Materials Today: Proceedings*. Vol. 26. Elsevier Ltd.

Sharma, Daulat Kumar, Devang Mahant, and Gautam Upadhyay. 2019. "Manufacturing of Metal Matrix Composites: A State of Review." in *Materials Today: Proceedings*. Vol. 26.

Shirvanimoghaddam, Kamyar, Salah U. Hamim, Mohammad Karbalaei Akbari, Seyed Mousa Fakhrhoseini, Hamid Khayyam, Amir Hossein Pakseresht, Ehsan Ghasali, Mahla Zabet, Khurram Shahzad Munir, Shian Jia, J. Paulo Davim, and Minoo Naebe. 2017. "Carbon Fiber Reinforced Metal Matrix Composites: Fabrication Processes and Properties." *Composites Part A: Applied Science and Manufacturing* 92.

Shivashankar, H., R. Sangamesh, and S. M. Kulkarni. 2019. “Processing and Investigation of Mechanical Characteristics on the Polydimethylsiloxane/Carbon Black Composites.” *Materials Research Express* 6(10). doi: 10.1088/2053-1591/ab3b7e.

Shukla, Vineeta. 2019. “Review of Electromagnetic Interference Shielding Materials Fabricated by Iron Ingredients.” *Nanoscale Advances* 1(5).

Sijo, M. T., and K. R. Jayadevan. 2016. “Analysis of Stir Cast Aluminium Silicon Carbide Metal Matrix Composite: A Comprehensive Review.” *Procedia Technology* 24:379–85. doi: 10.1016/j.protcy.2016.05.052.

Sperling, L. H. (Leslie Howard). 2006. *Introduction to Physical Polymer Science*. Wiley.

Stankova, N. E., P. A. Atanasov, Ru G. Nikov, R. G. Nikov, N. N. Nedyalkov, T. R. Stoyanchov, N. Fukata, K. N. Kolev, E. I. Valova, J. S. Georgieva, and St A. Armyanov. 2016. “Optical Properties of Polydimethylsiloxane (PDMS) during Nanosecond Laser Processing.” *Applied Surface Science* 374. doi: 10.1016/j.apsusc.2015.10.016.

Sugatri, Rana Ida, Yudo Chandrasa Wirasadewa, Kurniawan Eko Saputro, Ersan Yudhapratama Muslih, Radyum Ikono, and Muhamad Nasir. 2018. “Recycled Carbon Black from Waste of Tire Industry: Thermal Study.” *Microsystem Technologies* 24(1). doi: 10.1007/s00542-017-3397-6.

Sui, Guopeng, Dingyao Liu, Yuhang Liu, Wenjing Ji, Qin Zhang, and Qiang Fu. 2019. “The Dispersion of CNT in TPU Matrix with Different Preparation Methods: Solution Mixing vs Melt Mixing.” *Polymer* 182. doi: 10.1016/j.polymer.2019.121838.

Sun, Wen Jin, Ling Xu, Li Chuan Jia, Chang Ge Zhou, Yang Xiang, Ru Hua Yin, Ding Xiang Yan, Jian Hua Tang, and Zhong Ming Li. 2019. “Highly Conductive and Stretchable Carbon Nanotube/Thermoplastic Polyurethane Composite for Wearable Heater.” *Composites Science and Technology* 181. doi: 10.1016/j.compscitech.2019.107695.

Szeluga, Urszula, Bogumiła Kumanek, and Barbara Trzebicka. 2015. “Synergy in Hybrid Polymer/Nanocarbon Composites. A Review.” *Composites Part A: Applied Science and Manufacturing* 73.

Tadmor, Rafael, Ratul Das, Semih Gulec, Jie Liu, Hartmann E. N’guessan, Meet Shah, Priyanka S Wasnik, and Sakshi B. Yadav. 2017. “Solid-Liquid Work of Adhesion.” *Langmuir* 33(15). doi: 10.1021/acs.langmuir.6b04437.

Takahashi, Toru, Shunsuke Tsubo, Ken Inoue, Ryo Suzuki, Hidenobu Murata, and Masaru Tachibana. 2023. “Effect of Dispersibility of Carbon Nanotubes on the Hardness and Thermal Properties of Polyphenylene Sulphide/Carbon Nanotube Composites Obtained Using Solution Mixing and Melt Blending Methods.” *Materials Science and Engineering: B* 295. doi: 10.1016/j.mseb.2023.116579.

Takeichi, T., and N. Furukawa. 2012. “5.25 - Epoxy Resins and Phenol-Formaldehyde Resins.” in *Polymer Science: a Comprehensive Reference: Volume 1-10*. Vols. 1–10.

Tang, Long Cheng, Li Zhao, Fei Qiang, Qian Wu, Li Xiu Gong, and Jin Ping Peng. 2019. "Mechanical Properties of Rubber Nanocomposites Containing Carbon Nanofillers." in *Carbon-Based Nanofillers and Their Rubber Nanocomposites: Fundamentals and Applications*.

Tarfaoui, M., K. Lafdi, and A. El Moumen. 2016. "Mechanical Properties of Carbon Nanotubes Based Polymer Composites." *Composites Part B: Engineering* 103. doi: 10.1016/j.compositesb.2016.08.016.

Tavman, Ismail H. 2015. "Preparation and Characterization of Conductive Polymer Nanocomposites Based on Ethylene–Vinylacetate Copolymer (EVA) Reinforced with Expanded and Unexpanded Graphite." *Advanced Materials Research* 1114:92–99. doi: 10.4028/www.scientific.net/amr.1114.92.

Thongruang, Wiriya, Richard J. Spontak, and C. Maurice Balik. 2002. *Bridged Double Percolation in Conductive Polymer Composites: An Electrical Conductivity, Morphology and Mechanical Property Study*. doi: https://doi.org/10.1016/S0032-3861(02)00180-5.

Tian, He, Yi Shu, Xue Feng Wang, Mohammad Ali Mohammad, Zhi Bie, Qian Yi Xie, Cheng Li, Wen Tian Mi, Yi Yang, and Tian Ling Ren. 2015. "A Graphene-Based Resistive Pressure Sensor with Record-High Sensitivity in a Wide Pressure Range." *Scientific Reports* 5. doi: 10.1038/srep08603.

Tiwari, Santosh K., Raghvendra Kumar Mishra, Sung Kyu Ha, and Andrzej Huczko. 2018. "Evolution of Graphene Oxide and Graphene: From Imagination to Industrialization." *ChemNanoMat* 4(7).

Umar, Ehtisham, Muhammad Ikram, Junaid Haider, Walid Nabgan, Muhammad Imran, and Ghazanfar Nazir. 2023. "3D Graphene-Based Material: Overview, Perspective, Advancement, Energy Storage, Biomedical Engineering and Environmental Applications a Bibliometric Analysis." *Journal of Environmental Chemical Engineering* 11(5).

Urban, Francesca, Grzegorz Lupina, Alessandro Grillo, Nadia Martucciello, and Antonio Di Bartolomeo. 2020. "Contact Resistance and Mobility in Back-Gate Graphene Transistors." *Nano Express* 1(1). doi: 10.1088/2632-959X/ab7055.

Vargaftik, N. B., B. N. Volkov, and L. D. Voljak. 1983. "International Tables of the Surface Tension of Water." *Journal of Physical and Chemical Reference Data* 12(3). doi: 10.1063/1.555688.

Wang, Jibin, Qiuying Li, Chifei Wu, and Haiyan Xu. 2014. "Thermal Conductivity and Mechanical Properties of Carbon Black Filled Silicone Rubber." *Polymers and Polymer Composites* 22(4). doi: 10.1177/096739111402200405.

Wei, Yuhong, Xiaoshi Li, Yunfan Wang, Thomas Hirtz, Zhanfeng Guo, Yancong Qiao, Tianrui Cui, He Tian, Yi Yang, and Tian Ling Ren. 2021. "Graphene-Based Multifunctional Textile for Sensing and Actuating." *ACS Nano* 15(11). doi: 10.1021/acsnano.1c05701.

Wen, Yingfeng, Chao Chen, Yunsheng Ye, Zhigang Xue, Hongyuan Liu, Xingping Zhou, Yun Zhang, Dequn Li, Xiaolin Xie, and Yiu Wing Mai. 2022. "Advances on

Thermally Conductive Epoxy-Based Composites as Electronic Packaging Underfill Materials—A Review." *Advanced Materials* 34(52).

Wolf, Marc P., Georgette B. Salieb-Beugelaar, and Patrick Hunziker. 2018. "PDMS with Designer Functionalities—Properties, Modifications Strategies, and Applications." *Progress in Polymer Science* 83.

Yan, Chaoyi, Jiangxin Wang, and Pooi See Lee. 2015. "Stretchable Graphene Thermistor with Tunable Thermal Index." *ACS Nano* 9(2). doi: 10.1021/nn507441c.

Yan, Jing, and Young Gyu Jeong. 2014. "Multiwalled Carbon Nanotube/Polydimethylsiloxane Composite Films as High Performance Flexible Electric Heating Elements." *Applied Physics Letters* 105(5). doi: 10.1063/1.4892545.

Yan, Jing, and Young Gyu Jeong. 2015. "Synergistic Effect of Hybrid Carbon Fillers on Electric Heating Behavior of Flexible Polydimethylsiloxane-Based Composite Films." *Composites Science and Technology* 106. doi: 10.1016/j.compscitech.2014.11.016.

Yao, Hong Bin, Jin Ge, Chang Feng Wang, Xu Wang, Wei Hu, Zhi Jun Zheng, Yong Ni, and Shu Hong Yu. 2013. "A Flexible and Highly Pressure-Sensitive Graphene-Polyurethane Sponge Based on Fractured Microstructure Design." *Advanced Materials* 25(46):6692–98. doi: 10.1002/adma.201303041.

Yao, Xudan, Stephen C. Hawkins, and Brian G. Falzon. 2018. "An Advanced Anti-Icing/de-Icing System Utilizing Highly Aligned Carbon Nanotube Webs." *Carbon* 136:130–38. doi: 10.1016/j.carbon.2018.04.039.

Yetisgin, Abuzer Alp, Hazal Sakar, Hakan Bermek, and Levent Trabzon. 2020. "Highly Conductive PDMS/Carbon Nanotube/Graphene Nanocomposites and Effect of Sulfuric Acid Treatment on Conductivity." *ArXiv*.

Young, T. 1805. "III. An Essay on the Cohesion of Fluids." *Philosophical Transactions of the Royal Society of London* 95. doi: 10.1098/rstl.1805.0005.

Yuen, Siu Ming, Ma Chen-Chi, Hsin Ho Wu, Hsu Chiang Kuan, Wei Jen Chen, Shu Hang Liao, Chia Wen Hsu, and Han Lang Wu. 2007. "Preparation and Thermal, Electrical, and Morphological Properties of Multiwalled Carbon Nanotube and Epoxy Composites." *Journal of Applied Polymer Science* 103(2). doi: 10.1002/app.25140.

Zhang, Wei, Abbas A. Dehghani-Sanij, and Richard S. Blackburn. 2007. "Carbon Based Conductive Polymer Composites." Pp. 3408–18 in *Journal of Materials Science*. Vol. 42.

Zhao, Yanan, Eusebio Duarte Cabrera, Dan Zhang, Jingyao Sun, Tairong Kuang, Willie Yang, Matthew J. Lertola, Avraham Benatar, Jose M. Castro, and L. James Lee. 2018. "Ultrasonic Processing of MWCNT Nanopaper Reinforced Polymeric Nanocomposites." *Polymer* 156. doi: 10.1016/j.polymer.2018.09.053.

Zhao, Zehui, Huawei Chen, Xiaolin Liu, Zelinlan Wang, Yantong Zhu, and Yuping Zhou. 2021. "The Development of Electric Heating Coating with Temperature Controlling Capability for Anti-Icing/de-Icing." *Cold Regions Science and Technology* 184. doi: 10.1016/j.coldregions.2021.103234.

Zhou, Rui, Pengcheng Li, Zeng Fan, Donghe Du, and Jianyong Ouyang. 2017. "Stretchable Heaters with Composites of an Intrinsically Conductive Polymer, Reduced Graphene Oxide and an Elastomer for Wearable Thermotherapy." *Journal of Materials Chemistry C* 5(6):1544–51. doi: 10.1039/c6tc04849h.

Zhu, Yanwu, Shanthi Murali, Weiwei Cai, Xuesong Li, Ji Won Suk, Jeffrey R. Potts, and Rodney S. Ruoff. 2010. "Graphene and Graphene Oxide: Synthesis, Properties, and Applications." *Advanced Materials* 22(35). doi: 10.1002/adma.201001068.

Zhu, Yinlong, Xin Chen, Kaimei Chu, Xu Wang, Zhiqiang Hu, and Haijun Su. 2022. "Carbon Black/PDMS Based Flexible Capacitive Tactile Sensor for Multi-Directional Force Sensing." *Sensors* 22(2). doi: 10.3390/s22020628.

APPENDIX A

CONDUCTIVITY MEASUREMENTS WITH DETAILED INFORMATION

Table A.1. Resistance and conductivity measurements of composite samples

Sample	L (m)	W (m)	t (m)	R (Ω)	Avg R (Ω)	Std. Dev. (%)	Cond. (S/m)	Avg Cond. (S/m)
			0.0014	9200			0.14	
			0.0014	10380			0.14	
			0.0015	12100			0.13	
			0.0016	11500			0.12	
%25 K70/PDMS	0.0695	0.036	0.0014	10200	9831	1342	0.14	0.14
			0.0017	9700			0.11	
			0.0010	8600			0.19	
			0.0012	8300			0.16	
			0.0013	8500			0.15	
			0.0020	340			2.74	
			0.0023	330			2.37	
			0.0022	327			2.51	
			0.0016	333			3.33	
%30 K70/PDMS	0.0687	0.037	0.0016	330	340	15	3.52	3.17
			0.0016	322			3.43	
			0.0015	360			3.57	
			0.0015	365			3.69	
			0.0016	355			3.37	

(cont. on next page)

Table A.1. (cont.)

			0.0012	160			13.67	
			0.0011	125			14.55	
			0.0015	125			10.41	
			0.0015	126			10.69	
%35 K70/PDMS	0.0705	0.036	0.0020	112	123	21	7.98	10.79
			0.0019	97			8.10	
			0.0015	98			10.62	
			0.0014	110			11.64	
			0.0017	150			9.47	
			0.0017	128000			0.01	
			0.0018	133000			0.01	
			0.0015	128000			0.01	
			0.0013	108000			0.01	
%10 XE2B/PDMS	0.05	0.04	0.0015	75000	110222	26257	0.01	0.01
			0.0016	148000			0.01	
			0.0013	77000			0.01	
			0.0015	109000			0.01	
			0.0012	86000			0.01	
			0.0019	330			2.37	
			0.0020	270			2.26	
			0.0017	258			2.65	
			0.0016	273			2.82	
%15 XE2B/PDMS	0.05	0.04	0.0016	280	276	25	2.86	2.57
			0.0017	294			2.61	
			0.0019	252			2.37	
			0.0019	246			2.37	
			0.0016	280			2.79	

Table A.2. Effect of surfactant on resistance and conductivity of composite samples

Sample	L (m)	W (m)	t (m)	R (Ω)	Avg R (Ω)	Std. Dev. (%)	Cond. (S/m)	Avg Cond. (S/m)
%30 K70/PDMS/ TX-100	0.07	0.04	0.0025	250	239	71	2.82	2.96
			0.0022	150			3.26	
			0.0025	333			2.88	
			0.0023	300			3.05	
			0.0027	200			2.65	
			0.0020	180			3.61	
			0.0025	160			2.87	
			0.0026	250			2.68	
			0.0025	330			2.83	
%30 K70/PDMS/ SDS	0.07	0.04	0.0012	470	358	57	4.47	3.11
			0.0018	310			3.06	
			0.0018	350			2.94	
			0.0017	330			3.19	
			0.0021	320			2.56	
			0.0020	363			2.64	
			0.0018	298			3.03	
			0.0019	350			2.81	
			0.0016	430			3.27	
%30 K70/PDMS/ F127	0.07	0.04	0.0010	490	500	38	3.67	3.09
			0.0014	520			2.78	
			0.0014	468			2.82	
			0.0012	485			3.23	
			0.0012	530			3.18	
			0.0012	530			3.20	
			0.0013	438			3.00	
			0.0013	560			3.00	
			0.0013	480			2.93	

(cont. on next page)

Table A.2. (cont.)

			0.0013	430			3.46	
			0.0016	520			2.95	
			0.0020	463			2.36	
			0.0017	435			2.73	
%30 K70/PDMS/ CTAB	0.07	0.04	0.0016	384	438	57	2.84	3.00
			0.0019	396			2.51	
			0.0016	367			2.97	
			0.0012	420			3.74	
			0.0013	530			3.48	